

Institute of Crop Science  
University of Hohenheim  
Prof. Dr. Nicolaus von Wirén

# **Identification of Regulatory Factors Determining Nutrient Acquisition in Arabidopsis**

Dissertation

Submitted in fulfillment of the requirements for the degree

“Doktor der Agrarwissenschaften”

(Dr. Sc. agr. / Ph.D. in Agricultural Sciences)

to the

Faculty of Agricultural Sciences

presented by

**Ricardo Fabiano Hettwer Giehl**

From Rio Grande do Sul, Brazil

2011

This thesis was accepted as a doctoral dissertation in fulfilment of the requirements for the degree “Doktor der Agrarwissenschaften” by the Faculty of Agricultural Sciences at the University of Hohenheim, on 27<sup>th</sup> June 2011.

Date of oral examination: 18<sup>th</sup> July 2011.

Examination Committee

Supervisor and Reviewer

Prof. Dr. Nicolaus von Wirén

Co-reviewer

Prof. Dr. Gerd Weber

Additional examiner

Prof. Dr. Klaus Harter

Vice-Dean and Head of the Committee

Prof. Dr. Andreas Fangmeier

## Table of contents

<b>1</b>	<b>Summary .....</b>	<b>4</b>
<b>2</b>	<b>Zusammenfassung .....</b>	<b>6</b>
<b>3</b>	<b>General introduction.....</b>	<b>8</b>
3.1	Regulation of macronutrient accumulation.....	8
3.1.1	Local signaling of macronutrient availability .....	9
3.1.2	Long-distance signaling of macronutrients .....	15
3.2	Regulation of micronutrient accumulation.....	18
3.2.1	Local signaling circuits regulating micronutrient homeostasis .....	19
3.2.2	Systemic regulation of micronutrient homeostasis .....	24
3.3	Objectives of the thesis.....	29
<b>4</b>	<b>Local supply of iron triggers lateral root elongation in <i>Arabidopsis thaliana</i> by altering auxin distribution .....</b>	<b>31</b>
4.1	Introduction.....	31
4.2	Materials and Methods .....	33
4.2.1	Plant material and growth conditions.....	33
4.2.2	Root growth measurements .....	34
4.2.3	Histochemical analysis .....	34
4.2.4	Microscopy analyses .....	35
4.2.5	Mineral element and chlorophyll analyses.....	35
4.2.6	Screening of <i>Ds</i> -transposon insertion lines under localized Fe .....	36
4.2.7	Expression analysis.....	37
4.2.8	Histochemical localization of ferric Fe .....	37
4.2.9	Ferric-chelate reductase activity.....	38
4.3	Results.....	38
4.3.1	Localized supply of iron stimulates lateral root development in <i>Arabidopsis</i> .....	38
4.3.2	Influence of the mode of iron supply on the nutritional status of the shoot .....	40
4.3.3	Influence of FIT and IRT1 on lateral root development under localized iron supply .....	44
4.3.4	Influence of shoot-derived Fe signals on lateral root development.....	47

4.3.5	Effect of localized Fe supply on the development of lateral roots .....	51
4.3.6	Localized Fe supply alters auxin distribution in lateral roots .....	54
4.3.7	Enhanced elongation of lateral roots in response to local Fe is dependent on an AUX1-mediated auxin transport .....	54
4.3.8	Screening of <i>Ds</i> -transposon-tagged Arabidopsis lines for their response to localized Fe supply .....	58
4.3.9	Loss of <i>GATA3</i> expression abolishes the stimulation of lateral root elongation in response to localized Fe availability .....	62
4.3.10	Regulation of <i>GATA3</i> expression by Fe .....	63
4.4	Discussion .....	65
4.4.1	Localized Fe supply differentially regulates lateral root number and lateral root length .....	66
4.4.2	The local regulation of lateral root development by Fe .....	67
4.4.3	AUX1-mediated auxin distribution is required for the increased lateral root elongation under localized Fe .....	69
4.4.4	Involvement of the putative DNA-binding protein <i>GATA3</i> in the regulation of lateral root elongation under localized Fe .....	70
<b>5</b>	<b>Ionomics-based identification of a transcription factor involved in the signaling of P deficiency in Arabidopsis roots .....</b>	<b>77</b>
5.1	Introduction .....	77
5.2	Material and methods .....	80
5.2.1	Screening of <i>Ds</i> -transposon lines .....	80
5.2.2	Phenotypical characterization of <i>ngal1</i> mutants .....	81
5.3	Results .....	85
5.3.1	Element profiling of <i>Ds</i> -transposon insertion lines affected in the expression of transcription factors .....	85
5.3.2	Isolation of a <i>Ds</i> -transposon-tagged line hypersensitive to low P .....	87
5.3.3	Role of <i>NGAL1</i> in lateral root development .....	93
5.3.4	The short-root phenotype of <i>ngal1-1</i> is specific for P starvation .....	94
5.3.5	The effect of <i>NGAL1</i> on some P starvation-induced responses .....	96
5.3.6	The short-root phenotype of <i>ngal1-1</i> is not due to a nutritional defect ...	99
5.3.7	<i>NGAL1</i> is expressed in root tips and is up-regulated by P-starvation ...	101
5.3.8	<i>NGAL1</i> modulates stem-cell maintenance under low P .....	103
5.4	DISCUSSION .....	106

5.4.1 Ionomics-based screen of Ds-transposon-tagged lines allowed the identification of transcription factors involved in the regulation of ion homeostasis.....	106
5.4.2 Involvement of NGAL1 in P and K accumulation.....	110
5.4.3 Impact of NGAL1 on root architecture .....	112
5.4.4 The local regulation of root architectural changes in response to P is dependent on a functional NGAL1 .....	115
<b>6 General discussion.....</b>	<b>117</b>
6.1 Nutrients as signals for root development.....	118
6.2 Nutrient signals differentially modulate the development of primary and lateral roots .....	120
6.3 Role of transcription factors in the signaling cascades affecting root development .....	124
<b>7 References .....</b>	<b>127</b>
<b>8 Acknowledgements .....</b>	<b>150</b>
<b>9 Curriculum vitae .....</b>	<b>152</b>

## 1 Summary

The acquisition and translocation of mineral nutrients involves the orchestrated action of a series of physiological and biochemical mechanisms, which are, in turn, regulated by nutrient availability and demand. Furthermore, root morphological changes play an outstanding role for nutrient acquisition, especially when the availability of a certain nutrient is low. Although for most nutrients the molecular mechanisms involved in their acquisition from soils have been described, much less is known about the regulatory pathways underlying the uptake and translocation of nutrients in plants. Thus, the main aim of the present study was to characterize root morphological responses to nutrient supply and to identify novel regulatory components.

The first part of the present thesis describes the morphological response of *Arabidopsis* roots to the essential element iron (Fe), which has a particularly low solubility in soils. Relative to a homogenous supply of Fe, localized Fe supply to horizontally-separated agar plates doubled lateral root length without a particular effect on lateral root number. The internal tissue Fe rather than external Fe triggered the local elongation of lateral roots. In addition, the Fe-stimulated emergence of lateral root primordia and root cell elongation was accompanied by a higher activity of the auxin reporter *DR5:GUS* in lateral root apices. A crucial role of the auxin transporter *AUX1* in Fe-triggered lateral root elongation was indicated by Fe-regulated *AUX1* promoter activities in lateral root apices and by the failure of *aux-1* mutants to elongate lateral roots into Fe-enriched agar patches. Furthermore, a screening was designed to identify novel regulatory components involved in the Fe-dependent stimulation of lateral roots. One member of the GATA family of transcription factors was found to play a role in the local, root-endogenous regulation of lateral root development in response to local supplies of Fe. It was concluded that a Fe sensing mechanism in roots regulates lateral root development by modulating auxin transport.

The second part of the thesis describes the use of multi-elemental analyses to identify novel regulators of nutrient accumulation in *Arabidopsis*. Firstly, it is shown that the disruption of transcription factors expression can lead to significant

alterations in the accumulation of one or more nutrients in shoots. In addition, this approach allowed the identification of a so-far uncharacterized transcription factor – NGAL1 – that regulates primary root elongation in response to phosphorus (P) supply. The loss of NGAL1 resulted in hypersensitive inhibition of primary root growth under low P and a P-independent increase in lateral root elongation. The results presented here indicate that NGAL1 participates in a signaling pathway that modulates meristematic activity by controlling the expression of important root patterning regulators according to the local availability of P.

## 2 Zusammenfassung

Die Aufnahme und Translokation von Mineralstoffen in Pflanzen wird durch das Zusammenspiel einer Reihe von physiologischen und biochemischen Mechanismen bedingt, welche wiederum von Nährstoffverfügbarkeit im Boden und Nährstoffbedarf der Pflanze reguliert werden. Dabei spielt die Veränderung der Wurzelmorphologie bei der Nährstoffaufnahme eine besonders bedeutende Rolle, vor allem wenn die Verfügbarkeit eines bestimmten Nährstoffs begrenzt ist. Obwohl für die meisten Nährstoffe die molekularen Mechanismen ihrer Aneignung aus dem Boden bereits beschrieben sind, ist vergleichsweise wenig über die regulatorischen Signalwege bekannt, die der Aufnahme und Translokation von Nährstoffen in Pflanzen zugrundeliegen. Das Ziel der vorliegenden Arbeit ist daher die Charakterisierung von morphologischen Reaktionen der Wurzel auf das Nährstoffangebot und die Identifikation neuer regulatorischer Komponenten.

Im ersten Teil der Arbeit wurde die morphologische Reaktion von Arabidopsiswurzeln auf das essentielle Spurenelement Eisen (Fe) beschrieben, welches im Boden besonders schwer löslich ist. Im Vergleich zu einem homogenen Angebot von Fe verdoppelte sich bei einer lokal determinierten Zugabe von Fe in horizontal geteilten Agarplatten die Länge der Lateralwurzeln, wohingegen die Anzahl der Lateralwurzeln nicht beeinflusst war. Die lokale Verlängerung der Lateralwurzeln wurde dabei eher von gewebinternem Fe, als von extern vorliegendem Fe gesteuert. Des Weiteren wurde das durch Fe stimulierte Entstehen von Lateralwurzelpseudomeren und die Elongation von Wurzelzellen von einer höheren Aktivität des Auxinreporters *DR5::GUS* in Lateralwurzelspitzen begleitet. Die Fe-regulierte *AUX1* Promoter-Aktivität in Lateralwurzelspitzen und die ausbleibende Elongation von Lateralwurzeln in Fe-angereicherten Agarsegmenten bei *aux-1* Mutanten, wiesen auf eine besonders wichtige Rolle des Auxintransporters AUX1 in der Fe-gesteuerten Elongation von Lateralwurzeln hin. Im Weiteren wurde ein Selektionsverfahren entwickelt, um neue regulatorische Komponenten der Fe-abhängigen Stimulation von Lateralwurzeln zu identifizieren. Dadurch wurde ein Mitglied der Familie der GATA-Transkriptionsfaktoren identifiziert, das eine Rolle bei der lokalen, auf die



Wurzel beschränkten Regulation der Entwicklung von Lateralwurzeln bei lokalem Fe-Angebot spielt. Dieser Teil der Arbeit liess schließen, dass die Entwicklung von Lateralwurzeln durch einen „Fe-Sensing“-Mechanismus der Wurzeln vermittelt wird, dem eine lokale Modulation des Auxin-Transports zugrundeliegt.

Der zweite Teil der Arbeit zielte auf eine Identifizierung von neuen Regulatoren der Nährstoffakkumulation in Pflanzen ab, indem Nährstoffprofile einer kleinen Mutantenpopulation in Arabidopsis erfasst wurden. Zunächst wurde gezeigt, dass eine fehlende Funktion von Transkriptionsfaktoren zu einer signifikanten Änderung der Akkumulation von einem oder mehreren Elementen im Sprossgewebe führen kann. Darüber hinaus ermöglichte dieser Ansatz die Identifikation des bisher nicht charakterisierten Transkriptionsfaktors, NGAL1, der die Elongation der Primärwurzel in Abhängigkeit eines lokalen Angebots von Phosphor (P) reguliert. Der Verlust von NGAL1 führte unter P-Mangel zu einer hypersensitiven Hemmung des Primärwurzelwachstums und einer P-unabhängigen Steigerung der Seitenwurzelbildung. Die hier beschriebenen Ergebnisse deuten darauf hin, dass NGAL1 die meristematische Aktivität der Wurzelspitze an die lokale Verfügbarkeit von P anpasst, indem NGAL1 wichtige Regulatoren der Stammzellidentität im Wurzelapex beeinflusst.

### **3 General introduction**

Fourteen mineral nutrients are essential for the growth and development of plants. Since the availability of these nutrients dependent on many chemical and physical properties of soils, plants are frequently challenged to mobilize those nutrients which are sparingly available. Evidence is emerging that plants are able to monitor their nutrient status at the whole-plant level as well as local variations in nutrient provision in plant tissues. This requires a series of sensing and signaling mechanisms devoted to detect and integrate the status of a certain nutrient. Some of these mechanisms act at a rather short distance, and report the intracellular demand or the demand of neighboring cells. Other sensing signaling mechanisms, however, are necessary to integrate the long-distance information of nutrient demand and availability at the whole-plant level. In this chapter, the current knowledge regarding macro- and micronutrient signaling is reviewed.

#### **3.1 Regulation of macronutrient accumulation**

Classified as macronutrients are those elements required by plants in comparatively large quantities, such as nitrogen (N), potassium (K), sulfur (S), phosphorus (P), magnesium (Mg) and calcium (Ca) (Marschner, 1995). Except for Ca and K, all other macronutrients are incorporated into organic molecules, such as amino acids (N and S), nucleic acids (N and P), phospholipids (P) and chlorophylls (Mg). Ca and K, in turn, remain in their ionic elementary form and function mainly as osmolytes (particularly K) or as stabilizers of cell walls and membranes as well as second messengers in signaling cascades (Ca). Because of the participation of macronutrients in essential processes of plant growth and development, many molecular components are committed to the uptake of macronutrients from the soil solution and their subsequent allocation into different tissues and cellular compartments (Amtmann and Blatt, 2009). Not surprisingly, intricate regulatory mechanisms modulate many of the components involved in macronutrient uptake, translocation and internal use, to meet the plant's demand. Plants appear to monitor both the plant macronutrient status and local fluctuations of their availability in the rooted soil. Thus, it is also plausible to assume that

distinct signaling molecule(s) are involved in these local and systemic responses. Although signaling components have been characterized for most macronutrients (Amtmann et al., 2006; Schachtman and Shin, 2007; Doerner, 2008; Gojon et al., 2009; Miller et al., 2009), the main focus in this section shall be set on N and particularly P, for which a great deal of understanding on local and systemic regulation has been accumulated in recent years.

### **3.1.1 Local signaling of macronutrient availability**

Although the concentration of most macronutrients in soils is usually high, complex chemical and physical interactions in soils often result in the shortage of one or more nutrients (Marschner, 1995). In order to more efficiently mobilize and utilize limited nutrients, plants must promptly respond to fluctuations in nutrient concentrations as well as to changes in the demand of different plant organs during distinct developmental stages.

The existence of a local regulation of macronutrient homeostasis was demonstrated by gene expression analyses. When K or P was withheld from the nutrient solution, changes in the expression of many K or P deficiency-regulated genes were observed in roots within 60 minutes (Wang et al., 2002). Since within this time no significant concentration change is expected to happen in the shoot, it is very likely that these responses were subject to a root-borne sensing and signaling pathway. This view was supported by a fast up-regulation of certain genes under P starvation, even when plants had their shoots being removed (Wang et al., 2002). In the case of N, the diversity of N forms that can be taken up by different transport systems is reflected in the existence of complex regulatory pathways involved in sensing and transmitting the information on the availability of these N forms. In this context, it has been shown that the expression of the high-affinity nitrate transporter *NRT2.1* was mainly stimulated in Arabidopsis roots that received nitrate supply, whereas the ammonium transporter *AMT1.1* was up-regulated in the N-starved roots (Gansel et al., 2001). Thus, it has been suggested that *AMT1.1* is primarily controlled by the local availability of ammonium rather than by long-distance signals (Gansel et al., 2001).

In the case of P, evidence has been obtained that inorganic orthophosphate (Pi), the P form which is taken up by plants (Raghothama, 1999), can function as a local signal. This view is supported by the observation that P starvation-inducible genes were quickly down-regulated (within 30 min) when Pi was resupplied to P-deficient plants (Müller et al., 2004). This response occurred well before any changes in shoot Pi or carbohydrate concentrations could be detected. More recently, a genome-wide transcriptome study indicated that the majority of P deficiency-regulated genes responded to the local presence of Pi (Thibaud et al., 2010). Further evidences for the existence of a Pi sensing mechanism in plants were provided from the study of the Pi analog, phosphite, which supposedly cannot be assimilated by plants (Carswell et al., 1996; Carswell et al., 1997). The supply of phosphite to otherwise P-deficient plants suppressed a series of P deficiency-induced responses, such as the expression of the Pi transporter *AtPT2* or the ectopic formation of root hairs, without affecting the Pi nutritional status of the plants (Ticconi et al., 2001). Altogether, it is the current view that in the local signaling, Pi itself is most likely the molecule which is sensed (Figure 1).

Besides some physiological and biochemical changes, also root morphological and architectural adaptations appear to be regulated by local Pi signaling. In fact, the frequently occurring heterogeneous distribution of nutrients in the soil imposes an additional challenge to plants: to reach and successfully colonize the sites where nutrients are available. Experimental and genetic evidence indicates that plants are able to monitor nutrient fluctuations and thus redirect root growth towards the sites where nutrients are more available (Zhang et al., 1999; Linkohr et al., 2002; Remans et al., 2006b; Lima et al., 2010). When grown under low P, plants show a remarkable increase in root hair density and length (Bates and Lynch, 1996; Ma et al., 2001; Schmidt and Schikora, 2001). Interestingly, the ectopic formation of root hairs is observed specifically in roots that are in direct contact with P-free medium (Bates and Lynch, 1996; Ma et al., 2001; Schmidt and Schikora, 2001). These observations indicate that stimulated root hair growth is independent of the overall plant P status. Enhanced root formation represents an important adaptive strategy for plants growing under limited P, since mutants defective in root hair development, such as *root hair defective2 (rhd2)*, show a

significantly lower Pi accumulation and modest reproductive development when cultivated under P-deficient conditions (Bates and Lynch, 2001).

More recently, a mutant showing inhibited root hair growth specifically under low P was selected from a genetic screen (Li et al., 2010). Because *per1* mutants did not show changes in Pi uptake and were rescued by the supplementation of the Pi analog phosphite, it has been suggested that *per1* mutants are defective in local Pi signaling. Complementation analysis of the *PER1* locus on chromosome 3 identified a synonymous substitution in the gene coding for UBP14, an ubiquitin-specific protease (Li et al., 2010). Thus, UBP14 represents the first molecular component identified to play a role in the regulation of epidermal cell fate specification in response to local Pi availability (Figure 1).

In addition to morphogenetic modifications, changes that are also displayed at the level of the root architecture are regulated by local Pi. Under low P, primary root elongation is typically inhibited while lateral root growth is markedly stimulated (Williamson et al., 2001; Lopez-Bucio et al., 2002; Lopez-Bucio et al., 2003). This adaptation is thought to enhance the plant's exploratory capacity in the upper parts of the soil, where Pi is usually more abundant. Evidence that the primary root inhibition is dependent on a local Pi signaling response came from the observation that the contact of the primary root tip of *Arabidopsis thaliana* plants with a low P patch inhibits further root elongation, irrespective of the plant nutritional status (Linkohr et al., 2002; Svistoonoff et al., 2007). Additional genetic evidence has reinforced the idea that P deficiency-induced primary root inhibition is responsive to the local Pi availability. Indeed, the conditional phenotype of *pdr2* mutants suggests that PDR2 represents a Pi-sensitive checkpoint that adjusts root architectural changes according to the external Pi availability (Ticconi et al., 2004). When transferred to a horizontal split-agar system, *pdr2* mutants exhibited a stronger inhibition of primary root elongation when placed in contact with a P-free agar segment, even if the upper part of the root system was grown on adequate Pi supply (Ticconi et al., 2004).

Although primary root inhibition is considered a widespread response to low P, the analysis of different *A. thaliana* accession lines indicated that there is a considerable natural variation for this trait (Chevalier et al., 2003; Reymond et al.,

2006). This natural variation was exploited by Reymond et al. (2006) to map quantitative trait loci (QTLs) involved in remodeling root architecture under low P in a recombinant inbred line (RIL) population originated from Bay-0 (limited primary root inhibition under low P) and Shahdara (strong primary root inhibition). One of the three major QTLs for primary root growth, *LPR1*, was mapped to the gene At1g23010 (Svistoonoff et al., 2007). Both *LPR1* and its close paralog *LPR2* encode multicopper oxidases that are mainly expressed in the primary root tip. In *lpr1* and *lpr2* loss-of-function mutants, the inhibition of primary root elongation in response to low P is markedly attenuated (Svistoonoff et al., 2007). These observations suggest that *LPR1* and *LPR2* are involved in Pi sensing at the primary root meristem. More recently, it has been demonstrated that both *PDR2* and *LPR1* are likely to act in a common regulatory pathway that adjusts meristematic activity to external P availability (Ticconi et al., 2009). Moreover, based on the observation that a triple *pdr2lpr1lpr2* mutant was less inhibited in primary root growth than *pdr2* and wildtype plants in low P, it was proposed that *PDR2* most likely acts downstream of *LPR1* and *LPR2* (Figure 1). The current view indicates that *PDR2* maintains the expression of two key regulators of radial root patterning and stem cell specification - *SCARECROW* (*SCR*) and *SHORT ROOT* (*SHR*) – under P starvation, thus maintaining a basal level of meristematic activity (Ticconi et al., 2009).

In the case of N, it has been demonstrated that plant roots can sense a local availability of nitrate and preferentially stimulate the elongation of those lateral roots which are in contact with the nutrient (Zhang and Forde, 1998; Zhang and Forde, 2000). Up to now, few genes have been identified to play a role in the regulation of root development in response to local nitrate. One of them, *ANR1*, encodes a putative MADS-box transcription factor (Zhang and Forde, 1998). The repression of *ANR1* by antisense and co-suppression prevented to a large extent the stimulation of lateral root elongation in the nitrate-supplied patch (Zhang and Forde, 1998). Surprisingly, the dual-affinity nitrate transporter *NRT1.1* was found to represent another component in the nitrate signaling pathway (Remans et al., 2006b). When the *NRT1.1*-deficient mutant *chl1* was grown in a split-root setup, it did not fully express the typical stimulation of lateral root elongation on the nitrate-

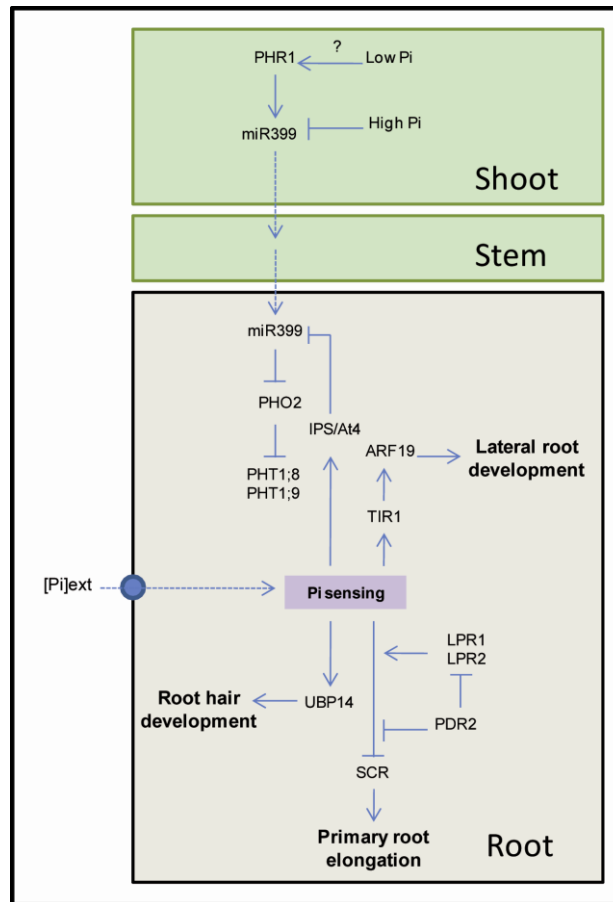


**Figure 1. Schematic representation of local and systemic regulatory modules controlling P homeostasis in plants.** A root-endogenous Pi sensing mechanism monitors the external availability of Pi. If primary roots reach a P-starved medium, primary root elongation is inhibited whereas root hair formation and lateral root initiation are enhanced. Primary root elongation is modulated according to the external Pi availability and is regulated by a signaling cascade that involves the ER-localized LPR1/2 and PDR2 (Svistonoff et al., 2007; Ticconi et al., 2009). These proteins control the expression of stem-cell regulators, such as SCR, thus adjusting the meristematic activity to the external availability of Pi. The development of root hairs is also controlled by local variations in Pi availability. The contact with a P-deficient medium triggers the formation of extra root hairs in response to a signaling pathway that includes UBQ14 (Li et al., 2010). In addition, the stimulation of lateral root development by low P has been shown to involve an increased in auxin sensitivity mediated by the auxin receptor TIR1 (Perez-Torres et al., 2008). Phosphorous starvation induces the expression of *TIR1*, thus allowing the activation of ARF19, and perhaps other ARFs (Perez-Torres et al., 2008), which regulate the auxin-dependent initiation of lateral root primordia (Okushima et al., 2007). In addition to the local P signaling, also systemic signals reporting the whole-plant P status control many root P starvation responses. One of these systemic signaling modules involves *miR399*, *PHO2* and *IPS/At4*. A low P status in the shoots is sensed by a yet unknown mechanism that induces the expression of *miR399* in a PHR1-dependent manner (Bari et al., 2006). Mature *miR399* is then translocated via the phloem into the roots (Pant et al., 2008), where it negatively regulates the expression of the E2 ubiquitin conjugase *PHO2* (Aung et al., 2006; Bari et al., 2006; Pant et al., 2008). The *miR399*-mediated down-regulation of *PHO2* activity increases the expression of root-expressed Pi transporters, such as *PHT1;8* and *PHT1;9*, leading to increased Pi uptake (Aung et al., 2006; Bari et al., 2006). The long-distance signal of P-starvation is also integrated into the local signaling circuit, since P starvation also leads to the concomitant induction of the ribo-regulators *IPS1* and *At4* that, in turn, regulate *PHO2* expression by modulating the silencing activity of *miR399* (Franco-Zorrilla et al., 2007). The sensing of a P sufficient status in leaves represses *miR399* expression and releases *PHO2* from the *miR399*-dependent inhibition, thus down-regulating *PHT1;8* and *PHT1;9* and reducing Pi uptake.

supplied side (Remans et al., 2006b). Importantly, because uptake was not significantly affected by the loss of NRT1.1, the reduced lateral root growth of *chl1* mutants was most likely indicative of defective signaling rather than an indirect effect of reduced uptake. Furthermore, the expression of *ANR1* in the root tip was largely down-regulated in *chl1* mutants, strongly indicating that NRT1.1 acts upstream of ANR1 in the nitrate-dependent signaling cascade that regulates lateral root development (Remans et al., 2006b). In addition to NRT1.1, also the high-affinity nitrate transporter NRT2.1 has been implicated in the modulation of root architecture in response to nitrate availability (Remans et al., 2006a). Although part of this role could be assigned to the nitrate uptake function of NRT2.1, lateral root initiation under low N was found to be directly affected by NRT2.1 independently of nitrate uptake.

More recently, it has been demonstrated that local availabilities of nitrate and ammonium have complementary effects on the root architecture of *Arabidopsis* plants, since ammonium enhanced the initiation of lateral roots whereas nitrate stimulated their subsequent elongation (Lima et al., 2010). Similar to nitrate, also the local ammonium signaling involves a transporter protein: the ammonium transporter AMT1;3. However, not only inorganic N forms affect root architecture. It has also been shown that glutamate availability is able to directly affect root growth (Walch-Liu et al., 2006; Walch-Liu and Forde, 2008). The external supply of glutamate strongly reduced the elongation of the primary root, by inhibiting the meristematic activity in the apical meristem (Walch-Liu et al., 2006). Interestingly, the supply of nitrate ( $\geq 0.5\text{mM}$ ) was able to counteract the inhibitory effect of glutamate on primary root growth (Walch-Liu and Forde, 2008). Furthermore, because the NRT1.1-deficient mutant *chl1-5* was sensitive to glutamate even in the presence of nitrate, it was suggested that NRT1.1-dependent nitrate sensing at the primary root tip alleviates the negative impact of glutamate on primary root growth (Walch-Liu and Forde, 2008). These observations further supported the idea that besides mediating nitrate transport, NRT1.1 displays also a regulatory function. Thus, the current view is that the NRT1.1-mediated nitrate sensing at the root tip suppresses the glutamate inhibition of primary root growth (Walch-Liu and Forde, 2008; Forde and Walch-Liu, 2009), thereby modulating root architecture in response to the soil availability of inorganic N and organic N pools.



### 3.1.2 Long-distance signaling of macronutrients

To maintain optimal growth under a wide range of environmental conditions, plants rely not only on the proper monitoring of signals reporting external nutrient availability at the root level, but also on the information of internal nutrient concentrations and demands in far-located organs, such as leaves and fruits. Earlier physiological experiments strongly indicated that many P and N starvation responses are under the control of long-distance signals (Drew and Saker, 1975; Laine et al., 1995; Burleigh and Harrison, 1999; Gansel et al., 2001). When *Medicago truncatula* plants were grown in a split-root setup, P starvation-induced genes were systematically down-regulated in the root half exposed to low P (Burleigh and Harrison, 1999). This indicated that at least part of the P-deficiency responses in roots is systematically regulated by the overall P status. A similar regulation has also been reported for nitrate, since nitrate uptake is induced in nitrate-fed and repressed in nitrate-free root portions splitted between compartments with contrasting nitrate availabilities (Drew and Saker, 1975; Laine et al., 1995). Indeed, the expression of the high-affinity nitrate transporter *AtNRT2.1* is preferentially induced in root parts exposed to nitrate (Gansel et al., 2001).

Besides the regulation of physiological and molecular responses, systemic signals do also modulate root architectural changes. Whereas localized supply of nitrate stimulates the elongation of lateral roots directly exposed to this nutrient (Drew, 1975; Zhang and Forde, 1998; Zhang et al., 1999), the supply of high nitrate levels systemically inhibits lateral root development (Zhang et al., 1999). Systemic inhibition by high tissue nitrate levels was further supported by the observation that the nitrate reductase-deficient *nia1nia2* mutant, which accumulates more internal nitrate due to reduced nitrate assimilation rates (Wilkinson and Crawford, 1993), is more sensitive to nitrate inhibition (Zhang et al., 1999).

Although shoot-borne signals are able to repress P and N starvation responses in roots, in either case the nature of these systemic signals is still not clear. In the case of P, the simplest scenario would indicate that  $P_i$  itself could serve not only as a local, but also as a long-distance signal. However, this is likely not the case,

since the repression of P deficiency responses in P-free parts of roots is observed well before any considerable change in P concentration can be detected in leaves (Burleigh and Harrison, 1999). Instead, many studies have indicated other potential signals for the systemic regulation of P starvation responses.

Sugars have been hypothesized to serve as long-distance signals that regulate P-deficiency responses in roots (Karthikeyan et al., 2007; Hammond and White, 2008). The stimulation of lateral root growth and the expression of a set of P starvation-responsive genes have been shown to be dependent on the supply of sucrose (Jain et al., 2007; Karthikeyan et al., 2007). In addition, P starvation typically leads to increased accumulation of starch and sucrose in shoots and roots (Ciereszko and Barbachowska, 2000; Müller et al., 2007). Shoot-to-root transport of sucrose in the phloem increases under P starvation (Ciereszko et al., 2005). Since the supply of glucose or glucose analogues failed to alter the expression of P starvation-induced genes (Müller et al., 2005; Karthikeyan et al., 2007), it has been suggested that sucrose rather than its breakdown products acts as the potential signaling compound. This hypothesis is further reinforced by the fact that *pho3* mutants are defective in the expression of *SUC2*, a sucrose-proton symporter involved in sucrose loading of the phloem (Lloyd and Zakhleniuk, 2004). In *pho3* mutants, P starvation-induced responses are markedly attenuated although P levels in shoots and roots are significantly reduced, even under sufficient Pi supply (Zakhleniuk et al., 2001). Furthermore, as a consequence from the loss of *SUC2* activity, *pho3* plants accumulate larger amounts of starch and soluble sugars in leaves (Zakhleniuk et al., 2001). Altogether, these observations indicate that sucrose might act as a systemic signal regulating P starvation responses in roots.

Apart from the putative systemic signaling mediated by sugars, the components of another long-distance regulatory circuit of P starvation responses have been elucidated in more detail (Doerner, 2008; Lin et al., 2009; Rouached et al., 2010; Yang and Finnegan, 2010; Figure 1). These findings were greatly facilitated by the identification of the *Arabidopsis* mutant *pho2*, which exhibits a two- to four-fold increase in Pi concentrations in leaves, even though showing almost unchanged root Pi levels (Delhaize and Randall, 1995). Reciprocal grafting studies indicated

that the underlying gene acts primarily in the roots, since the *pho2* genotype in roots is sufficient to phenocopy the whole plant *pho2* phenotype (Bari et al., 2006). In addition, because a subset of Pi starvation-induced genes is markedly up-regulated in *pho2* roots, despite the greater shoot Pi contents (Bari et al., 2006), it has been suggested that *pho2* mutants display a defective long-distance Pi signaling. Two independent studies identified *PHO2* (also known as *UBC24*) as a member of the E2 ubiquitin conjugase family (Aung et al., 2006; Bari et al., 2006). Aung et al. (2006) were able to demonstrate that *PHO2* expression is regulated by *microRNA399* (*miR399*). The constitutive overexpression of *miR399* led to marked suppression of *PHO2* expression and greater accumulation of Pi in shoots, thus mimicking the *pho2* mutation (Aung et al., 2006). Under sufficient Pi, *PHO2* targets a set of P deficiency-responsive proteins for degradation, including two root-expressed Pi transporters (*PHT1;8* and *PHT1;9*; Aung et al., 2006; Bari et al., 2006). Indeed, Pi overaccumulation in *pho2* shoots could be extensively prevented by the suppression of both *PHT1;8* and *PHT1;9* by RNA interference, indicating that the up-regulation of these two Pi transporters is causing the *pho2* phenotype (Bari et al., 2006). The expression of *miR399* is strongly up-regulated after the onset of P deficiency in leaves (Fujii et al., 2005; Aung et al., 2006; Bari et al., 2006; Pant et al., 2008). In addition, the MYB-type transcription factor *PHR1* appears to be important for the regulation of *miR399* expression, since *miR399* transcripts are down-regulated in *phr1* mutants (Bari et al., 2006), but up-regulated in *PHR1* overexpressors (Nilsson et al., 2007).

A major breakthrough for the understanding of the long-distance control of P responses in roots was the observation that *miR399* can move from leaves to roots in order to regulate *PHO2* expression (Lin et al., 2008; Pant et al., 2008). Mature *miR399* could be detected in phloem exudates and its specific overexpression in leaves of chimeric plants resulted in increased *miR399* levels in the grafted wildtype rootstock and reduced *PHO2* expression (Pant et al., 2008). Thus, the current view indicates that during early P limitation in leaves the induction of *miR399* expression serves as a long-distance signal to down-regulate *PHO2* expression in roots, thereby enhancing Pi uptake via the activation of the Pi transporters *PHT1;8* and *PHT1;9* (Figure 1). However, it is noteworthy that this signaling module controls only a subset of the P deficiency-induced responses in

roots, since e.g. other Pi transporters from the *PHT1* family are not significantly affected in *pho2* mutants (Aung et al., 2006).

An additional level of control in the *miR399*-*PHO2* signaling module is mediated by *IPS1* (*INDUCED BY Pi STARVATION1*) and *At4*, two members of the *Mt4*/TPS11 family of non-coding RNAs. Although earlier studies showed that both genes are strongly up-regulated in response to P limitation (Burleigh and Harrison, 1999; Franco-Zorrilla et al., 2002; Shin et al., 2006), their function remained largely unknown for many years. Strikingly, *IPS1* contains a motif which is complementary to *miR399*, except for a few critical bases located exactly in the motif required for the microRNA-guided cleavage of mRNA targets (Franco-Zorrilla et al., 2007). Amazingly, it was demonstrated that *IPS1* is able to sequester *miR399*, thus preventing *miR399*-mediated cleavage of *PHO2* transcripts (Figure 1). This hypothesis was elegantly corroborated by demonstrating that the expression of a modified version of *IPS1*, in which the mismatched bases were replaced by fully complementary ones, restored wildtype levels of *miR399* activity and repressed *PHO2* expression (Franco-Zorrilla et al., 2007). Thus, this mechanism offers an additional level of control, in which the long-distance P starvation signal is further adjusted at a local level, probably in order to fine-tune P acquisition in roots to the whole plant demand. In this context, the regulation of *miR399* activity by *IPS1* likely enable plants to quickly respond to local, root-endogenous fluctuations of Pi availability even before the shoot P status is significantly changed. In addition, the integration of short-range signals into the long-distance regulatory circuit offers the roots a certain degree of autonomy over the whole-plant signaling. Recently, additional microRNAs significantly induced or repressed by P starvation have been identified by means of deep sequencing (Hsieh et al., 2009). These findings suggest that there are even more levels of microRNA-mediated regulation of Pi homeostasis to be characterized.

### **3.2 Regulation of micronutrient accumulation**

Conversely to macronutrients, micronutrients are usually required in low amounts. In addition, many are toxic when present inside plant cells at high concentrations. Therefore, it is not surprising that plants have also evolved a set of mechanisms to

finely adjust micronutrient acquisition to the physiological and structural requirements of plant cells. If the external availability of a micronutrient is insufficient to cover the plant's demand, physiological and/or morphological responses are up-regulated to improve micronutrient acquisition and increase internal utilization. The initiation of such mechanisms must be coordinated across different plant organs, which may differ in their requirements or the size of their internal stores, and therefore depends on the use of signals, such as hormones, ions or metabolites, reporting the nutritional status of the micronutrient at the organ, tissue or cellular level from close or distant positions within the plant.

### **3.2.1 Local signaling circuits regulating micronutrient homeostasis**

The homeostasis of micronutrients at the cellular level is composed of a tight control of acquisition, efflux and storage processes. In the case of boron (B), for which metabolism plays a minor role, homeostasis appears to be primarily regulated by influx and efflux. Boron uptake by the NIP5;1 transporter in *Arabidopsis* roots is transcriptionally up-regulated under B deficiency (Takano et al., 2006), while cellular toxicity is avoided by the activation of B exporters (Miwa et al., 2007). By contrast, Fe homeostasis additionally requires the up-regulation of genes involved in Fe acquisition from the rhizosphere and Fe remobilization from the vacuole, whereas the build-up of Fe storage capacities is suppressed (Lanquar et al., 2005; Arnaud et al., 2006). In the strategy I plant *Arabidopsis*, in which Fe acquisition from the rhizosphere is mediated by the induction of plasma membrane proton-ATPases, the transmembrane reductase FRO2 and the Fe(II) transporter IRT1, the basic helix-loop-helix (bHLH) transcription factor FIT directly up-regulates the corresponding genes in response to Fe deficiency (Colangelo and Guerinot, 2004; Jakoby et al., 2004; Yuan et al., 2005); (Figure 2). In graminaceous plants like rice, where Fe acquisition is driven by phytosiderophores, there is also a bHLH-type transcription factor (Ogo et al., 2006; Ogo et al., 2007) which mediates the transfer of a Fe deficiency signal to the corresponding target genes. However, OsIRO2 is in turn transactivated by an interplay of two further transcription factors, namely IDEF1, an ABI3/VP1-type

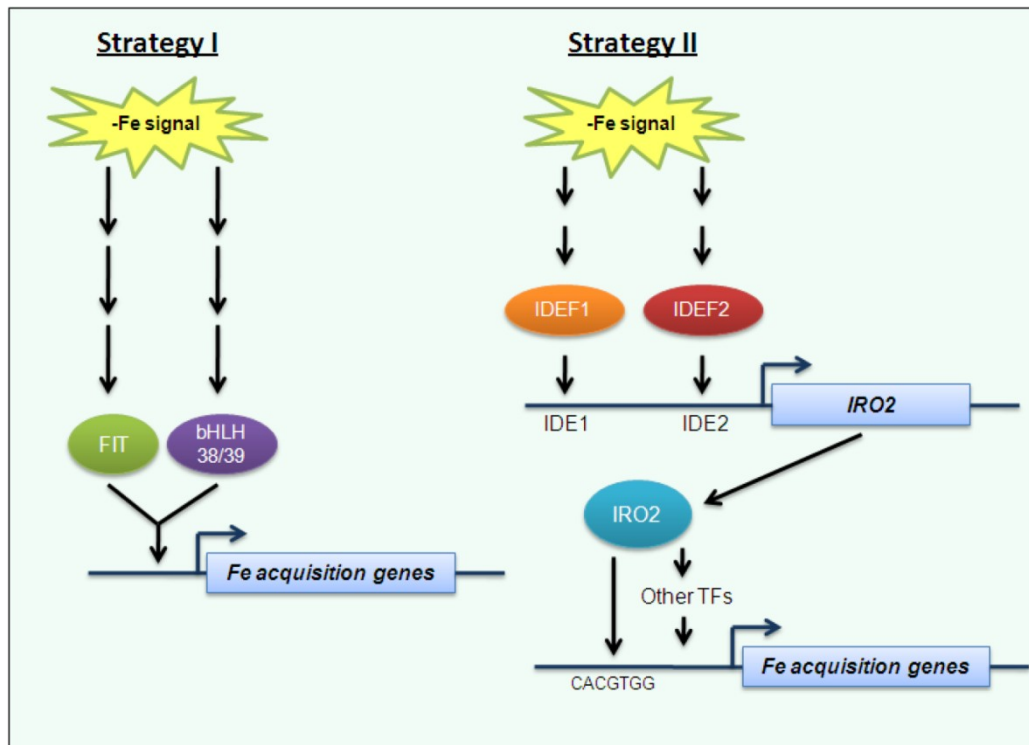


**Figure 2. Transcriptional regulation of Fe acquisition genes in strategy I and strategy II plants.** In the strategy I plant *Arabidopsis*, it has been shown that the expression of Fe acquisition genes is cooperatively regulated by the transcription factors FIT and either bHLH38 or bHLH39 (Yuan et al., 2008). Since both genes are also up-regulated under Fe deficiency (Colangelo and Gueriot, 2004; Jakoby et al., 2004; Yuan et al., 2005), they likely act downstream of a signalling cascade activated under Fe limitation. A promoter activity approach, however, suggested that the induction of *bHLH38* (and *bHLH39*) and *FIT* is mediated by distinct pathways (Wang et al., 2007). In graminaceous plants (strategy II), IDE1 and IDE2, two cis-acting elements present in the promoter of many Fe deficiency-inducible genes (Kobayashi et al., 2003), have been identified as regulators of Fe deficiency responses. In rice, a candidate gene approach has shown that IDE1 is transactivated by IDEF1, a transcription factor of the ABI3/VP1 family (Kobayashi et al., 2007). In addition, a yeast one-hybrid screening identified IDEF2, a NAC domain transcription factor that binds to IDE2 (Ogo et al., 2008). In rice, both IDEF1 and IDEF2 appear to regulate specific sets of Fe-regulated genes at least partially via the transcription factor IRO2, a Fe deficiency-inducible bHLH identified in a transcription profiling analysis (Ogo et al., 2006). The promoter region of *IRO2* contains a sequence similar to IDE suggesting that it acts downstream of the IDE-IDEF regulatory circuit (Ogo et al., 2007). Since the IRO2 binding sequence 5'-CACGTGG-3' is absent in the promoter of many Fe deficiency-inducible genes, it is plausible that additional transcription factors participate in their regulation in response to Fe limitation (Ogo et al., 2007).

transcription factor, and IDEF2, a NAC-domain transcription factor (Kobayashi et al., 2007; Ogo et al., 2008). In this section, the main focus shall be put on the molecular identities of the upstream components linking the Fe deficiency signal to the transcriptional regulation of genes involved in Fe homeostasis and their positions in the signaling cascade (Figures 3 and 4).

Nitric oxide (NO) has been recognized as an early component in Fe signaling (Murgia et al., 2002; Arnaud et al., 2006; Graziano and Lamattina, 2007; Chen et al., 2010b; Ramirez et al., 2010). Besides improving Fe availability inside the plant (Graziano et al., 2002), NO appears to be involved in the modulation of Fe deficiency responses in root cells (Graziano and Lamattina, 2007). In tomato roots, Fe deficiency triggered a rapid and sustained NO accumulation, primarily in rhizodermal cells, coinciding with the expression of the Fe acquisition genes *SIIRT1* (*Fe(II) transporter1*) and *SIFRO1* (*ferric chelate reductase1*). When the rise of NO was prevented by treating Fe-deficient roots with the NO scavenger 2-(4-carboxyphenyl)-4,4,5,5-tetramethylimidazoline-1-oxyl-3-oxide (cPTIO), the expression of *SIFRO1*, *SIIRT1* and the tomato homolog of *FIT* - *SIFER* - was inhibited (Graziano and Lamattina, 2007). The NO-induced response was dependent on the presence of FER, since *fer* plants were insensitive to NO supply, suggesting that NO acts upstream of FER to initiate molecular adaptations to Fe deficiency (Figure 3). However, it remains to be investigated whether NO is imported or synthesized in rhizodermal cells and what is the intracellular site of NO production under Fe deficiency.

Conversely to the up-regulation of acquisition mechanisms upon Fe starvation, an excess of Fe is caught up by an increased accumulation of the Fe storage protein ferritin (Lobreaux et al., 1995). More recently, a loss-of-function approach demonstrated that the major function of plant ferritins is not to store and release Fe, but to scavenge free reactive Fe, thereby preventing oxidative damage (Ravet et al., 2009). Again, NO acts as an upstream signal, since Fe supply to Arabidopsis cell cultures evoked a quick burst of NO in plastids and led to increased *Fer1* (*Ferritin1*) gene expression (Arnaud et al., 2006). The activation of *Fer1* further involved a 26S-proteasome-dependent degradation of a not yet identified repressor. Thus, NO appears as an upstream signal in two oppositely regulated pathways (Figure 3).

Another example of the diversity of signals evolved to regulate micronutrient responses has been shown for copper (Cu). Under Cu limitation the expression of genes coding for non-essential Cu-containing proteins is down-regulated in a process primarily regulated by micro-RNAs (Yamasaki et al., 2007; Abdel-Ghany

and Pilon, 2008; Pilon et al., 2009). However, when Cu reaches toxic levels it induces the formation of reactive oxygen species (ROS) as well as  $\text{Ca}^{2+}$  influx in roots (Yeh et al., 2007). In rice, these reactions evoke the activation of the MAP kinases OsMPK3 and OsMPK6 that are putatively involved in the signaling of high Cu.

Although some components of micronutrient signaling cascades have been elucidated, the mechanisms and sites of micronutrient sensing inside the plant cell are still unknown. In yeast, mitochondria have been recognized as those compartments in which Fe is sensed (Chen et al., 2004; Rutherford et al., 2005; Kumanovics et al., 2008). Yeast cells impaired in mitochondrial Fe–S cluster synthesis showed a constitutive up-regulation of the Fe regulon, even when Fe was sufficient (Chen et al., 2004). The two transcription factors Aft1 and Aft2, which are activators of Fe deficiency responses in yeast, responded downstream of a signal derived from the mitochondrial Fe–S cluster biosynthesis pathway, but not from cytosolic Fe (Rutherford et al., 2005; Kumanovics et al., 2008). That points to a role of mitochondrial Fe metabolism in the regulation of cellular Fe acquisition. In plants, plastids may be involved in micronutrient signaling in addition to mitochondria. The loss of PIC1, a membrane protein presumably involved in Fe transport across the inner envelope of chloroplasts, resulted in ferritin accumulation and increased Cu-dependent superoxide dismutase expression (Duy et al., 2007). These responses were accompanied by an induction of *IRT1* and indicated disturbed cellular Fe homeostasis (Duy et al., 2007). Interestingly, a transcriptional profiling of Fe deficiency responses in *Arabidopsis* revealed that cellular Fe homeostasis was highly dependent on the heme biosynthesis and Fe-S cluster assembly in the plastids (Yang et al., 2010). Thus, it would not be surprising if this organelle turns out as a Fe-sensing compartment in plant cells (Figure 3).

Micronutrient shortage may also result in morphological changes, especially in rhizodermal cells. Root hair formation and patterning are altered in response to Fe and manganese (Mn) deficiencies (Schmidt et al., 2000; Schikora and Schmidt, 2001; Müller and Schmidt, 2004; Konno et al., 2006; Yang et al., 2008). In response to both deficiencies, a large proportion of rhizodermal cells form



bifurcated tips. In the case of Fe, these morphological responses were hindered by ethylene and auxin antagonists as well as in mutants defective in ethylene and auxin signaling (Schmidt et al., 2000; Perry et al., 2007). Manganese deficiency changes the developmental programs of rhizodermal cells and, unlike Fe but similar to P, induces a re-differentiation of atrichoblasts into root hair-forming cells (Yang et al., 2008). Surprisingly, the expression of genes involved in epidermal cell fate specification, such as *CAPRICE* (*CPC*), was not affected by Mn deficiency. Instead, Mn deficiency was able to partially rescue the root hair-less phenotype of the *cpc* mutant, indicating that the Mn deficiency signal - similar to the P deficiency signal - is perceived downstream of the cell fate specification cascade. Altogether, these pieces of evidence suggest that Fe and Mn starvation signals are integrated at different stages in the postembryonic rhizodermal cell fate decision.

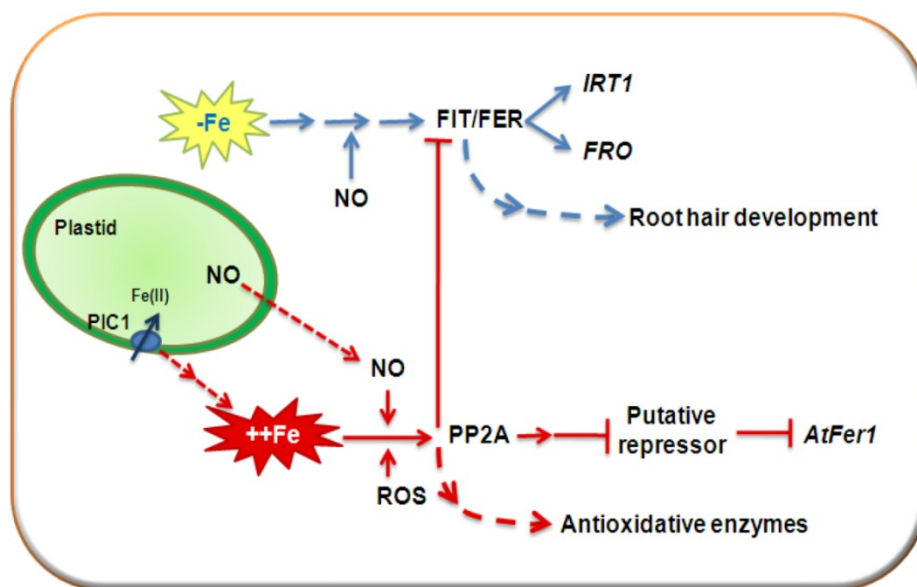


**Figure 3. Schematic representation of cellular signaling events involved in the modulation of physiological and morphological responses to Fe deficiency or excess in root cells.** Iron deficiency is sensed inside the cell via a still unknown mechanism and leads to a fast production (or import into the cell) of nitric oxide (NO). NO acts upstream of the Fe deficiency-regulated transcription factor FER (tomato) or FIT (*Arabidopsis*) (Graziano and Lamattina, 2007) that up-regulate the expression of Fe(II) transporter (*IRT1*) and ferric chelate reductase (*FRO2*) genes. The Fe starvation-induced formation of root hairs is also under control of FER/FIT, although the cell fate specification cascade is probably not involved in the process (Perry et al., 2007). Iron overload provokes a burst of NO in plastids, which represses the Fe uptake machinery upstream of FER/FIT. The NO burst upon Fe overload induces a PP2A-type phosphatase that promotes *Fer1* expression via a 26 S proteasome-dependent degradation of a yet unknown repressor that inhibits *Fer1* when Fe is limited (Arnaud et al., 2006). Since loss of PIC1, a putative Fe transporter in the chloroplast envelope, leads to up-regulation of *Fer1* (Duy et al., 2007), PIC1 might be involved in the signaling of Fe overload. The signaling cascades induced under Fe overload are marked in red, while those responding to Fe deficiency are marked in blue.

### 3.2.2 Systemic regulation of micronutrient homeostasis

Besides sensing the local availability of micronutrients, root cell adaptations underlie a regulation of remote signals from neighboring cells or tissues and from the shoot. For Fe, evidence for a long-distance signal coordinating the response of one part of the root system with the Fe nutritional status of another part has been provided by split-root experiments (Vert et al., 2003) and by characterizing mutants unable to down-regulate Fe deficiency responses in roots (Delhaize, 1996; Grusak and Pezeshgi, 1996; Ling et al., 1999). In fact, Fe deficiency responses were initiated even in Fe-replete root fractions if another part of the roots was exposed to Fe limitation (Vert et al., 2003).

Root-derived signals controlling shoot responses have been found for Cu, which generates ROS when supplied at high levels. Within 5 min, the supply of 100  $\mu$ M CuSO<sub>4</sub> to canola roots provoked an enhanced glutathione synthesis in leaves to counteract ROS formation, even though changes in Cu accumulation in leaves had not yet been observed (Russo et al., 2008). Thus, a root-derived signal might have pre-adapted the leaves to an upcoming stress even before the stressor had arrived. Biochemical assays indicated that phospholipase C and D are involved in generating this long-distance signal (Navari-Izzo et al., 2006; Russo et al., 2008).

Signals generated in one cell layer might also spread radially or longitudinally within the root, thus activating responses in adjacent cells or cell layers. Cell type-specific transcriptional profiles in Fe-starved *Arabidopsis* roots demonstrated that most genes are regulated in a longitudinal and radial zone-specific manner (Dinneny et al., 2008). There was a strong transcriptional response of stress-responsive genes in the stele, indicating that (i) Fe deficiency might be sensed in the innermost root tissue and (ii) a systemic signal might coordinate the activation of Fe deficiency-responsive gene sets. For this task, ethylene might represent a promising candidate spreading the Fe-deficiency information across the whole root, because its synthesis is enhanced in Fe-deficient roots (Romera et al., 1999; Li and Li, 2004; Wu et al., 2011) and ethylene is easily transported from inner to outer root cells due to its volatile nature. When Fe-deficient *Arabidopsis* plants were treated with ethylene inhibitors, the expression of many Fe deficiency-

regulated genes, such as *FIT*, *bHLH38*, *bHLH39*, *FRO2*, *IRT1*, *NAS1*, *NAS2* and *FRD3* was markedly repressed, whereas the same genes were induced by supplementation of ethylene or its immediate precursor, 1-aminocyclopropane-1-carboxylic acid (ACC; Lucena et al., 2006; Garcia et al., 2010). These observations support the view that Fe limitation is translated into an ethylene signal that, in turn, increases Fe acquisition via FIT-mediated transcriptional regulation (Figure 3). However, so far there are no evidences indicating that ethylene (or ACC) acts as a long-distance signal reporting the Fe status from the shoot. Thus, ethylene appears more as an intra-organ signal distributing the message of a Fe deficient status within the root.

In addition to ethylene, cytokinins (CKs) have also been demonstrated to modulate Fe uptake in roots. Besides being able to inhibit root growth (Dello Iorio et al., 2007), CKs repressed the transcription of Fe-regulated genes involved in Fe uptake, irrespective of the plant Fe status (Séguéla et al., 2008). This CK-mediated regulation functions independently of AtFIT, since the expression of *IRT1* and *FRO2* was repressed by CK analogs also in *fit1* plants. However, CK-mediated repression required the CK receptors CRE1/WOL/AHK4 and AHK3 (Séguéla et al., 2008). Taken together, these results indicate that CKs not only modulate root growth but also Fe acquisition independent of the plant Fe demand (Figure 4).

Evidence for the existence of a shoot-derived signal has been obtained from the study of the pea mutants *dgl* and *brz* that exhibit up-regulated Fe acquisition irrespective of external Fe supply (Grusak and Pezeshgi, 1996). The grafting of either *brz* or *dgl* mutant shoots onto wildtype roots resulted in higher ferric chelate reductase activity, suggesting that a shoot-borne signal regulates the activity of this root enzyme (Grusak and Pezeshgi, 1996; Figure 3). Likewise, the Arabidopsis *frd3* mutant is also unable to down-regulate Fe-deficiency responses in roots even under Fe-sufficient growth conditions (Delhaize, 1996; Yi and Guerinot, 1996; Rogers and Guerinot, 2002). This gene most likely encodes a xylem loader of the Fe(III) chelator citrate, so that leaves of the *frd3* mutant continuously suffer from Fe deficiency while Fe accumulates in the root tissue (Durrett et al., 2007). As the up-regulation of Fe acquisition genes in *frd3* roots

cannot be repressed by a root satiety signal, a systemic signal has been postulated that derives from the shoot and is perceived in roots upstream of FIT/FER (Lucena et al., 2006; Figure 4).

Since Fe concentrations in the phloem sap may correlate with those in leaves, phloem-derived Fe itself has been proposed to control root responses under variable Fe availability (Maas et al., 1988). Lacking synthesis of the aminocarboxylate-type Fe chelator nicotianamine (NA) resulted in constitutive Fe deficiency and led to the *chloronerva* phenotype in tomato, expressing in interveinal chlorosis in leaves, even though Fe accumulated at high levels in the shoot (Ling et al., 1999). Since NA forms a stable complex with Fe(II) at neutral and slightly alkaline pH (von Wirén et al., 1999) and putative Fe–NA transporters have been identified in the phloem tissue (Koike et al., 2004), it is tempting to speculate that NA-complexed Fe itself represents a phloem-mobile signal. Alternatively, Fe might travel through the phloem as a peptide-bound Fe complex as observed in the phloem sap of *Ricinus communis* (Krüger et al., 2002). However, whether these complexed Fe forms contribute to the systemic regulation of root responses awaits further investigation.

Although the nature of the long-distance signal for Fe homeostasis is unknown, the question of whether this signal is a positive or negative modulator of the micronutrient acquisition machinery has been addressed. Spraying Fe-deficient leaves of tobacco plants with Fe(II)-EDTA reduced the expression of *NtIRT1* and *NtFRO2* (Enomoto et al., 2007). Furthermore, the removal of leaves from Fe-deficient plants quickly and gradually repressed the expression of both genes, whereas there was no alteration when this procedure was undertaken with Fe-sufficient plants. In tomato, both *FER* expression and FER protein accumulation were down-regulated in Fe-sufficient wildtype roots but up-regulated in Fe-sufficient *chloronerva* roots (Brumbarova and Bauer, 2005). These observations suggest that the long-distance signal from the shoot acts as a positive modulator of Fe-deficiency responses in roots. More recently, split-root experiments with

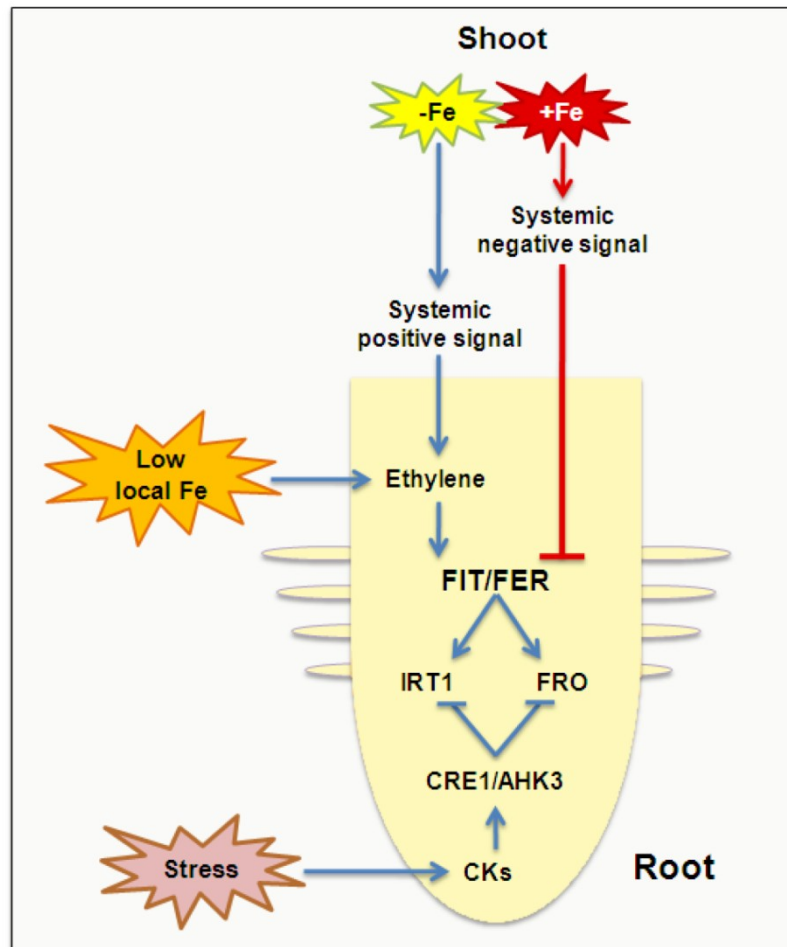


**Figure 4. Schematic representation of systemic signaling involved in the regulation of strategy I-type responses to Fe deficiency.** If the shoot demand for Fe increases, a signal is sent from the shoot to the root to activate the strategy I acquisition machinery via a signaling pathway involving ethylene and the bHLH transcription factors FIT/FER (Lucena et al., 2006). The same signaling cascade might be evoked in roots in response to low local Fe availability. In this model, ethylene might also mediate longitudinal and radial signaling in roots, thereby integrating Fe-deficiency signals at the whole-root level. Conversely, if the shoot is Fe sufficient, a yet unknown shoot-borne signal (possibly a chelated form of Fe delivered via the phloem) represses the expression of *FIT/FER* and, thus, of *IRT1* and *FRO* (Enomoto et al., 2007). Whenever the plant is challenged by growth-limiting stress conditions, cytokinins (CKs) repress root growth as well as the Fe uptake machinery in a pathway dependent on both CK receptors CRE1/WOL/AHK4 and AHK3, but independent of FIT/FER and the Fe nutritional status (Séguéla et al., 2008).

promoter-reporter plants in *Arabidopsis* showed that the expression of *BHLH100*, another basic helix–loop–helix transcription factor up-regulated under Fe deficiency, was independent of FIT and regulated by other local and systemic signals (Wang et al., 2007). Since FIT can physically interact with other BHLH transcription factors from the same subfamily (Yuan et al., 2008),

heterodimerization of these signal-transducing proteins might provide a level at which systemic and local signals are integrated into a coordinated response.

Also for zinc (Zn) evidence for the existence of a systemic Zn deficiency response has recently been provided. The heterologous expression of TgMTP1 from the Zn hyperaccumulator *Thlaspi goesingense* in *Arabidopsis thaliana* enhanced Zn accumulation in the shoot (Gustin et al., 2009). Since TgMTP1 localizes to the tonoplast, a TgMTP1-mediated sequestration of Zn into leaf vacuoles most likely accounted for the induction of Zn deficiency responses both in the shoot and the root. This would suggest that a long-distance signaling cascade communicating the shoot Zn status to the roots does also exist for Zn. However, the components of this cascade remain to be unveiled.

### 3.3 Objectives of the thesis

The characterization of molecular players involved in the uptake, translocation and allocation of nutrients in plants strongly indicates that most of these processes are under the control of signaling circuits reporting both the local availability of the nutrient and the nutritional status of the plant. In the present study, the main goals were to characterize regulatory mechanisms in root responses to nutrient supply and to identify novel regulatory components. Thus, two different approaches were chosen in order to fulfill this task. In the first, changes in root architecture in response to the local availability of Fe were studied as evidence for a local sensing mechanism. In this case, the main objective was to understand how the availability of a micronutrient is integrated into the program of lateral root development. Iron was chosen because a considerable amount of mutants affected in uptake and translocation are available, which could be used to test different hypotheses on how local Fe affects lateral root development. In the second approach, elemental profiling was used to screen for insertion lines affected in the expression of transcription factors and showing particularly high or low nutrient concentration. Since proteins with DNA-binding activity have been implicated in a multitude of signaling pathways, the goal here was to identify novel regulators of nutrient accumulation.

Chapter 4 provides a detailed investigation on root architectural changes induced by heterogeneous (or patchy) availability of Fe. Since Fe solubility in many soils is low and its diffusion extremely limited, it was expected that root architectural changes could facilitate Fe acquisition when Fe is only available in local patches. These changes were investigated in a series of *in vitro* experiments using different Fe- and hormone-related mutants, reporter lines and other molecular tools. In addition, a screening of insertion lines affected in the expression of DNA-binding proteins was undertaken, in order to identify novel components involved in the modulation of root development in response to a local availability of Fe.

In Chapter 5, an elemental profiling approach was used to identify novel regulators of the accumulation of nutrients and trace elements in plants. Elemental analysis of insertion lines represents an unbiased and relatively fast method to identify molecular components affecting the accumulation of nutrients in plants. However,

although insertion mutants with distinct concentrations of Fe were identified, these mutants did not show prominent phenotypical changes when grown under limited or toxic supplies of Fe. Instead, one insertion line, which showed a significantly altered accumulation of K and P, exhibited strong root architectural phenotypes when grown under limited P supply. In this insertion mutant, the expression of the B3-type transcription factor *NGAL1* is defective due to a *Ds*-transposon insertion. A series of physiological and molecular experiments were undertaken in order to investigate the role *NGAL1* in the modulation of root architectural changes in response to P starvation.

In the last part of this thesis (Chapter 6), a general discussion integrates the findings from this work into the current model of nutrient signaling in plants. Furthermore, this section highlights how nutrient availability is sensed and signaled in order to regulate developmental programs that shape the root architecture and, ultimately, affect nutrient accumulation and efficiency in plants.



## **4 Local supply of iron triggers lateral root elongation in *Arabidopsis thaliana* by altering auxin distribution**

### **4.1 Introduction**

Lateral root formation is a post-embryonic process (Dubrovsky et al., 2001) that starts with the priming of pericycle cells in the basal meristem of the parental root (De Smet et al., 2007). Upon activation by auxin, pericycle founder cells undergo a precisely coordinated sequence of divisions that gives rise to the lateral root primordium (Dubrovsky et al., 2001). Once established, the primordium can further develop and a lateral root can eventually emerge from the parental root. The plant hormone auxin appears as central in the regulation of many developmental steps required for lateral root formation (Casimiro et al., 2001; Wu et al., 2007). As a consequence of such a key role, many mutants defective in auxin transport and signaling show defects in lateral root development (Fukaki et al., 2002; Marchant et al., 2002; Geldner et al., 2004; Okushima et al., 2007). All developmental steps are genetically programmed and highly responsive to environmental cues. Among the most critical environmental factors, nutrient availability can profoundly shape root architecture (Lopez-Bucio et al., 2003; Hodge, 2006).

Mild N, S or P deficiency usually extend the root system and increase root-to-shoot ratios (Marschner, 1995; Lopez-Bucio et al., 2003), whereas a local supply of nitrate or Pi to otherwise N- or P-deficient plants stimulates lateral root development (Drew, 1975; Zhang et al., 1999; Linkohr et al., 2002). Furthermore, a localized supply of nitrate or Pi promotes lateral root elongation in *Arabidopsis*, whereas only local nitrate supply additionally increases lateral root density (Zhang et al., 1999; Linkohr et al., 2002). Thus, lateral root formation is affected by nutrients at different developmental stages (e.g. initiation versus elongation) and in a nutrient-specific manner. In the case of N, it has been shown that ammonium and nitrate have complementary effects on lateral root architecture, with ammonium mainly enhancing initiation and nitrate the elongation of lateral roots (Lima et al., 2010). With respect to nitrate, the dual-affinity nitrate transporter NRT1.1 triggers a specific nitrate signaling pathway that stimulates lateral root

growth in response to a localized supply of nitrate (Remans et al., 2006). Moreover, NRT1.1 turned out to facilitate auxin transport under non-repressive nitrate supplies, thus offering an example on how nutritional signals are integrated into the phytohormonal regulatory network (Krouk et al., 2010b). A role of auxin is also well established for P deficiency-induced lateral root formation which appears to rely on higher auxin sensitivity in pericycle cells mediated by the auxin receptor TIR1 (Perez-Torres et al., 2008). However, apart from N and P responses, relatively less is known on nutrient-dependent modulations of lateral root development and their interaction with hormonal signals.

As lateral root growth shortens diffusion pathways of nutrients in the soil solution to the root surface, it was hypothesized that profound changes in lateral root architecture should be expected for those nutrients that are sparingly soluble. In particular the solubility of the micronutrient Fe is very low in well-aerated and alkaline soils but may increase locally, as for example under reducing conditions in soil microsites (Marschner, 1995). With regard to the frequently occurring uneven distribution of organic matter and microbial activity but also of air- or water-conducting pores, Fe availability varies locally and changes in a gradual or patchy pattern within the root zone (Hinsinger et al., 2005). Reports on morphological changes of the root system to varying Fe availabilities mostly refer back to earlier work and describe exclusively adaptations to Fe deficiency (Römheld and Marschner, 1981; Landsberg, 1986). Iron deficiency also induces the ectopic formation of root hairs (Schmidt et al., 2000) by modulating the length, position and abundance of root hairs (Perry et al., 2007). Moreover, low Fe availability frequently leads to the formation of branched root hairs (Müller and Schmidt, 2004) through a signaling cascade probably involving auxin and ethylene (Schmidt et al., 2000; Schmidt and Schikora, 2001). In contrast to morphological responses, physiological adaptations to low Fe availabilities have been extensively described with a plasma membrane-localized  $H^+$ -ATPase, the membrane-bound ferric Fe(III) reductase FRO2 and the divalent metal cation transporter IRT1 being major components of a Fe deficiency-inducible strategy for enhanced Fe acquisition in Arabidopsis (Kim and Gueriot, 2007; Giehl et al., 2009). Both *IRT1* and *FRO2* are rapidly up-regulated under Fe starvation via the basic helix-loop-helix (bHLH) transcription factor FIT (Bauer et al., 2007). *FIT*, in turn, is also up-regulated in

response to Fe deficiency suggesting that the Fe sensing event acts upstream of this transcription factor (Colangelo and Guerinot, 2004; Jakoby et al., 2004). Resupply of Fe to Fe-starved plants induces *IRT1* and *FRO2* gene expression within 24 h showing that Fe acts in the short run as an inducer of both genes (Vert et al., 2003). When plants were grown in a split-root setup, the expression of *IRT1* and *FRO2* were enhanced in the Fe-supplied but not in the Fe-deficient root parts, indicating that these components of Fe acquisition were subject to both, a systemic and a local regulation (Vert et al., 2003). To date, the relation between these physiological and any morphological adaptations of the root system to varying Fe availabilities remained unaddressed.

Aiming at better understanding responses of the root system to varying Fe availabilities, in this study changes in lateral root architecture under homogenous or local Fe supply in wild-type and mutant plants defective in Fe acquisition or translocation are compared. Furthermore, the influence of the Fe nutritional status of the shoot in lateral root responses to Fe was investigated. The auxin transporter AUX1 was identified as a Fe-sensitive component in the auxin signaling pathway modulating lateral root development.

## 4.2 Materials and Methods

### 4.2.1 Plant material and growth conditions

The wild-type (*Arabidopsis thaliana*) ecotypes used in this study were Nossen-0 (No-0), Columbia-0 (Col-0) and Columbia-*glabrous1* (Col-*gl*). The following and previously described mutants and transgenic lines (in Col-0 background) were used: *aux1-T* (SALK\_020355C; Fischer et al., 2006), *tir1-T* (SALK\_151603C; Men et al., 2008); *pin2-T* (SALK\_122916C); *irt1* (Varotto et al., 2002); *fit-3* (Jakoby et al., 2004); *pro35S::FIT* (Jakoby et al., 2004); *proCYCB1;1::GUS* (Ferreira et al., 1994); *DR5::GUS* (Ulmasov et al., 1997); *proAUX1-AUX1:YFP* (Swarup et al., 2004); *axr1-3* (Lincoln et al., 1990); *frd3-1* (Rogers and Guerinot, 2002); and *nit1-3* (Normanly et al., 1997). Seeds were surface sterilized in 70% (v/v) ethanol and 0.05% (v/v) Triton X-100. The seeds were planted in sterile plates containing half-strength MS (Murashige and Skoog, 1962) medium without iron, supplemented

with 0.5% sucrose, 2.5 mM MES (pH 5.6) and 1% (w/v) Difco Agar (Becton Dickinson). The 7 day old seedlings were transferred to separated agar plates (SAP) containing agar medium as described above and Fe(III)-EDTA at indicated concentrations. Before agar segments were separated, the medium was supplemented with 75  $\mu$ M of ferrozine [3- (2-pyridyl)-5,6-diphenyl-1,2,4-triazine sulfonate] (Serva®) to render traces of Fe contaminants in the agar unavailable (Jain et al., 2009). Thus, all root responses recorded here were most likely initiated by lower concentrations of available Fe. Three seedlings per plate were transferred to segmented plates with the primary root touching the middle segment, oriented in a vertical position and cultured under a 22°C/19°C and 10/14 h light/dark regime at a light intensity 120  $\mu$ mol photons m<sup>-2</sup> s<sup>-1</sup>.

### 4.2.2 Root growth measurements

After 15 days of incubation on SAP, root systems were scanned by an Epson Expression 10000XL scanner (Seiko, Epson) at 300 dpi resolution. Traces in the background of the images were removed by Adobe Photoshop 5.0 version LE software. Root growth measurements were taken from scanned images using WhinRHIZO version Pro2007d software (Regents Instruments Canada Inc.). Lateral root primordia were counted using conventional light microscopy (Olympus BH, Germany). Developmental stages of lateral root initials were classified according to Malamy and Benfey (1997). All the experiments were performed at least twice and yielded similar results.

### 4.2.3 Histochemical analysis

For histochemical studies, seven-day-old *Arabidopsis proCYCB1::GUS* (*cycb1::uiad*) (Ferreira et al., 1994) or *DR5::GUS* (Ulmasov et al., 1997) lines germinated in ½ MS Fe-free media were transferred to segmented agar plates with the primary root apex touching the middle segment. Just before the primary root left the middle segment (3 days on treatment) and after it was growing for 3 days in contact with the third segment (3 days on treatments), root systems from the middle segment were excised and stained for GUS activity. For the staining,

root samples were incubated overnight at 37°C in a GUS reaction buffer containing 0.4 mg mL<sup>-1</sup> of 5-bromo-4-chloro-3-indolyl-β-D-glucuronide, 50 mM sodium phosphate, pH 7.2, and 0.5 mM ferrocyanide and 0.5 mM ferricyanide. After 12 h, roots were cleared and mounted as described by Malamy and Benfey (1997). For each treatment 30 to 40 roots were analyzed. Before plants were transferred to treatments, a GUS staining analysis on roots growing in the top segment revealed that  $1.00 \pm 0.01$  lateral roots were at the pre-emerged stage and  $1.43 \pm 0.53$  were already emerged.

### 4.2.4 Microscopy analyses

Lateral root meristem and epidermal cell lengths were measured on pictures of lateral roots from about 14 seedlings taken by a Zeiss microscope (Axiovert 200M, Jena, Germany) equipped with an AxioCam HR camera. Meristem length was assessed as the distance between the quiescent center and the first elongating cell and was measured with the AxioVision40 version 4.8.1.0 software (Zeiss, Germany). The same software was also used to determine the length of epidermal cells. YFP and GFP images were obtained with a confocal microscope LSM 510 META (Zeiss, Göttingen, Germany). Excitation light produced by an argon laser was adjusted to 488 nm and emission filters of 510 to 525 nm and 505 to 530 nm allowed the detection of GFP and YFP fluorescence signals, respectively. Image superimposition and fluorescence quantification were made by means of the Zeiss LSM 510 software version 3.0. The same microscope settings were used to record all confocal sections.

### 4.2.5 Mineral element and chlorophyll analyses

Shoots of agar-grown plants were briefly rinsed with double-distilled H<sub>2</sub>O and dried at 80°C. Samples consisting of approximately 30 shoots were digested with HNO<sub>3</sub> in polytetrafluoroethylene (PTFE) vials in a pressurized microwave digestion system (UltraCLAVE IV, MLS GmbH, Germany). Elemental analysis was performed by inductively coupled plasma mass spectrometry (ICP-MS, ELAN 6000, Perkin Elmer Sciex), equipped with a standard Scott-type spray chamber

and a cross-flow nebulizer. The internal standard rhodium ( $10 \text{ mg L}^{-1}$ ) was used to correct for the drift of the instrument. The certified reference material SRM 1575a ('pine needles'; National Institute of Standards and Technology/NIST) was used for quality control, and the recovery rate was  $>95\%$ . Chlorophyll concentrations were determined by incubating shoot samples with spectrophotometric grade *N,N'*-dimethyl formamide (Sigma-Aldrich, Germany) at  $4^\circ\text{C}$  for 48 h. The absorbance at 647 nm and 664 nm was then measured in extracts according to Porra et al. (1989).

#### 4.2.6 Screening of *Ds*-transposon insertion lines under localized Fe

Aiming at identifying regulatory components involved in the stimulation of lateral root growth in response to localized Fe, 302 transgenic lines harboring *Ds*-transposon insertion in genes encoding putative DNA-binding proteins (Kuromori et al., 2004; Ito et al., 2005) were screened. *Ds*-transposon and wildtype (accession No-0) seeds were germinated under Fe-deficient  $\frac{1}{2}$  MS medium (Murashige and Skoog, 1962). After seven days, seedlings were transferred to segmented agar plates containing half-strength MS salts, 0.5% sucrose,  $75 \mu\text{M}$  of ferrozine (Serva®) and  $25 \mu\text{M}$  of Fe supplied only in the middle segment (localized). Three replicates with three seedlings in each plate were used per *Ds*-transposon-tagged line. In addition, one replicate with  $25 \mu\text{M}$  Fe being supplied homogeneously over the three segments was used as a control. For the wildtype (No-0), multiple replicates were used. Plates were kept in a growth cabinet under the conditions described above (item 4.2.1). After 15 days, plates were scanned by an Epson Expression 10000XL scanner (Seiko, Epson) at 300 dpi resolution and the fresh weight of the whole root was recorded. Selected for further characterizations were those lines that showed significant reduction of lateral root growth specifically when grown under localized supply of  $25 \mu\text{M}$  Fe. These lines displayed also a reduced root fresh weight index (fresh root biomass under localized Fe divided by the biomass of the same line under homogeneous Fe).

#### 4.2.7 Expression analysis

For quantitative real-time PCR total RNA was extracted from root tissues using the Trizol RNA extraction kit (Invitrogen). RNA was quantified and treated with DNase I (Invitrogen). One microgram of total RNA was reverse transcribed into cDNA using oligo(dT)<sub>24</sub> primers and the SuperScriptII Reverse Transcriptase Kit (Invitrogen). Quantitative real-time PCR analysis was performed using an Eppendorf mastercycler realplex (Eppendorf, Germany) and QuantiTect SYBR Green qPCR Mix (Qiagen). Gene-specific primers were used for *IRT1* (*IRT1*-For, 5'-CGGTTGGACTTCTAAATGC-3'; *IRT1*-Rev, 5'-CGATAATCGACATTCCACCG-3'), *FIT* from Séguéla et al. (2008; *FIT*-For, 5'-GGAGAAGGTGTTGCTCCATCTC-3'; *FIT*-rev, 5'-GTCTCGAATTTGAACGGAT TGG-3'), *GATA3* (*GATA3*-For, 5'-GCCGGATGAAGATGTGGAA-3'; *GATA3*-Rev, CGAGACCGTTTGGTTCTGG-3'). Relative transcript abundance was calculated by the Mastercycler ep realplex software package version 2.0. In addition, for the semi-quantitative *GATA3* expression in *gata3* insertion mutants, the following primer pair was used (*gata3*-For 5'-CCTCTGTTTCTTCGCCATTC-3'; *gata3*-Rev 5'-TCACCTGTTTCTTCACC CAAC-3').

#### 4.2.8 Histochemical localization of ferric Fe

Iron(III) in roots of wild-type or *frd3-1* mutant plants was stained according to a Perl's staining protocol for Arabidopsis described by Stacey et al. (2008). Root segments from the middle segment were excised, rinsed three times with 10 mM EDTA followed by three rinses with ultra-pure water (18.2 Milli-Q cm<sup>-1</sup>). The samples were vacuum infiltrated with Perl's staining solution, composed of equal volumes of 4% (v/v) HCl and 4% (w/v) K-ferrocyanide and incubated for 15 min. Samples were left for another 15 min in the staining solution and rinsed three times with ultra-pure water. Stained samples were imaged using a stereo microscope (Zeiss, Stemi 2000-C, Germany) equipped with a CCD digital camera (Sony DXC-390P). Representative pictures of all tested conditions were taken using Adobe Photoshop 5.0 version LE.

#### 4.2.9 Ferric-chelate reductase activity

Wildtype (Col-0) and *aux1-T* plants were grown for 14 days under homogeneous or localized supply of 50  $\mu\text{M}$  Fe-EDTA. Root segments from the middle segment were then assayed for ferric reductase activity according to the protocol described by Waters et al. (2006). The activity was determined by placing the root segments in 2 mL buffer solution containing 0.2 mM  $\text{CaSO}_4$ , 5 mM MES (pH 5.5), and 0.2 mM ferrozine (Serva®). The reaction was initiated by adding Fe(III)-EDTA to a final concentration of 0.1 mM and allowed to continue for 30 min. The activity was determined by measuring the absorbance (562 nm) of the solution at the end of the reaction. Fresh weight of the root segments was recorded and the activity expressed as  $\mu\text{mol Fe(II) g}^{-1} \text{FW h}^{-1}$ .

### 4.3 Results

#### 4.3.1 Localized supply of iron stimulates lateral root development in *Arabidopsis*

To investigate changes in root architecture of *Arabidopsis thaliana* in response to Fe deficiency, wild-type plants (No-0) were grown on Fe-deficient  $\frac{1}{2}$  MS medium solidified with agar. Traces of Fe arising from inevitable Fe contamination by nutrient salts in the agar medium were inactivated by addition of the Fe(II)-chelator ferrozine (Serva®). When shoots of Fe-deficient plants turned chlorotic, primary root length was not affected (Figure 5A-C), whereas lateral root number and average lateral root length strongly decreased (Figure 5A, D-E). This observation suggested that especially lateral root architecture changes in dependence of the Fe nutritional status of the plant or external Fe availabilities.

Aiming at monitoring the lateral root response to local Fe availabilities, plants were grown on segmented agar plates (Zhang and Forde, 1998), to which increasing concentrations of Fe(III)-EDTA were supplied either to all three segments (homogenous supply) or only to the middle segment (localized supply). Under homogenous Fe supply, root and shoot growth and in particular lateral root



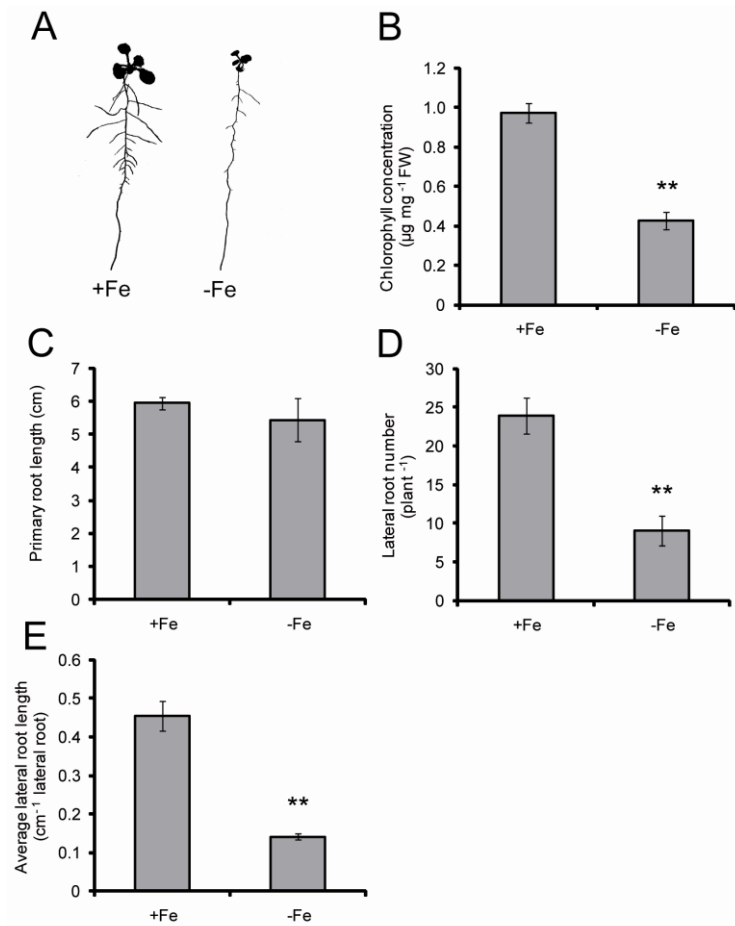


**Figure 5. Influence of Fe deficiency on root architectural changes in Arabidopsis plants.** Ten-day-old seedlings germinated on half-strength MS medium were transferred either to 75  $\mu\text{M}$  Fe (+Fe) or to 0  $\mu\text{M}$  Fe + 10  $\mu\text{M}$  of the Fe(II) chelator ferrozine (-Fe). After 10 days, (A) plants were scanned and (B) chlorophyll concentration in the shoots, (C) the length of the primary root, (D) the number of lateral roots, and (E) the average length of lateral roots were determined. Bars represent means  $\pm$  SD ( $n = 5$  replicates with five plants each). \*\* denotes significant difference according to Student's *t* test ( $P < 0.001$ ).

development in the upper, middle and lower root segment improved with increasing Fe concentrations up to 50  $\mu\text{M}$  with no considerable changes in phenotype beyond that concentration (Figure 6A, C-H), except at 500  $\mu\text{M}$  homogenous Fe supply when primary root length and the number of lateral roots in the bottom segment started to decline (Figure 6H, I). Relative to 10  $\mu\text{M}$  Fe, 25  $\mu\text{M}$  localized Fe supply enhanced mean lateral root length by 15-fold resulting in a twofold higher lateral root length than under homogenous supply (Figure 6B, E). With further increasing local Fe supply lateral root length decreased down to the level of plants grown under homogenous Fe supply (Figure 6E). Importantly, the

enhanced lateral root elongation in response to localized supply was restricted to the Fe-treated agar segment (Figure 6E), since such response was not observed in the upper or lower Fe-deficient segments (Figure 6C, G). Up to 25  $\mu\text{M}$  Fe supply, a steep increase was also observed for the number of lateral roots, but in contrast to lateral root length, lateral root number remained constant with further increasing Fe supply (Figure 6E, F). In addition, lateral root number did not differ significantly between the two modes of Fe supply (Figure 6F). Taken together, these data indicated that mean lateral root length responded more sensitively to changes in localized Fe supply than lateral root number.

Since differences exist among chelating agents in the affinity and specificity for Fe and other metals (Chaney, 1988; Norwell, 1991) the lateral root development was compared under the localized supply of 25  $\mu\text{M}$  Fe, either being chelated by ethylenediamine-tetraacetic acid (EDTA) or by N,N-di-(2-hydroxybenzoyl)-ethylenediamine-N,N-diacetic acid (HBED), two chelating agents with distinct affinities for Fe and other metal micronutrients (Chaney, 1988). Lateral root length and number as well as chlorophyll concentrations were not significantly different irrespective of which Fe(III) chelator was used (Figure 7). Therefore, changes in root architecture observed were not due to an indirect effect of the Fe(III)-chelating agent and/or interactions of the chelator with other micronutrients.

### **4.3.2 Influence of the mode of iron supply on the nutritional status of the shoot**

Either mode of Fe supply resulted in a maximum production of shoot fresh biomass at 25  $\mu\text{M}$ , but a homogenous supply of 500  $\mu\text{M}$  Fe repressed growth while a localized supply of the same Fe concentration did not (Figure 8A). Over the concentration range of 25 to 75  $\mu\text{M}$  Fe, root biomass production was significantly larger under localized relative to homogenous supply (Figure 8B). Since primary root length was not significantly affected in the same concentration range by the mode of Fe supply (Figure 6I), the enhanced root biomass production under localized Fe supply resulted almost exclusively from the growth of lateral roots (Figure 6E).

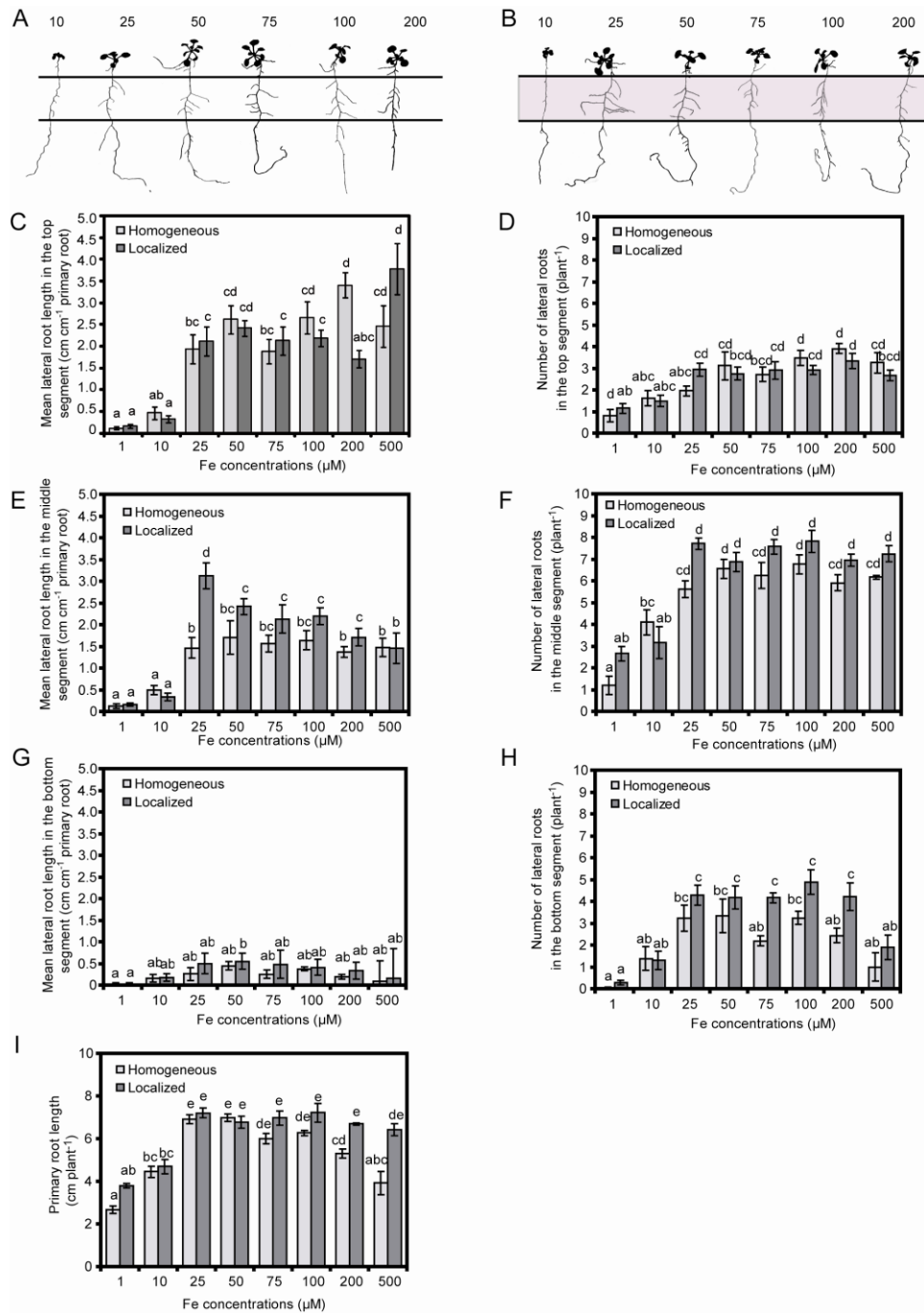


**Figure 6. Effect of homogeneous and localized Fe supplies on lateral root development of *Arabidopsis* plants.** (A,B) Root architecture of wildtype plants (accession No-0) in response to Fe supply. Seedlings were grown on half-strength MS medium without Fe for 7 days before transfer to segmented agar plates (SAP) containing half-strength MS and 75  $\mu\text{M}$  ferrozine. Fe(III)-EDTA was added at the indicated concentrations to all three segments (A; homogeneous supply) or only to the middle segment (B; localized supply). Plants were scanned after 15 days of growth on Fe treatments. Horizontal lines represent the borders between the three segments. The grey color in (B) indicates Fe being supplied only to the middle segment. Mean lateral root length in the (C) top, (E) middle and (G) bottom segment, and number of visible lateral roots ( $> 0.5$  mm) in the (D) top, (F) middle and (H) bottom segment. (I) Primary root length over all three compartments as determined by image analysis. Bars indicate means  $\pm$  SE,  $n = 8$  plates each containing 3 plants. Different letters indicate significant differences among means ( $P < 0.05$  by Tukey's test).

To address the question of whether homogenous Fe supply confers an advantage to plants growing under low Fe availabilities, chlorophyll concentrations were determined as a measure of the Fe nutritional status of the shoot (Morales et al., 1990). Chlorophyll levels reached maximum values at 25  $\mu$ M Fe under either mode of Fe supply (Figure 8C) indicating that an enhanced elongation of lateral roots into the Fe-containing patch enabled the plants to meet the Fe demand of their shoots if Fe supply is spatially restricted. Moreover, the mode of Fe delivery did not significantly affect the shoot concentrations of Fe or other nutrients, since element concentrations that were altered with increasing Fe supply showed similar changes under homogenous and localized Fe supply (Table 1). As an exception to that, more Zn accumulated under elevated levels of localized relative to homogenous Fe supply. This elevation might be indicative for the involvement of IRT1 or further Fe-regulated metal transporters with poor substrate specificity (Korshunova et al., 1999; Vert et al., 2002) in the uptake of Zn from Fe-deficient

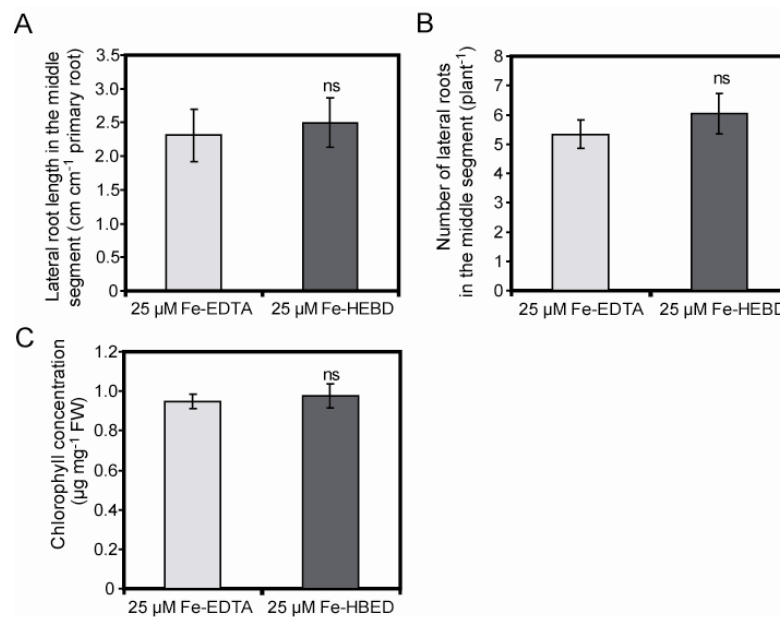


**Figure 7. Effect of Fe(III)-chelating agents on lateral root development in response to localized Fe supply.** (A) Number and (B) mean lateral root length and (C) chlorophyll concentrations in shoots of wildtype plants (No-0) that were supplied with 25  $\mu$ M Fe(III) chelated with either ethylenediamine-tetraacetic acid (EDTA) or by N,N-di-(2-hydroxybenzoyl)-ethylenediamine-N,N-diacetic acid (HBED) in the middle agar segment. Bars indicate means  $\pm$  SE,  $n = 7-8$  plates with 3 plants. *ns* denotes no significant difference according to Student's *t*-test ( $P < 0.05$ ).

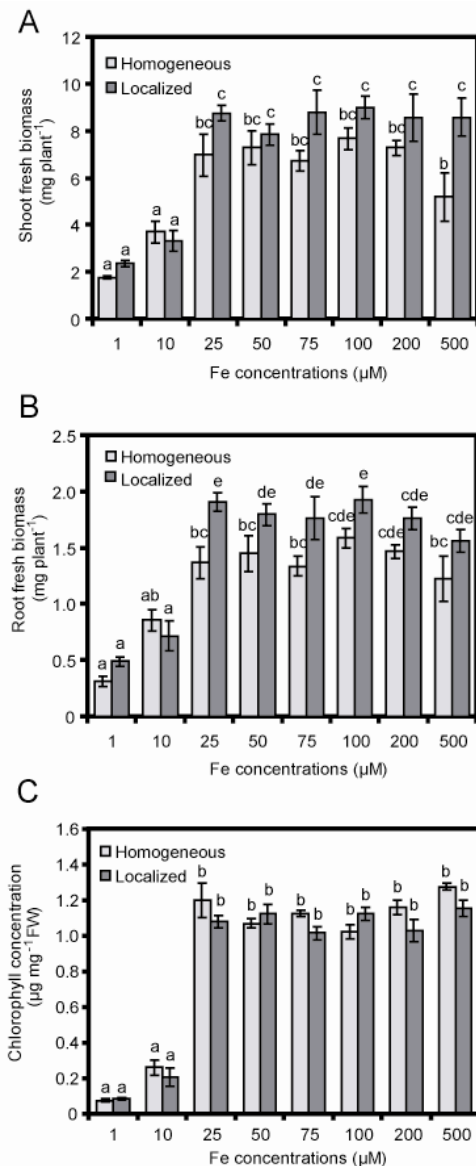


**Figure 8. Effect of the mode of Fe supply on the growth of *Arabidopsis* seedlings.** Fresh weight of (A) shoots or (B) roots, and (C) chlorophyll concentrations in shoots of seedlings grown for 15 days either on homogeneous or localized supply of different concentrations of Fe. Bars represent means  $\pm$  SE,  $n = 4$  replicates with 30 shoots each in replicate. Different letters indicate significant differences among means ( $P < 0.05$  by Tukey's test).

root segments. Thus, the shoot nutrient profile indicated that the morphological changes observed in the roots were not due to an undesirable effect of the mode of Fe supply on the accumulation of other essential macro- or microelements.

To verify the importance of lateral development on Fe acquisition under local supply, growth of the *arf7arf19* double mutant, which is severely impaired in lateral development (Okushima et al., 2007), was tested in SAP. Its corresponding wildtype Col-0 required a localized supply of 50 µM Fe for maximum lateral root elongation (data not shown), then leading to healthy growth with green leaves (Figure 9). Under the same conditions, young leaves of *arf7arf19* plants became chlorotic, indicative for an inadequate Fe nutritional status (Figure 9). Leaf

chlorosis was not observed in *arf7arf19* plants grown under homogeneous supply of 50  $\mu\text{M}$  Fe. This observation supported the view that the ability of roots to laterally explore Fe-enriched nutrient patches can be crucial to adequately cover the Fe demand of the shoot.

#### 4.3.3 Influence of FIT and IRT1 on lateral root development under localized iron supply

In Arabidopsis, many of the physiological Fe stress responses in roots are controlled by the transcription factor FIT (Colangelo and Guerinot, 2004; Jakoby et al., 2004). Interestingly, the tomato ortholog of FIT, SIFER, has been shown to additionally affect root hair formation (Ling et al., 2002). Thus the involvement of this Fe-regulated transcription factor in root architectural changes in response to localized Fe supply was assessed. In *fit* mutant plants the number of lateral roots was significantly lower than in wild-type plants at concentrations up to 50  $\mu\text{M}$  of localized Fe supply and achieved a similar number only at 200  $\mu\text{M}$  Fe, while lateral root length in *fit* plants was significantly reduced over the whole range of locally

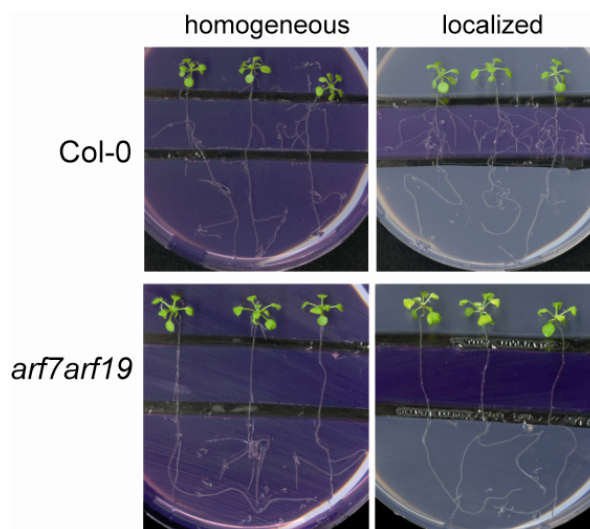


**Figure 9. Defective lateral root development in the double *arf7arf19* mutant results in leaf chlorosis under localized supply of Fe.** *arf7arf19* mutant seeds were germinated on Fe-free, half-strength MS medium for 7 days. Seedlings were then transferred to segmented agar plates supplied with 75  $\mu\text{M}$  ferrozine and with 50  $\mu\text{M}$  Fe-EDTA in all three segments or only in the middle segment. Pictures were taken after 15 days on treatment and representative plants are shown ( $n = 6$  replicates).

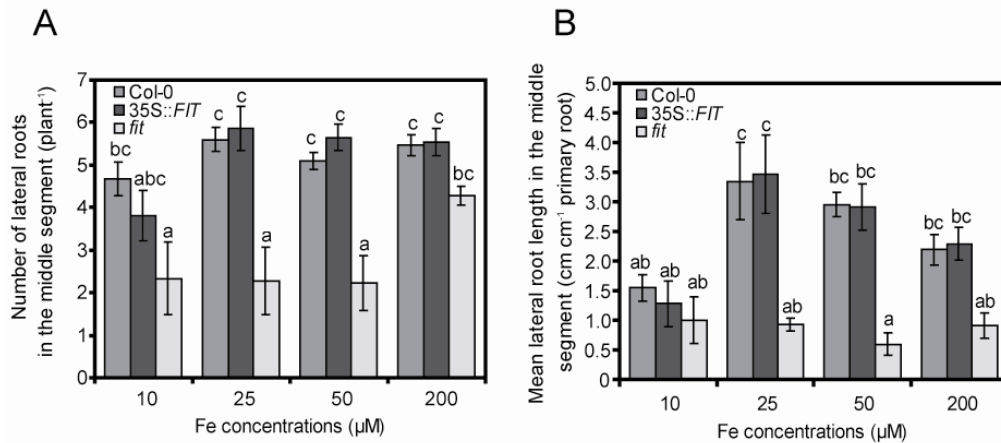


**Figure 10. Lateral root development in response to localized Fe supply in transgenic plants with deregulated expression of *FIT*.** (A) Number and (B) mean lateral root length in wildtype (Col-0), 35S::*FIT* and *fit* mutant plants as affected by the Fe concentration supplied to the middle segment. Seeds were germinated on Fe-free, half-strength MS medium for 7 days. Then, seedlings were transferred to segmented agar plates supplied with Fe in the middle segment at the indicated concentrations. After 15 days, the number of visible lateral roots (> 0.5 mm) and mean lateral root length in the middle segment was determined by image analysis. Bars indicate means  $\pm$  SE,  $n = 7$ -12 plates with 3 plants per plate. Different letters indicate significant differences among means ( $P < 0.05$  by Tukey's test).

supplied Fe concentrations (Figure 10). To investigate whether *FIT* overexpression can provoke an altered morphological response, 35S::*FIT* lines were tested for lateral root formation under local Fe supply. However, the constitutive expression of *FIT* did not significantly affect root architecture, since 35S::*FIT* lines generated a similar number and length of lateral roots as wild-type plants (Figure 10).

As *fit* plants suffer from impaired Fe uptake due to lower *IRT1* and *FRO2* expression (Colangelo and Gueriot, 2004), the failure of *fit* plants to increase lateral root length may reflect a role for *IRT1*/*FRO2*-dependent Fe acquisition in increasing lateral root length under localized Fe supply. Thus, it was investigated whether the Fe transporter *IRT1* was involved in the differential regulation of number and length of lateral roots under localized Fe supply. Whereas wild-type plants achieved their maximum number of lateral roots at 50 μM Fe, *irt1* plants developed very few lateral roots below 200 μM Fe supply and achieved a similar number as wild-type plants only when 600 μM Fe were added to the middle segment (Figure 11A). In contrast, lateral root length in *irt1* mutant plants could not be restored, even if Fe concentrations as high as 600 μM were supplied (Figure 11B). As a consequence, *irt1* shoots were chlorotic with chlorophyll concentrations

Table 1. Concentration of nutrients in shoots of Arabidopsis (accession No-0) plants grown for 15 days under different concentrations of Fe, supplied either homogeneously across all three segments (homogeneous) or only in the middle segment (localized). Shown are means and  $\pm$ S.E. ( $n = 4$  replicates of 30 shoots). Different letters indicate significant differences among means ( $P < 0.05$  by Tukey's test). Concentrations of S, P, K, and Ca are given in  $\text{mg g}^{-1}$ ; while the concentrations of Mg, Fe, B, Mn, and Zn are in  $\mu\text{g g}^{-1}$ .

Fe concentrations ( $\mu\text{M}$ )	S	P	K	Ca	Mg	Fe	B	Mn	Zn
Homogeneous supply									
10	15.50 $\pm$ 1.0 b	11.71 $\pm$ 1.5 ab	55.37 $\pm$ 1.1 a	4.68 $\pm$ 0.7 ab	2.19 $\pm$ 0.34 b	137 $\pm$ 24 ab	219 $\pm$ 27 b	198 $\pm$ 48 abc	708 $\pm$ 13 d
25	10.61 $\pm$ 0.5 ab	13.17 $\pm$ 0.4 b	52.88 $\pm$ 0.8 a	4.95 $\pm$ 0.1 ab	1.96 $\pm$ 0.02 ab	188 $\pm$ 20 ab	114 $\pm$ 7 a	221 $\pm$ 15 bc	400 $\pm$ 15 c
50	9.77 $\pm$ 0.6 ab	14.06 $\pm$ 0.8 b	54.64 $\pm$ 1.4 a	5.07 $\pm$ 0.1 b	1.87 $\pm$ 0.03 ab	151 $\pm$ 11 ab	109 $\pm$ 12 a	176 $\pm$ 6 abc	233 $\pm$ 30 b
200	8.63 $\pm$ 0.1 a	12.15 $\pm$ 1.6 ab	55.56 $\pm$ 1.1 a	3.96 $\pm$ 0.2 a	1.66 $\pm$ 0.06 a	235 $\pm$ 9 b	122 $\pm$ 14 a	138 $\pm$ 4 a	110 $\pm$ 20 a
Localized supply									
10	15.51 $\pm$ 1.7 c	10.38 $\pm$ 1.0 a	56.04 $\pm$ 3.7 a	4.95 $\pm$ 0.8 ab	2.20 $\pm$ 0.24 b	102 $\pm$ 13 a	195 $\pm$ 30 b	223 $\pm$ 71 bc	704 $\pm$ 79 d
25	11.34 $\pm$ 1.1 b	11.81 $\pm$ 0.4 ab	53.31 $\pm$ 1.9 a	4.95 $\pm$ 0.2 ab	2.08 $\pm$ 0.14 b	167 $\pm$ 26 ab	119 $\pm$ 15 a	248 $\pm$ 45 c	463 $\pm$ 93 c
50	10.15 $\pm$ 0.6 ab	12.69 $\pm$ 0.6 ab	53.37 $\pm$ 1.5 a	4.68 $\pm$ 0.6 ab	1.85 $\pm$ 0.11 ab	189 $\pm$ 38 ab	119 $\pm$ 22 a	167 $\pm$ 9 ab	330 $\pm$ 32 bc
200	9.86 $\pm$ 0.2 ab	12.19 $\pm$ 0.4 ab	51.86 $\pm$ 0.9 a	4.56 $\pm$ 0.4 ab	1.85 $\pm$ 0.05 ab	181 $\pm$ 16 ab	112 $\pm$ 16 a	142 $\pm$ 8 ab	294 $\pm$ 17 b



remaining far below wildtype levels (Figure 11C) supporting the requirement for IRT1 in the lateral root response to local Fe availabilities.

#### 4.3.4 Influence of shoot-derived Fe signals on lateral root development

Then, the question was addressed whether shoot Fe is able to influence lateral root development. To test this assumption, *irt1* and wild-type plants were grown under localized Fe supply with a fourth separated agar segment harboring the shoot and being supplemented with 100  $\mu\text{M}$  Fe(III)-citrate. In fact, shoot application of Fe(III)-citrate efficiently alleviated chlorosis and improved growth in wild-type and *irt1* plants (Figure 12A, B). While shoot Fe supply just slightly enhanced lateral root number and length in the wildtype, it completely restored lateral root development to wild-type levels in *irt1* (Figure 12C). Shoot Fe supply

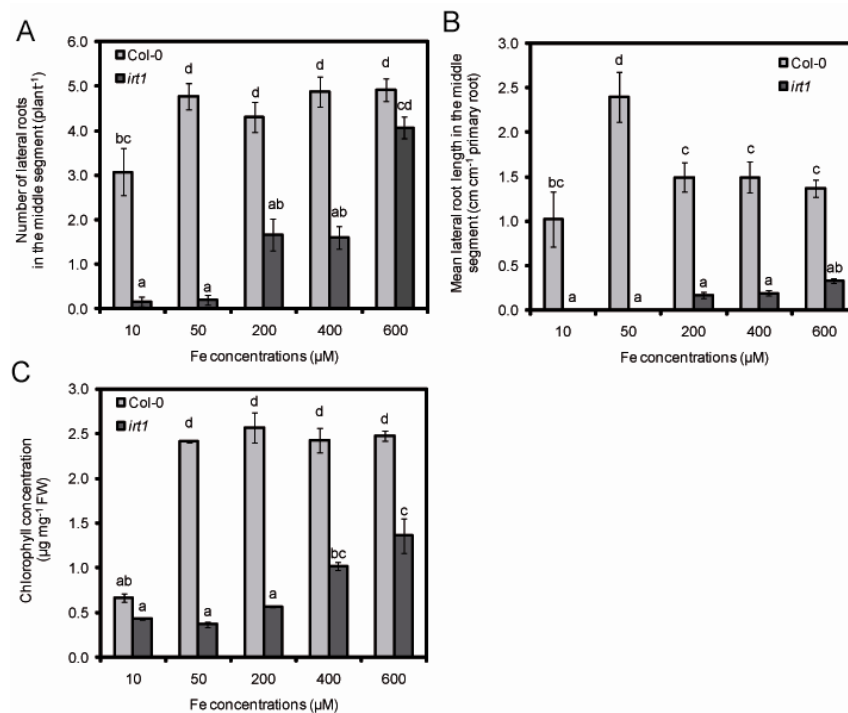


**Figure 11. Lateral root development in wildtype and *irt1* plants in response to localized Fe supply.** (A) Number and (B) mean length of lateral roots in wildtype (Col-0) and *irt1* mutant plants as affected by the Fe concentration supplied to the middle segment. Col-0 and *irt1* seeds were germinated on Fe-free, half-strength MS medium for 7 days. Seedlings were then transferred to segmented agar plates supplied with Fe in the middle segment at the indicated concentrations. After 15 days the number and mean length of visible lateral roots ( $> 0.5$  mm) in the middle segment were determined by image analysis. (C) Shoot chlorophyll concentrations were determined after 15 days of growth. Bars represent means  $\pm$  SE,  $n = 7$  replicates consisting of 3 plants. Different letters indicate significant differences among means ( $P < 0.05$  by Tukey's test).

now allowed *irt1* plants to respond to further increasing Fe concentrations to the middle root segment in the same manner as wild-type plants (Figure 12D). Hence, Fe supply to the shoots could completely restore lateral root formation under local Fe deficiency and thus circumvent IRT1-dependent Fe uptake by roots.

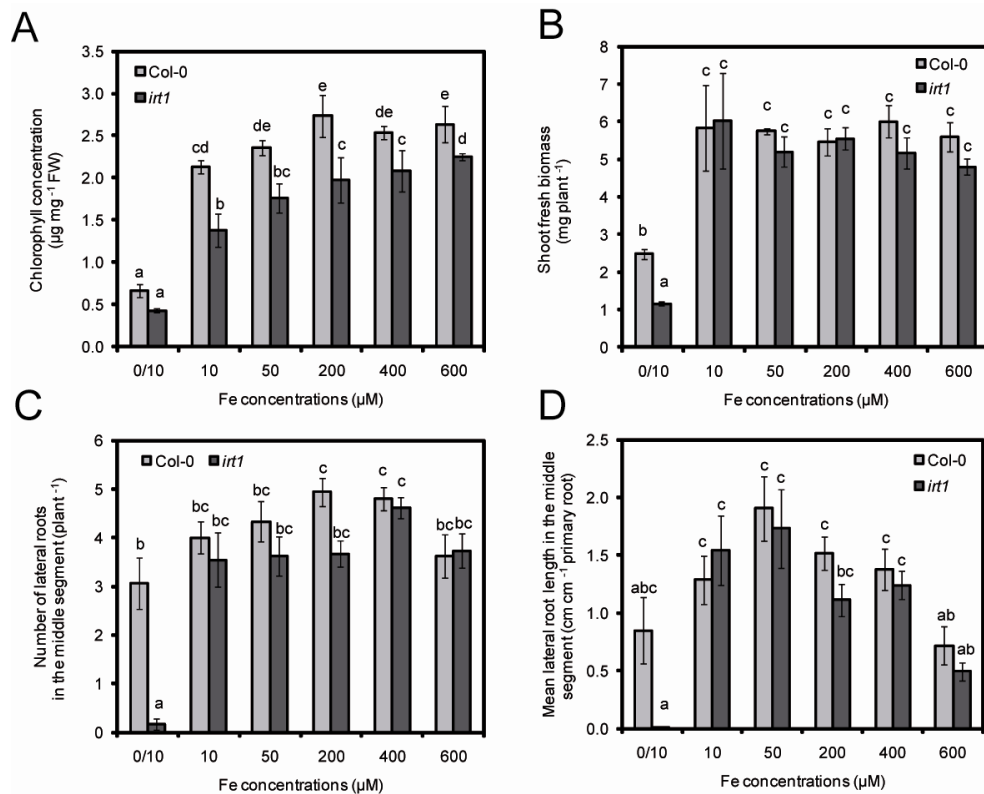


**Figure 12. Effect of shoot Fe supply on the development of lateral roots in wildtype (Col-0) and *irt1* on a tetrapartite agar plate.** (A) Chlorophyll concentrations, (B) shoot biomass, (C) Number and (D) mean length of lateral roots, of wildtype (Col-0) and *irt1* plants after growth for 14 days under increasing concentrations of Fe-EDTA in the middle agar segment. The shoot compartment was either supplied with 100 μM citrate at 10 μM local Fe supply (0/10) or with 100 μM Fe(III)-citrate at 10-600 μM local Fe supply. Bars indicate means ± SE, n = 6-7 plates with 3 plants each. Different letters indicate significant differences among means ( $P < 0.05$  by Tukey's test).

Lateral root elongation was then monitored in all three root compartments to further specify the influence of shoot-derived Fe. In fact, Fe supply to the shoots enhanced more significantly mean lateral root length in the upper Fe-free segment than in the middle segment (Figure 13A, B). Moreover, when shoots obtained Fe-citrate, Perl's staining of root Fe(III) was stronger than in roots without shoot Fe supply. These observations were indicative for basipetal Fe translocation from the shoots (Figure 13D). However, Fe application to shoots could not stimulate lateral

root elongation in the bottom root segment (Figure 13C). Even though the involvement of a shoot-derived systemic signal cannot be excluded, these results indicate that lateral root elongation is subject to a local control by the Fe concentration of the root tissue rather than to externally supplied Fe by itself.

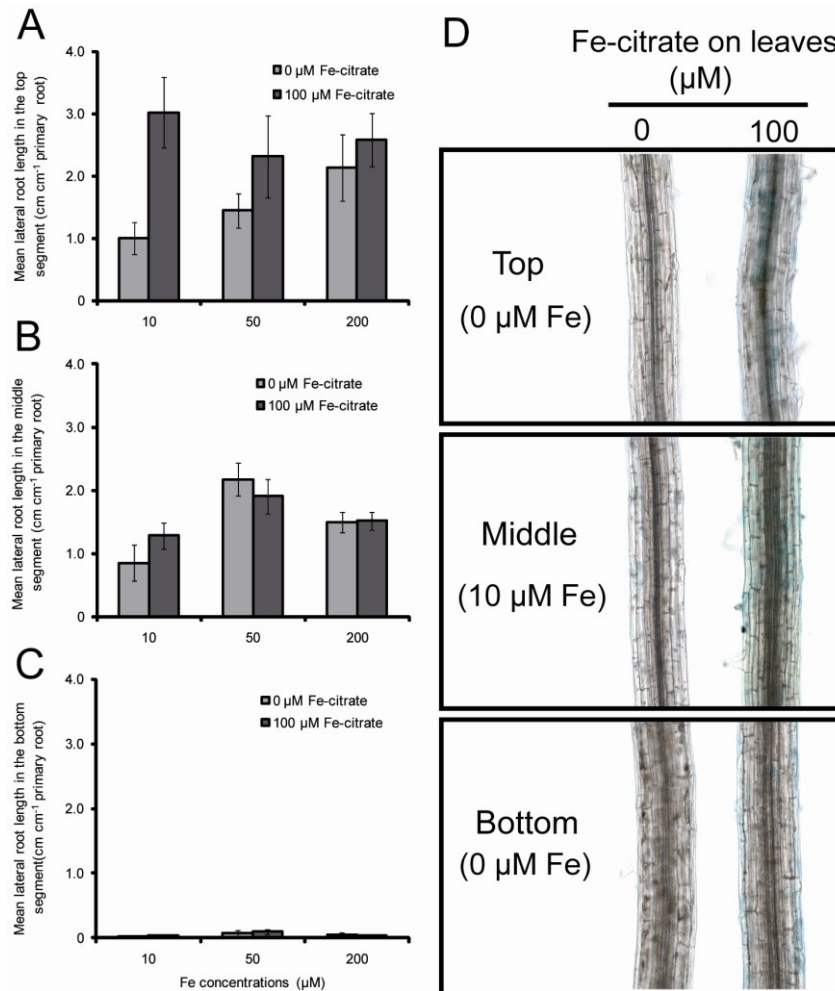


**Figure 13. Effect of shoot Fe supply on the development of lateral roots in wild-type plants.** (A-C) Mean lateral root length in the (A) top, (B) middle or (C) bottom segment of wildtype (Col-0) plants supplied with increasing concentrations of Fe-EDTA in the middle agar segment. The shoot compartment was either supplied with 100 μM citrate or 100 μM Fe(III)-citrate. Bars indicate means  $\pm$  SE, n = 6-7 plates with 3 plants each. (D) Histochemical localization of Fe(III) in plant roots locally supplied with 10 μM Fe-EDTA. The shoot compartment was either supplied with 100 μM citrate or 100 μM Fe(III)-citrate. Shown are representative root segments from the top, middle and bottom plate segments.

To address the possible involvement of a shoot-derived signal in lateral root development by an independent approach, the *ferric reductase defective3* (*frd3-1*) mutant and its allelic mutant *manganese accumulator1* (*man1*; also known as *frd3-3*) were used. Both mutants show a constitutive up-regulation of the Fe acquisition

machinery in roots despite accumulating more Fe in the root than wild-type plants, which also held true under the growth conditions used in this study (Figure 14; Delhaize, 1996; Rogers and Guerinot, 2002; Green and Rogers, 2004).

Lateral root development in wildtype and *frd3-1* plants was similar at any tested concentration of localized Fe supply. Only at 1  $\mu\text{M}$  Fe supply *frd3-1* mutant plants developed approximately two lateral roots more in their Fe-treated root segments than the corresponding wildtype (Figure 15A), while lateral root length followed the same concentration-dependent pattern in both lines (Figure 15B). Thus, the differential response between number and length of lateral roots, as it was observed in wildtype plants, remained conserved despite the loss of FRD3. A similar growth response was observed in *man1* (*frd3-3*) mutant plants (data not shown). These observations gained importance with respect to the chlorophyll levels which reflected a significantly lower Fe nutritional status in the *frd3-1* mutant than in wildtype plants at  $> 10 \mu\text{M}$  Fe supply (Figure 15C).

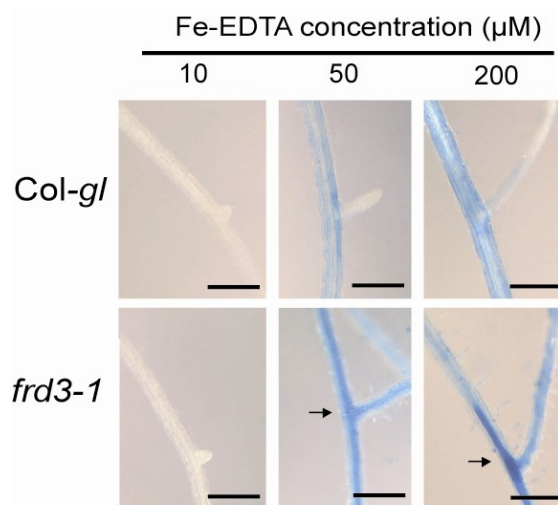


**Figure 14. Histochemical localization of Fe(III) in wildtype and *frd3-1* roots.** Roots of wildtype and *frd3-1* plants, grown on localized supply of 10, 50 or 200  $\mu\text{M}$  Fe-EDTA during 7 days, were washed with EDTA and ultra-pure water and subsequently vacuum infiltrated with Perl's stain solution for 15 min. Shown are representative plants for each genotype and treatment ( $n=10$  plants each). Scale bars = 150  $\mu\text{m}$ . Arrows indicate Fe(III) localization close to the vasculature in *frd3-1* roots supplied with 50 or 200  $\mu\text{M}$  Fe-EDTA.

Considering that Fe-deficient plants have been proposed to release a shoot signal responsible for the up-regulation of Fe acquisition mechanisms in roots (Grusak and Pezeshgi, 1996; Vert et al., 2003), a lacking repression of lateral root length at  $\geq 25 \mu\text{M}$  Fe was expected in *frd3-1* mutants. However, regarding the unaffected lateral root response in chlorotic *frd3-1* mutant plants (Figure 15A, B), evidence for the involvement of a shoot-borne signal was not obtained. These results indicated that Fe-dependent lateral root elongation was independent of a FRD3-mediated regulation by the Fe nutritional status of the shoot.

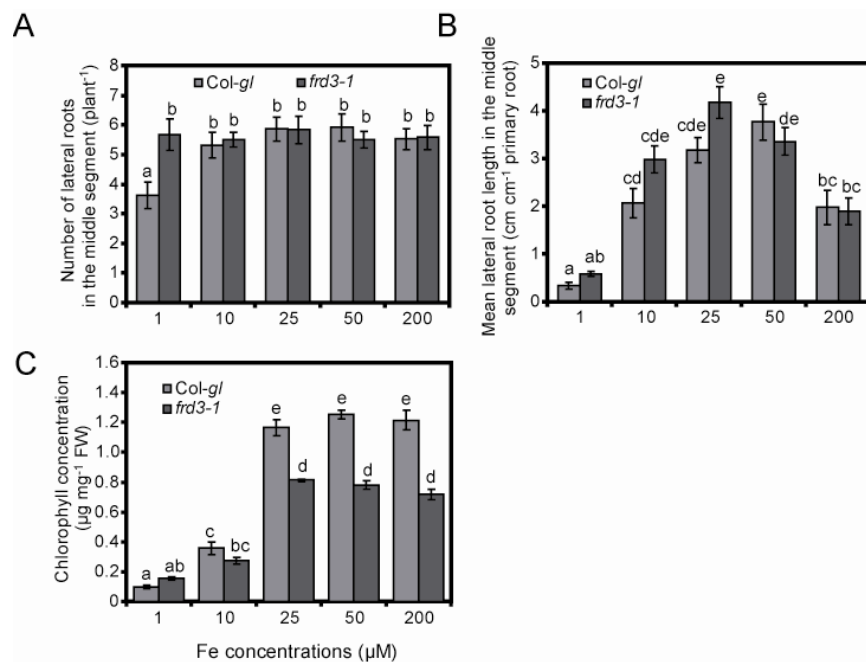


**Figure 15. Lateral root development in wildtype and *frd3-1* plants.** (A) Lateral root number, (B) lateral root length and (C) chlorophyll concentration in the shoots of wildtype (*Col-gl*) and *frd3-1* mutant plants. Seeds were germinated on Fe-deficient, half-strength MS medium for 7 days before transfer to segmented agar plates locally supplied with Fe(III)-EDTA only to the middle segment. Plant roots were scanned and the chlorophyll concentration determined after 15 days on Fe treatments. Bars represent means  $\pm$  SE,  $n = 7$ -12 plates with 3 seedlings per plate. Different letters indicate significant differences among means ( $P < 0.05$  by Tukey's test).

#### 4.3.5 Effect of localized Fe supply on the development of lateral roots

As localized Fe affected primarily the elongation of lateral roots (Figure 6), it was assessed how lateral root primordia progressed during their development using transgenic *proCYCB1;1::GUS* reporter lines (Ferreira et al., 1994), which allow tracking lateral root primordia before their emergence. The primary root tip of Fe-deficient *proCYCB1;1::GUS* seedlings was exposed to localized Fe supply and the

developmental stages of pre-emerged lateral root initials after 3 and 6 days were determined according to the classification described by Malamy and Benfey (1997).

Although the total number of lateral root initials was only slightly enhanced by the local supply of 50 and 200  $\mu\text{M}$  Fe, the proportion of emerged lateral roots was markedly increased by these treatments after 6 days (Table 2). In fact, the rate of emergence of initiated lateral roots was increased by 56% or 40% by a localized Fe supply of 50 or 200  $\mu\text{M}$ , respectively. Conversely, at 10  $\mu\text{M}$  Fe supply, i.e. non-promoting conditions for lateral root development, homogenous Fe supply was more favorable for lateral root emergence than localized supply (Table 2). Taken together, these results suggest that the local presence of Fe has a lower impact on the priming and initiation of lateral root development, but rather stimulates the emergence and subsequent elongation of already initiated lateral root primordia.

The growth of primary and lateral roots is determined mainly by cell division in the mitotically active meristem and the differentiation and elongation of the cells that leave the meristem (Scheres et al., 2002). In order to assess cell division activity within the meristems of lateral roots, the expression of *proCYCB1;1::GUS* was observed and found not to be significantly affected by the mode of Fe application, although the supply of low (10  $\mu\text{M}$ ) or high (200  $\mu\text{M}$ ) concentrations of Fe

**Table 2.** Number of pre-emerged and emerged lateral root initials in response to the homogeneous or localized availability of Fe-EDTA. Lateral root initials of *proCYCB1;1::GUS* plants were counted and classified according to Malamy and Benfey (1997) after 6 days on Fe treatments. Values represent means  $\pm$  SE,  $n = 15$ -20 seedlings. The rate of lateral root emergence (emerged lateral roots per day) was obtained by calculating the number of emerged lateral roots formed between 3 and 6 days after transfer to treatments.

Fe concentrations ( $\mu\text{M}$ )	Pre-emerged	Emerged	Total	Rate of emergence
Homogenous				
10	1.0 $\pm$ 0.44	5.4 $\pm$ 0.81	6.4 $\pm$ 0.41	<b>1.24</b>
50	2.5 $\pm$ 0.42	3.6 $\pm$ 0.24	6.1 $\pm$ 0.38	<b>1.03</b>
200	2.8 $\pm$ 0.21	4.8 $\pm$ 0.20	7.6 $\pm$ 0.25	<b>1.27</b>
Localized				
10	3.0 $\pm$ 0.41	2.5 $\pm$ 0.87	5.5 $\pm$ 0.40	<b>0.72</b>
50	1.7 $\pm$ 0.33	5.5 $\pm$ 0.67	7.2 $\pm$ 0.48	<b>1.61</b>
200	1.8 $\pm$ 0.54	6.3 $\pm$ 0.42	8.1 $\pm$ 0.50	<b>1.78</b>

appeared to show a slightly reduced overall cell cycle activity when compared to 50  $\mu\text{M}$  (Figure 16A). As an alternative approach to verify the effect of Fe on cell differentiation, meristem length was measured. Again, no marked difference could be observed, suggesting that neither the mode of Fe supply nor a difference in the Fe concentration affected cell differentiation (Figure 16B). However, when epidermal cell length was determined, it was observed that the localized supply of 50  $\mu\text{M}$  Fe significantly increased the length of rhizodermal cells (Figure 16A, C). No such effect was observed for the other two Fe concentrations tested or for 50  $\mu\text{M}$  of homogenous Fe supply (Figure 16A, C). Thus, rather than affecting the meristem activity of lateral roots, the localized supply of Fe promotes the elongation of lateral root cells leaving the meristem.

A Fe concentrations in the middle segment ( $\mu\text{M}$ )

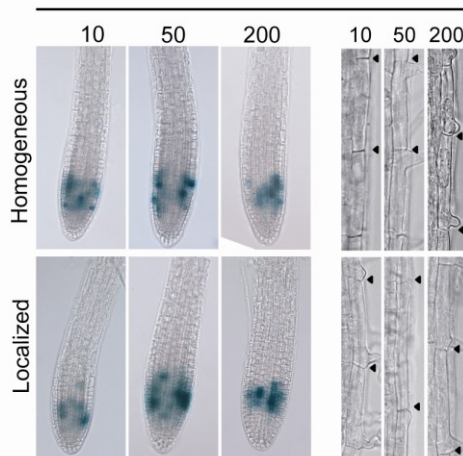
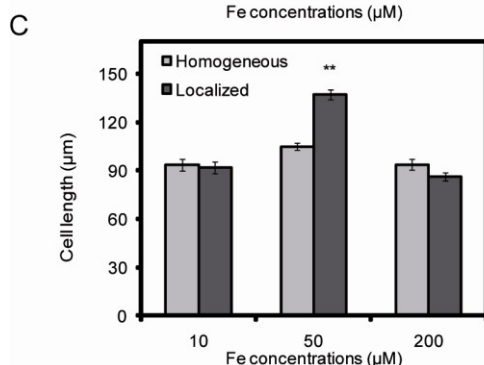
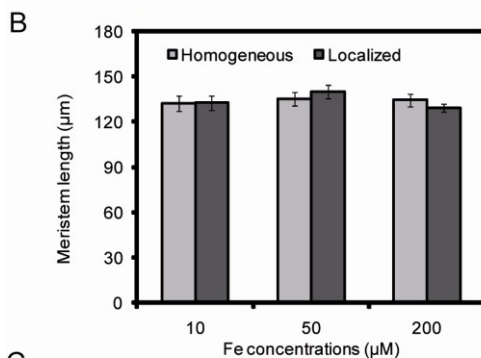


**Figure 16. Effect of homogeneous or localized Fe supply on cell division, differentiation and elongation.** (A) Seedlings of a *proCYCB1;1::GUS* line were germinated on Fe-deficient medium and transferred to segmented agar plates supplemented with 75  $\mu\text{M}$  ferrozine and with the indicated Fe(III)-EDTA concentrations only in the middle segment (localized supply) or in all three segments (homogeneous supply). (A, left panel) After 7 days, lateral roots from the middle segment were assayed for GUS activity. (A, right panel) Length of rhizodermal cells. Arrow heads indicate the boundaries of two consecutive epidermal cells. (B) Length of lateral root meristems and (C) length of individual rhizodermal cells. Bars represent means  $\pm$  SE,  $n = 3-4$  lateral roots from  $>14$  seedlings. \*\* denotes a significant difference according to Student's *t*-test ( $P < 0.01$ ).



#### 4.3.6 Localized Fe supply alters auxin distribution in lateral roots

Lateral root growth is coordinately controlled by environmental and hormonal signals, among which auxin takes in a central role in the regulation of all stages of lateral root development (Casimiro et al., 2003; Fukaki and Tasaka, 2009a; Peret et al., 2009). Therefore, it was examined whether Fe availability affects auxin accumulation in lateral roots by analyzing the activity of the auxin-responsive synthetic promoter DR5 (Ulmasov et al., 1997) under homogeneous or localized supply of Fe. Whereas DR5-GUS signals were weak at 10 or 200  $\mu\text{M}$  Fe irrespective of the mode of Fe supply, the supply of 50  $\mu\text{M}$  Fe only to the middle segment increased DR5-GUS activity in emerged and elongated lateral root tips (Figure 17A, B). However, in the primary root, a histochemical analysis of the *DR5::GUS* reporter did not show any significant change in auxin distribution under either mode of Fe supply (data not shown). These observations indicated that auxin distribution and accumulation in lateral roots is altered in response to locally supplied Fe. In order to discriminate whether this response indicates the existence of a signaling mechanism responsive to external or internal Fe concentrations, *DR5-GFP* expression was assessed in wildtype (Col-0) and *irt1* plants grown under localized supply of 50  $\mu\text{M}$  Fe. Relative to the wildtype, *DR5-GFP* expression in lateral root apices of the *irt1* mutant was markedly lower in both emerged and elongated lateral root cells (Figure 17C, D). Similar patterns were also observed when 200 and 600  $\mu\text{M}$  Fe were locally supplied to the roots (data not shown). Thus, these results indicate that IRT1-mediated Fe uptake is required for apical auxin accumulation in lateral roots.

#### 4.3.7 Enhanced elongation of lateral roots in response to local Fe is dependent on an AUX1-mediated auxin transport

Since auxin distribution depended on the mode of Fe supply (Figure 17), the response to local Fe supply was tested in mutants defective in auxin biosynthesis (*nit1-3*), transport (*pin2-T*; *aux1-T*) or sensitivity (*tir1-T* and *axr1-3*). While mean lateral root length was increased in *pin2-T*, *nit1-3* and *tir1-T* mutants to a similar extent as in wildtype (Col-0) plants, *aux1-T* and *axr1-3* plants showed a rather limited stimulation under a local availability of 50  $\mu\text{M}$  Fe (Figure 18).



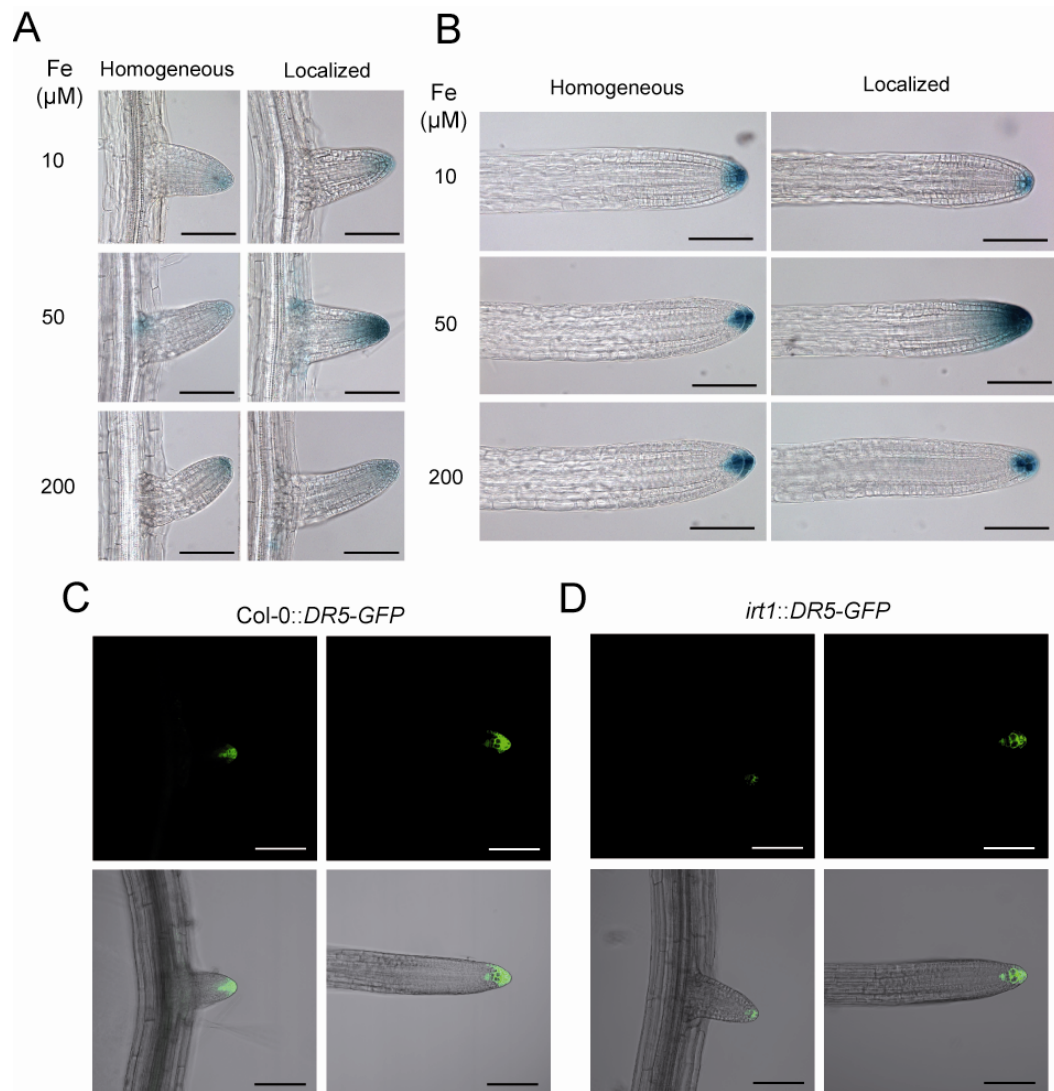


**Figure 17. Auxin accumulation is altered in response to local Fe.** (A, B) Expression of the auxin-responsive reporter *DR5-GUS* in (A) emerged and (B) elongating lateral roots. (C, D) Expression of the auxin-responsive reporter *DR5-GFP* in lateral roots of (C) wildtype (Col-0) and (D) *irt1* plants in response to localized supply of Fe. Seven-day-old seedlings germinated on Fe-deficient medium were transferred to segmented agar plates containing 50  $\mu\text{M}$  Fe-EDTA in the middle segment. Lateral roots were analyzed by (A, B) light microscopy or by (C, D) laser-scanning confocal microscopy after seven days on treatments ( $n \geq 10$  seedlings). The experiments were repeated twice and representative lateral roots are shown. Scale bars = 100  $\mu\text{m}$ .

Based on the reported involvement of the auxin influx carrier AUX1 in lateral root development (Casimiro et al., 2001; Marchant et al., 2002; De Smet et al., 2007), the role of AUX1 in Fe-dependent changes in root architecture was assessed. As expected, *aux1-T* plants showed a reduced number of lateral roots (Figure 19A; Marchant et al., 2002), irrespective of the treatments imposed. In contrast to wildtype plants that showed an 80% increase in mean lateral root length when

grown under localized supply of 50  $\mu\text{M}$  Fe, *aux1-T* plants were not able to significantly increase lateral elongation (Figure 19B and Figure 18). When 200  $\mu\text{M}$  Fe were supplied, both genotypes elongated lateral roots to a similar extent (Figure 19B). These observations indicated that the loss of *AUX1* expression prevents the Fe-dependent increase in lateral root elongation in response to localized Fe.

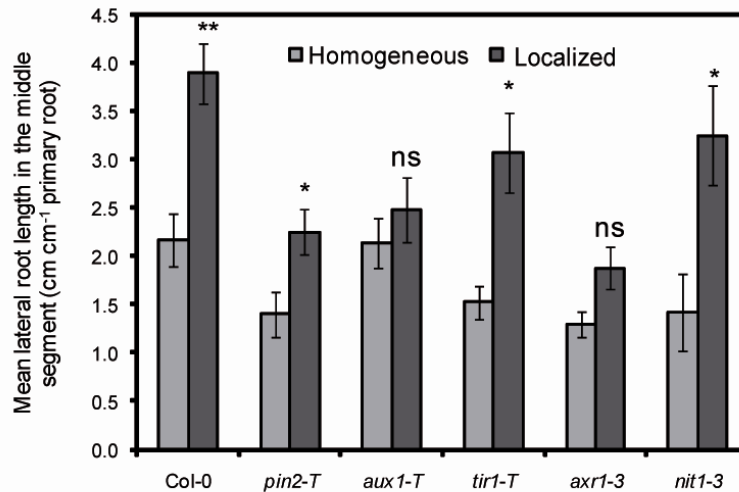


**Figure 18. Mean lateral root length in auxin mutants in response to homogeneous or localized Fe supply.** Seven-day-old wildtype (Col-0) and auxin mutant seedlings were transferred to split agar plates with homogeneous or localized supply of 50  $\mu\text{M}$  Fe-EDTA (+ 75  $\mu\text{M}$  ferrozine). After 15 days, plates were scanned and root architecture was analyzed. Bars indicate means  $\pm$  SE,  $n = 6-8$  plates with 3 plants. \*\* and \* denote significant difference according to Student's *t*-test at  $P < 0.01$  and  $P < 0.05$ , respectively. ns = no significant difference according to Student's *t*-test at ( $P < 0.05$ ).

Recently, it has been shown that Fe deficiency triggers an over-accumulation of indole-3-acetic acid (IAA) and that *aux1-7* mutant plants exhibit reduced ferric chelate reductase (FCR) activity under low Fe (Chen et al., 2010a). However, no significant difference in FCR activity was observed in *aux1-T* plants grown under homogeneous or localized supply of 50  $\mu\text{M}$  Fe, indicating that the missing stimulation of lateral root elongation in response to local Fe in *aux1-T* plants was not related to a defective Fe(III) reduction at the root surface (Figure 20). Collectively, these results indicate that *AUX1*-mediated auxin transport is necessary for the enhanced lateral root elongation observed in Fe-rich patches.

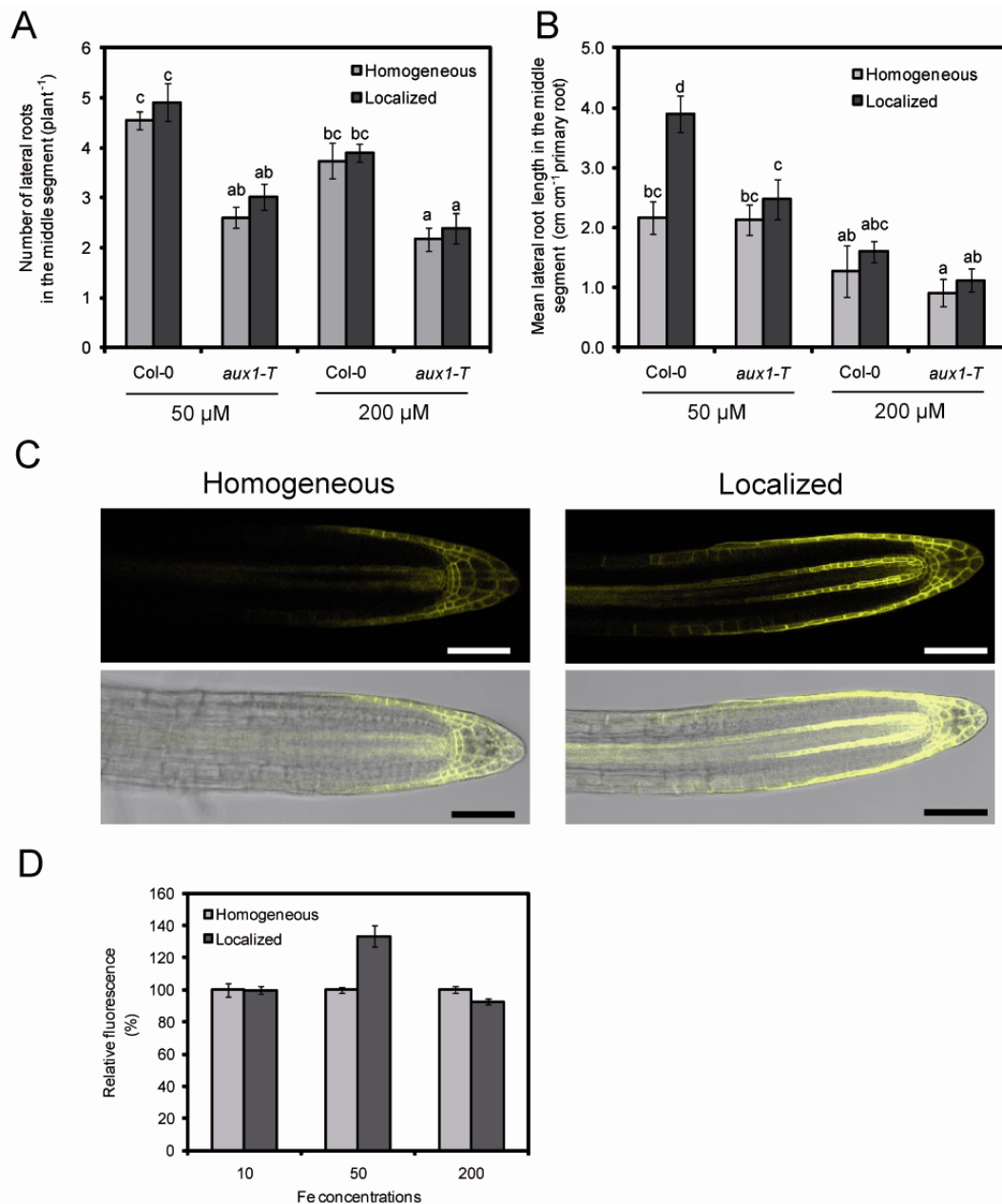


**Figure 19. Lateral root elongation under localized Fe supply is dependent on AUX1.** (A) Number and (B) mean length of lateral roots in wildtype (Col-0) and *aux1-T* plants after 15 days on treatments. Bars represent means  $\pm$  SE,  $n = 7$  plates with 3 seedlings per plate. Different letters indicate significant differences among means ( $P < 0.05$  by Tukey's test). (C) *proAUX1-AUX1::YFP* expression in lateral roots of wild-type plants grown on localized supply of 50  $\mu$ M Fe. Scale bars = 50  $\mu$ m. (D) Quantification of YFP fluorescence by image analysis of laser-scanning confocal images. Bars represent means  $\pm$  SE,  $n > 10$  seedlings.

To establish whether AUX1 expression is regulated by local Fe, its expression levels were determined by means of quantitative RT-PCR. However, no significant difference in expression could be detected (data not shown), possibly because whole roots (primary plus lateral roots) were harvested from the middle segment

for mRNA analysis. Alternatively, AUX1 accumulation in the apex of lateral roots was observed by using *proAUX1-AUX1:YFP* lines. The localized supply of 50  $\mu\text{M}$  Fe markedly increased AUX1-dependent fluorescence in the apex of emerged lateral roots (Figure 19C). In fact, as the measurement of AUX1-derived fluorescence confined to the lateral root apex revealed, the localized supply of 50  $\mu\text{M}$  to the middle segment increased AUX1 signal intensity by more than 30% relative to a homogeneous supply (Figure 19D). A localized supply of 10 or 200  $\mu\text{M}$  Fe had no impact on the relative intensities of *proAUX1-AUX1:YFP*-derived fluorescence (Figure 19D). Taken together, these results indicate that the localized availability of Fe stimulates lateral root elongation by increasing *AUX1* expression and subsequent auxin accumulation in the lateral root apex.

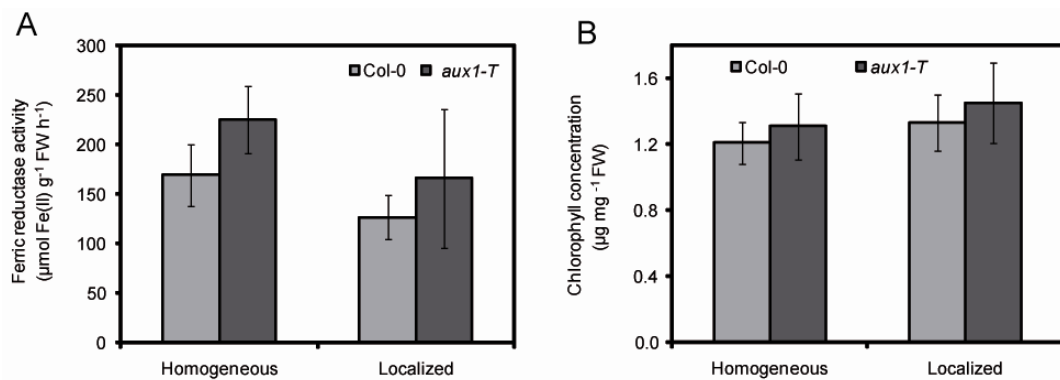


**Figure 20. Physiological characterization of *aux1-T* mutants under localized supply of Fe.** (A) Ferric chelate reductase activity in roots and (B) chlorophyll concentration in shoots of wildtype and *aux1-T* plants grown under homogeneous or localized supply of 50  $\mu\text{M}$  Fe-EDTA. Bars indicate means  $\pm$  SD,  $n = 5$  plates with 3 plants.

#### 4.3.8 Screening of *Ds*-transposon-tagged *Arabidopsis* lines for their response to localized Fe supply

The previous observations demonstrated that *Arabidopsis* plants stimulate lateral root development in Fe-containing patches. In order to identify further components involved in the regulation of lateral root elongation in response to localized Fe, a screening approach was used. Since No-0 wildtype plants showed a highly consistent twofold increase in the elongation of lateral roots when 25  $\mu\text{M}$  Fe-EDTA were supplied to the middle segment (Figure 6), these experimental settings

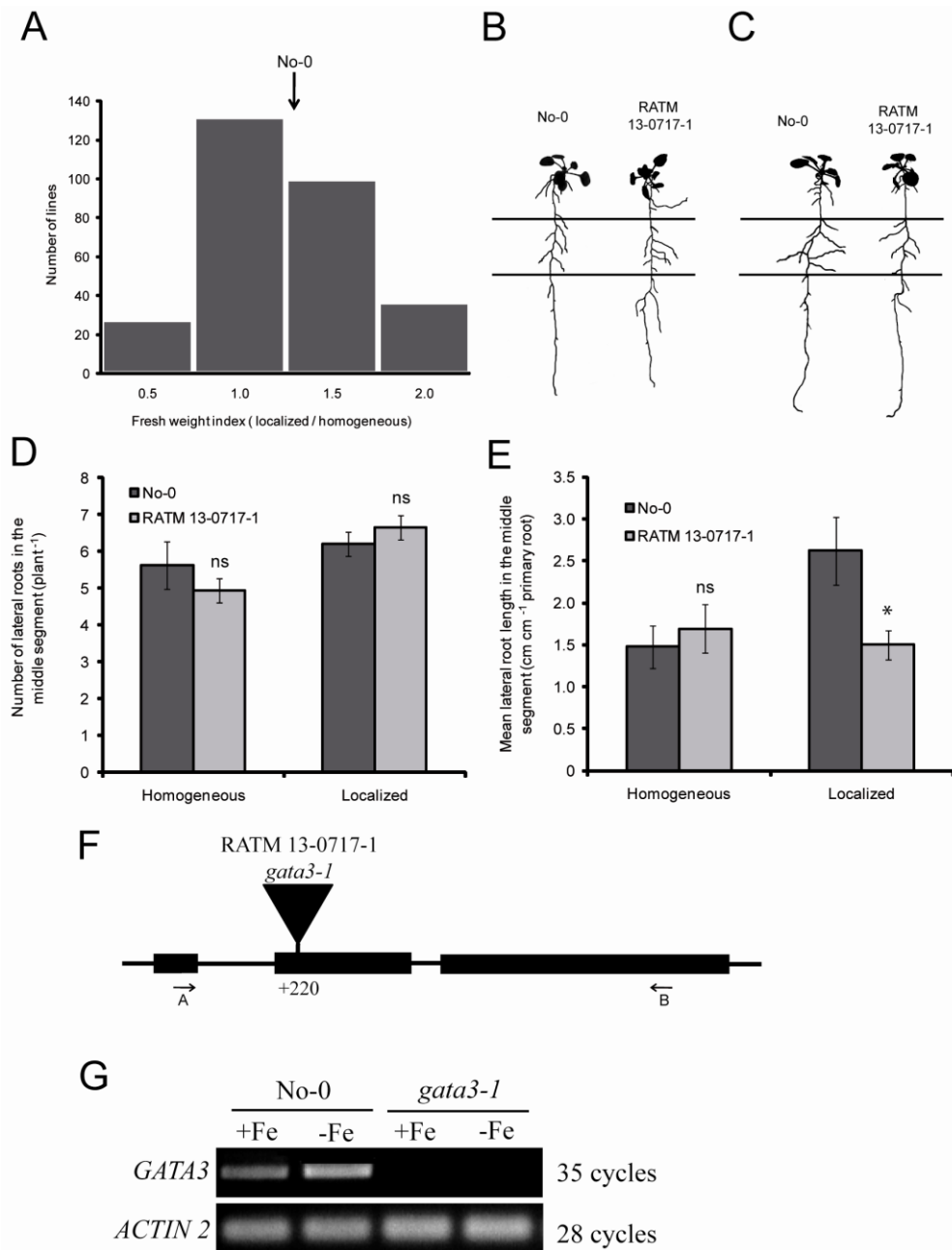


**Figure 21. Identification of a *Ds*-transposon-tagged line defective in Fe-dependent stimulation of lateral root elongation.** (A) Frequency distribution of lines according to root fresh weight index (root fresh weight under localized Fe supply divided by root fresh weight under homogeneous Fe). (B, C) Lateral root architecture of wildtype (No-0) and *Ds*-transposon line RATM 13-0717-1 under (B) homogeneous or (C) localized supply of 25  $\mu$ M Fe. (D) Number and (E) mean lateral root length of wildtype and RATM 13-0717-1. Seven-day-old seedlings germinated in  $\frac{1}{2}$  MS media without Fe were transferred to segmented agar plates supplemented with 75  $\mu$ M ferrozine and 25  $\mu$ M of Fe in all three segments (homogeneous) or only in the middle segment (localized). After 15 days on treatments, plates were scanned. (F) Exon-intron structure of *GATA3* showing the site of the *Ds*-transposon insertion in the second exon. Arrows (A and B) indicate *gata3-for* and *gata3-rev* primers (described in Materials and Methods), respectively, used for the expression analysis shown in Figure 1G. (G) RT-PCR analysis of *GATA3* expression in cDNA samples from wildtype (No-0) and *gata3-1* roots using primers A and B. Fifteen-day-old seedlings were transferred to  $\frac{1}{2}$  MS media supplement with 75  $\mu$ M Fe (+Fe) or without Fe (-Fe). The expression of the housekeeping gene *ACTIN2* served as control. \* denotes significant and ns not significant difference according to Student's *t*-test at  $P < 0.05$ .

were considered suitable for a screening strategy. Therefore, a collection of 302 transgenic lines harboring *Ds*-transposon insertions in genes predicted to encode for DNA-binding proteins was screened for Fe-dependent lateral root elongation. Transcription factors were chosen because of their central role in the regulation of many physiological and morphological processes, including lateral root development (Zhang and Forde, 1998; Xie et al., 2000; Wang et al., 2006).

*Ds*-transposon-tagged lines were grown with 25  $\mu$ M Fe either supplied locally only to the middle segment or homogeneously over all three segments. The aim was to identify *Ds*-transposon lines that were not able to stimulate lateral root elongation when Fe was available only in the middle segment, while showing similar lateral root development under homogeneous Fe supply as wildtype plants. In order to increase the experimental throughput, plates were scanned, but lateral root length was not quantified. Instead, lateral root development was assessed visually and by root biomass. Since previous experiments demonstrated that the increased lateral root elongation under localized Fe was reflected in increased root biomass production (Figures 6 and 7B), the root fresh weight index was determined, in which the fresh biomass of roots grown under localized Fe was divided by the biomass of the same transgenic lines when grown under homogeneous Fe. As shown in Figure 21A, wildtype plants had an index of  $\sim 1.3$ , indicating that root growth was stimulated under localized supply. Since it was shown before that primary root growth and lateral root number were not significantly affected by localized Fe supply, the increased fresh weight index in wildtype plants reflected the stimulated lateral root development in response to local Fe (Figure 6).

The majority of the transgenic lines screened showed root fresh weight indices ranging from 1.0 (weak response) to 2.0 (enhanced lateral root length under localized Fe), thus not deviating significantly from the wildtype (Figure 21A). However, 28 lines showed very limited lateral root elongation (index  $< 0.5$ ) particularly when exposed to localized availability of Fe. These lines were, therefore, tested once more under the same conditions. Among these lines, the *Ds*-transposon line RATM 13-0717-1 was the most prominent because it showed limited increased lateral root elongation when grown under localized Fe (Figure 21C, E), despite showing similar lateral root number and length as wildtype plants

under homogeneous supply of 25  $\mu\text{M}$  (Figure 21B, D). Since the transgenic lines used in this screen are homozygous and the genomic regions, where the *Ds*-transposon tags are inserted, are known (Kuromori et al., 2004; Ito et al., 2005), primers were designed to test the expression of the gene predicted to be mis-regulated in RATM 13-0717-1. The *Ds*-transposon is inserted into the second exon of At4g34680 (Figure 21F) and disrupts completely *GATA3* expression in roots (Figure 21G). The At4g34680 locus has been assigned to *GATA3*, encoding a DNA-binding protein from the GATA sub-family of zinc finger transcription factors (Manfield et al., 2007). Hereafter, the RIKEN line RATM 13-0717-1 was designated as *gata3-1*. These results indicate that the putative transcription factor *GATA3* might be involved in the regulation of lateral root development in response to localized Fe.

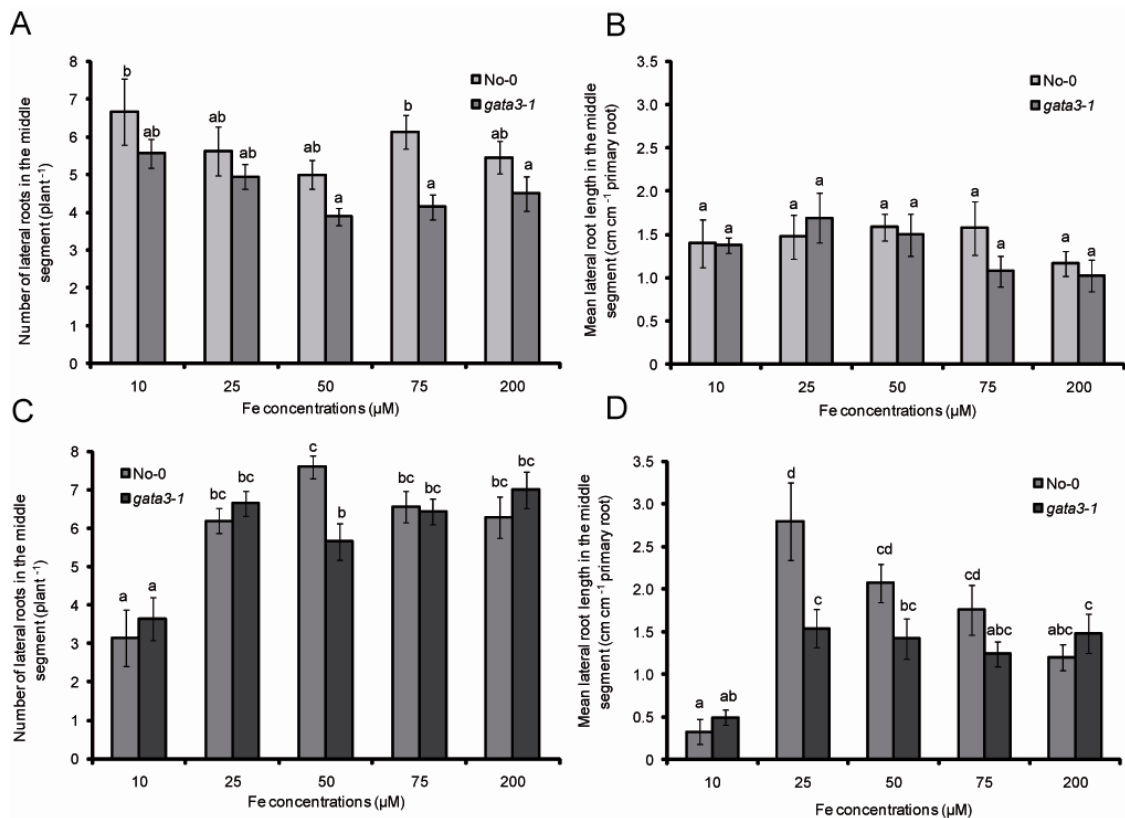


**Figure 22. Lateral root development in wildtype (No-0) and *gata3-1* plants in response to homogeneous or localized Fe supply.** (A, C) Lateral root number and (B, D) mean lateral root length in wildtype (No-0) and *gata3-1* plants. Seeds were germinated on Fe-free, half-strength MS medium for 7 days before transfer to segmented agar plates supplied (A, B) homogeneously or (C, D) locally with increasing concentrations of Fe(III)-EDTA. After 15 days on treatments, plant root were scanned and root parameters were measured by image analysis. Bars represent means  $\pm$  SE,  $n = 6$  plates with 3 seedlings in each. Different letters indicate significant difference among means ( $P < 0.05$  by Tukey's test).



### 4.3.9 Loss of *GATA3* expression abolishes the stimulation of lateral root elongation in response to localized Fe availability

To extend the understanding about the response of *gata3-1* plants to localized Fe, the lateral root development of this insertion mutant was characterized in response to a range of Fe concentrations either supplied homogeneously or locally. The number of lateral roots was only slightly affected in *gata3-1* plants irrespective of the mode of Fe application (Figure 22A and B). Mean lateral root length was also not significantly altered in *gata3-1* plants when Fe was supplied evenly over the three segments (Figure 22C). However, under localized Fe supply the mean lateral root length was significantly reduced in *gata3-1* plants particularly when 25  $\mu\text{M}$  Fe was supplied to the middle segment (Figure 22D). Similar responses were also observed in another independent line (SALK\_022107C; renamed here as *gata3-2*). In fact, *gata3-2* plants also showed no particular stimulation of lateral root elongation specifically under localized Fe relative to its respective wildtype accession Col-0 (Figure 23A, B).

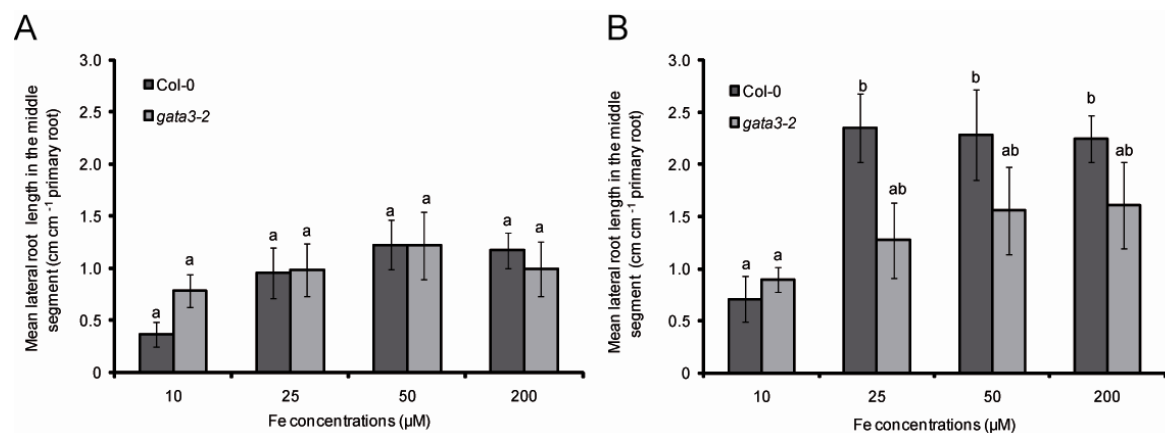


**Figure 23. Lateral root development in wildtype and *gata3-2* under homogeneous or localized Fe supply.** (A,B) Mean lateral root length in wildtype (Col-0) and *gata3-2* T-DNA insertion plants grown under (A) homogeneous or (B) localized supply of increasing concentrations of Fe(III)-EDTA. Seven-day-old seedlings germinated on Fe-free, half-strength MS medium were transferred to segmented agar plates supplemented with Fe in (A) all three segments (homogeneous) or (B) only in the middle segment (localized). After 15 days on treatments, plant root were scanned and root parameters were measured by image analysis. Bars represent means  $\pm$  SE,  $n = 6$  plates with 3 seedlings in each. Different letters indicate significant differences among means ( $P < 0.05$  by Tukey's test).



In order to test whether these differential responses were due to altered Fe acquisition, the two major components of the Strategy I Fe uptake machinery – namely Fe(III)-chelate reduction and *IRT1* expression – were compared in wildtype and *gata3-1* roots. The loss of *GATA3* expression did not affect *IRT1* expression under Fe-sufficient or Fe-deficient conditions (Figure 24A). In addition, no difference in Fe(III)-chelate reductase activity was observed between wildtype and *gata3-1* plants subjected to Fe deficiency for 6 days (Figure 24A, B). Altogether, these results indicate that the Fe acquisition machinery is not altered in *gata3-1* plants. Thus, *GATA3* appears to represent an essential component for the differential response of lateral root elongation of Arabidopsis plants to localized Fe availability.

#### 4.3.10 Regulation of *GATA3* expression by Fe

To gain more insights on the effect of Fe in the regulation of *GATA3* expression, relative expression levels in roots of Fe-fed plants were compared to those of plants grown under Fe limitation. The expression of *GATA3* was approximately twofold up-regulated after 6 days under Fe deficiency (Figure 25A). Furthermore, when expression were compared between roots sampled from the middle segment of plates homogenously or locally supplied with Fe, a strong up-regulation was observed specifically when 10  $\mu$ M Fe were supplied only to the middle segment (Figure 25B). Although this expression analysis was limited to only one sampling time these results indicate that *GATA3* expression is regulated by Fe deficiency rather than by its presence in the medium.

In order to establish whether *GATA3* expression is controlled by local or long-distance signals, the expression of this putative transcription factor was measured in wildtype and *frd3-1* roots exposed to localized supply of Fe. As shown in Figure 26A, *GATA3* expression levels were 50% lower in *frd3-1* roots when 10  $\mu$ M Fe was supplied. An increase in Fe concentrations supplied to the middle suppressed *GATA3* expression both in wildtype and *frd3-1* (Figure 26A). Since *frd3-1* plants exhibit a defective root-to-shoot translocation of Fe (Rogers and Guerinot, 2002; Green and Rogers, 2004; Durrett et al., 2007), significantly higher Fe levels

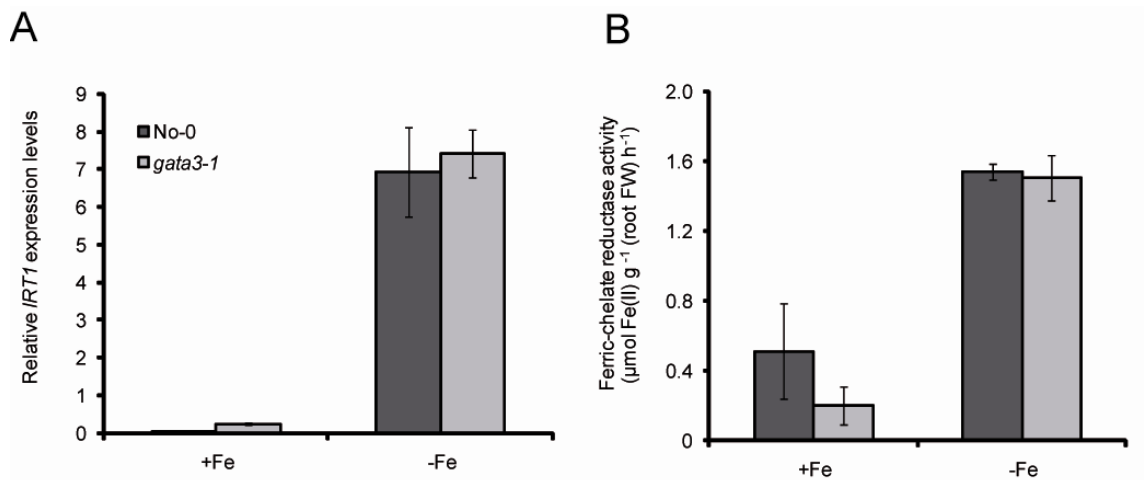


**Figure 24. GATA3 does not affect the expression of *IRT1* and the ferric-chelate reductase activity.** (A) Transcript levels of the Fe(II)-transporter *IRT1* as determined by quantitative RT-PCR in roots of wild-type (No-0) and *gata3-1* plants. Plants were grown for 15 days on half-strength MS and then transferred to either 75  $\mu\text{M}$  Fe (+Fe) or to a Fe-free (-Fe) media for 6 days. Bars represent means  $\pm$  SE ( $n = 3$  biological replicates). (B) Ferric-chelate reductase activity in wildtype (No-0) and *gata3-1* plants under +Fe or after 6 days under Fe deficiency. Fifteen-day-old seedlings germinated on half-strength MS medium were transferred to + Fe (75  $\mu\text{M}$  Fe) or -Fe (no Fe + 300  $\mu\text{M}$  ferrozine). Shown are means  $\pm$  SE,  $n = 6$  replicates.

might have accumulated in *frd3-1* roots even when the external supply was as low as 10  $\mu\text{M}$ . This could explain why *GATA3* mRNA levels were more suppressed in *frd3-1* already at 10  $\mu\text{M}$  Fe and at 200  $\mu\text{M}$  Fe (Figure 26A). Interestingly, the *GATA3* expression pattern differed significantly from that of the Fe(II)-transporter *IRT1*, whose expression was significantly up-regulated in *frd3-1* roots even under high Fe supply (Figure 6B). In addition, the expression pattern of the bHLH transcription factor *FIT* was also significantly different from *GATA3*. Although *FIT* expression was up-regulated under low Fe (10  $\mu\text{M}$  Fe-EDTA) both in wildtype and *frd3-1* roots, *FIT* expression remained at a higher level in *frd3-1* when 50  $\mu\text{M}$  Fe was supplied and were suppressed to wildtype levels only when 200  $\mu\text{M}$  Fe was supplied (Figure 26C). These results strongly indicate that, conversely to *FIT* and *IRT1*, *GATA3* expression is strictly controlled by the local Fe availability rather than by systemic signals from the shoot.

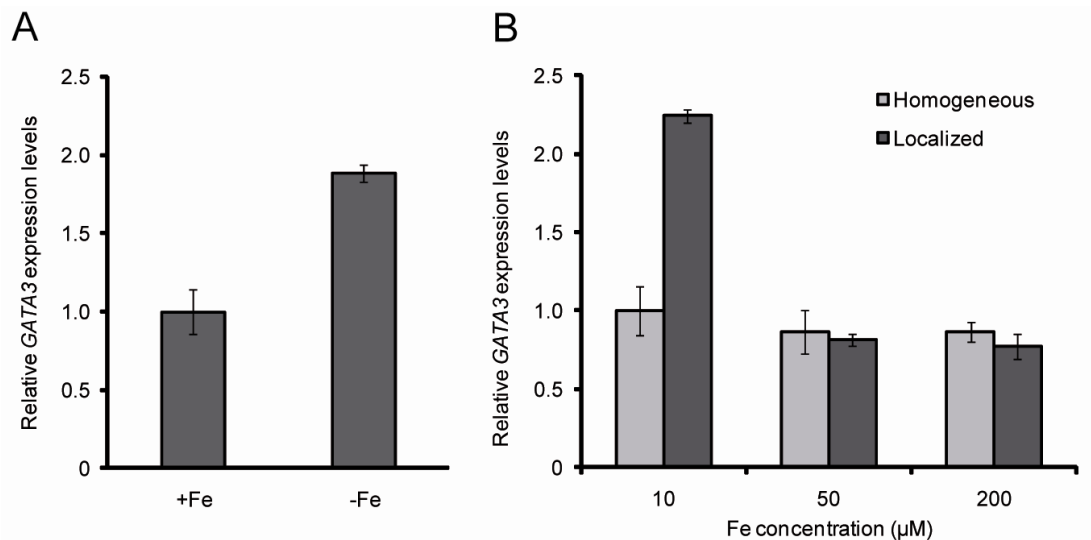


**Figure 25. *GATA3* expression is regulated by Fe.** (A) *GATA3* transcript levels as determined by quantitative RT-PCR in wildtype roots in response to Fe deficiency. Fifteen-day-old seedlings germinated on half-strength MS medium were grown for additional 6 days in the presence of 75 μM Fe (+Fe) or in the absence of Fe plus 15 μM ferrozine (-Fe). (B) Expression levels of *GATA3* in response to the homogeneous or localized supply of increasing concentrations of Fe. Root segments were harvested from the middle segments of wildtype plants (*Col-gl*) growing for 15 days under homogeneous or localized supply of Fe at the indicated concentrations. Bars represent means ± SE, n = 3.

#### 4.4 Discussion

Plant root development strongly depends on nutrient availability and changes in the root system architecture are mostly characterized by a differential growth response of root organs in a nutrient-specific or even nutrient form-specific manner. Apart from a general elongation of the total root system as observed under N, P and S deficiency (Marschner, 1995; Lopez-Bucio et al., 2003), so far only local supplies of ammonium, nitrate and phosphate have been shown to trigger lateral root proliferation (Drew, 1975; Linkohr et al., 2002; Remans et al., 2006; Lima et al., 2010). Here, it is shown that Fe availability has a particularly strong impact on lateral root development by interfering with auxin signaling and that a Fe-regulated GATA-type transcription factor is directly involved in this root architectural response.

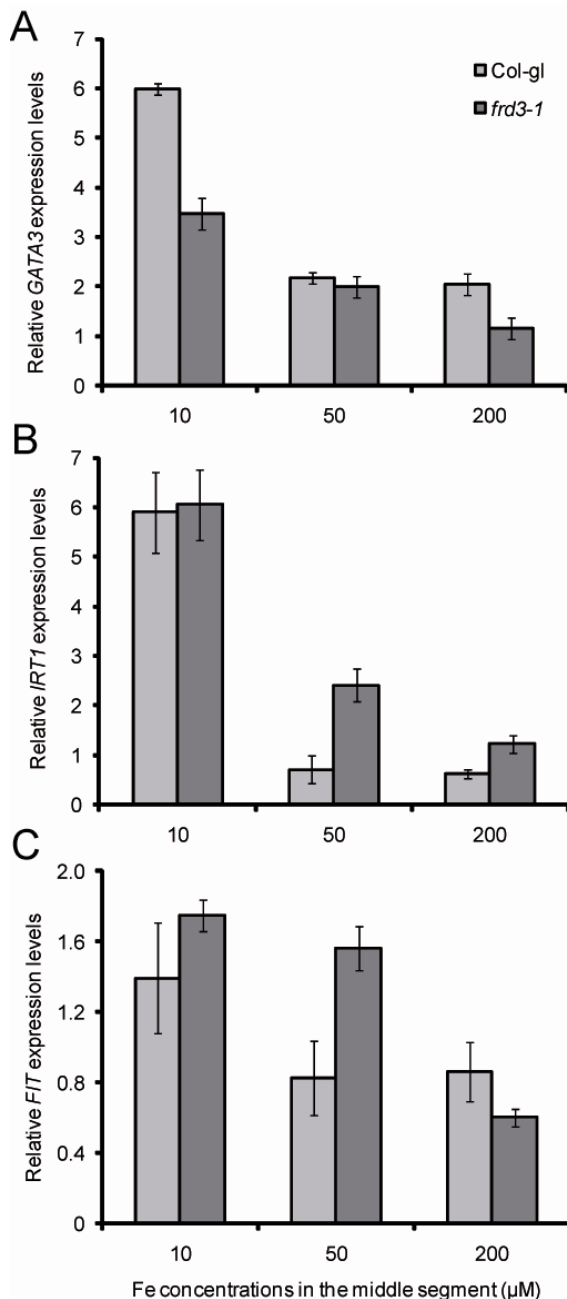


**Figure 26. GATA3 expression is regulated by the root Fe status.** Transcript levels of (A) *GATA3*, (B) *IRT1* and (C) *FIT* as determined by quantitative RT-PCR in roots of wildtype (Col-gl) and *frd3-1* mutant plants. Root segments were harvested from the middle segment of plants growing for 15 days under localized supply of Fe at the indicated concentrations. Bars represent means  $\pm$  SE,  $n = 3$ .

#### 4.4.1 Localized Fe supply differentially regulates lateral root number and lateral root length

The localized availability of Fe exerted a dual effect on lateral root development in *Arabidopsis*. Firstly, a direct comparison of lateral root growth responses to homogenous or localized supply of Fe revealed a twofold increase in lateral root length of wildtype plants grown on 25  $\mu\text{M}$  localized Fe supply relative to plants grown on homogenous Fe supply, while lateral root number was much less

affected (Figure 6E, F). This increase in lateral root length went along with enhanced cell elongation rather than cell division or differentiation (Figure 16A-C). However, during the very early stages of development, lateral root primordia of plants exposed to localized 50 or 200  $\mu\text{M}$  Fe emerged more quickly (Table 2). This suggests that Fe might also have an impact on cell division and/or differentiation, allowing lateral root initiation and/or emergence. This view is supported by the observation that localized nitrate-dependent stimulation of lateral root elongation was indirectly assigned to increased cell production rates in the lateral root tip, since cell length was not affected (Zhang et al., 1999). This supports the notion that nutrients may ultimately affect lateral root growth at different developmental processes.

Secondly, high local Fe supplies evoked an inhibition of lateral root length (Figure 6E, 11B) but not of lateral root number (Figure 6F, 11A). Thus, these two morphological root traits are subject to a differential regulation by local Fe availability. A growth-inhibitory effect of Fe has been reported for primary roots and suggested as the major cause for root shortening under local P deficiency, because low P levels may cause higher Fe availabilities and favor subsequent Fe toxicity (Ward et al., 2008). Indeed, a homogenous supply of elevated Fe concentrations also inhibited primary root elongation (Figure 6I). Since phosphate concentrations in the medium were the same and elemental analysis revealed that shoot phosphate concentrations were not affected by either mode of Fe supply at any level (Table 1), the Fe-mediated inhibition of lateral root growth under localized supply of 200 - 500  $\mu\text{M}$  Fe (Figure 6E) was most likely independent of any interactions with P.

#### 4.4.2 The local regulation of lateral root development by Fe

To improve Fe acquisition from the rhizosphere, *Arabidopsis* plants induce strategy I responses consisting of enhanced proton extrusion, Fe(III) reduction and  $\text{Fe}^{2+}$  transport (Kim and Guerinot, 2007; Giehl et al., 2009). The expression of the relevant genes, in particular *IRT1* and *FRO2*, are subjected to a local control, in which Fe acts as a local inducer, and a systemic control, in which a shoot-derived signal represses gene expression (Vert et al., 2003). Several lines of evidence

indicate that the regulation of lateral root development by Fe is different and primarily subject to a local rather than a systemic regulation: i) Lateral root elongation followed an optimum response to local Fe supplies and decreased at elevated external Fe levels (Figure 6E), even though the Fe nutritional status of the shoots did not change (Figure 8C, Table 1). This observation emphasizes that the Fe-dependent regulation of this morphological trait was not controlled by a long-distance Fe signal from the shoot, as it is the case for the expression of the Fe uptake machinery (Vert et al., 2003; Lucena et al., 2006; Enomoto et al., 2007). ii) Under localized Fe supply lateral root elongation in *frd3-1* mutants did not significantly differ from that of wildtype plants, although *frd3-1* shoots suffered from Fe deficiency (Figure 15B, C). Since FRD3 acts as a citrate loader into the xylem required for root-to-shoot translocation of Fe, *frd3-1* plants accumulate Fe in roots while the shoot remains Fe deficient (Durrett et al., 2007), thereby causing a weaker repression of strategy I responses in roots upon Fe resupply (Rogers and Guerinot, 2002). Under localized Fe supply, Fe-mediated stimulation of lateral root elongation was independent of FRD3, suggesting feedback control by Fe in a local rather than systemic regulatory loop. iii) Although the application of Fe to leaves stimulated lateral root elongation, this response was mainly restricted to the upper Fe-free segments (Figure 13A-C). The upper root part contained more Fe (Figure 13D), suggesting that Fe itself was translocated downwards to the root. In addition, Fe-citrate supply to leaves did not repress the stimulation of lateral root elongation under localized supply of 50  $\mu$ M Fe (Figure 13B). Collectively, these observations reinforce the view of a local control of lateral root elongation by Fe, although they additionally indicate that shoot-derived Fe can add up with externally available Fe to regulate lateral root growth. iv) Unlike lateral root elongation, elevated Fe supplies to *irt1* plants allowed to restore lateral root initiation up to wild-type levels, indicating that the lack of IRT1 in the initiation process was compensated for by excessive Fe supply; this was definitely not the case for lateral root elongation (Figure 11A, B). Thus IRT1, which is preferentially expressed in the rhizodermis of Fe-deficient plants (Vert et al., 2002), likely plays a role in Fe-dependent lateral root growth as the major Fe transporter being located upstream of the Fe sensing event triggering lateral root elongation. However, since an application of Fe-citrate to *irt1* shoots restored chlorophyll levels and lateral root

elongation to wild-type levels (Figure 12), IRT1 is only an essential upstream component in eliciting this morphological response if the Fe demand of the root tissue depends on the uptake of external Fe. In contrast to Fe-repressed lateral root elongation, the inhibitory effect of nitrate on lateral root elongation is mainly caused by systemic inhibition (Zhang et al., 1999).

#### **4.4.3 AUX1-mediated auxin distribution is required for the increased lateral root elongation under localized Fe**

Auxin has been recognized as the central player in lateral root development, since it affects many of the events necessary for lateral root initiation and elongation (Casimiro et al., 2001; Benkova et al., 2003). Although its role in nutrient-dependent changes in lateral root architecture is just beginning to be elucidated, first examples show that auxin signaling might be affected by nutrient supply at different developmental stages. Lateral root proliferation under P deficiency increases auxin sensitivity in pericycle cells by enhanced expression of the auxin receptor TIR1 and degradation of IAA/AUX repressors to unblock auxin signaling (Perez-Torres et al., 2008). In the case of lateral root elongation under localized nitrate supply, a nitrate-dependent repression of the nitrate transporter NRT1.1 proceeds apical auxin accumulation in the lateral root apex as a prerequisite for lateral root elongation (Krouk et al., 2010b). According to the higher *DR5* promoter activities (Figure 17A, B), Fe-mediated lateral root elongation also relies on auxin accumulation or an elevated auxin sensitivity in the lateral root apex, since *DR5* promoter activation did not occur under non-permissive external Fe concentrations or in the *irt1* mutant (Figures 11 and 17C, D). Considering that the requirement of IRT1 in lateral root elongation can be circumvented by shoot supply of Fe-citrate (Figure 12), it is likely that symplastic Fe is responsible for altered auxin activities in lateral root tips.

Screening of auxin-related mutants for Fe-responsive lateral root elongation pointed to the auxin importer AUX1 as a candidate for an integration of the local Fe nutritional status into the auxin signaling (Figure 18). AUX1 has been implicated in both acropetal and the basipetal routes of auxin transport in roots. Together with PIN2, AUX1 forms the basic machinery for basipetal auxin transport

from the root apex back to basal root zones (Swarup et al., 2001). Since *aux1-T* but not *pin2-T* mutants failed to elongate lateral roots in response to localized Fe (Figure 18), it is likely that acropetal rather than basipetal auxin transport represents a sensitive check point for this Fe-dependent morphological response. In support of this hypothesis, the *aux1-T* mutant failed to increase lateral root length at permissive Fe supplies while lateral root development was otherwise not affected (Figure 19A, B). Furthermore, only localized but not homogenous Fe supply increased *proAUX1-AUX1:YFP* expression levels in the lateral root meristems (Figure 19C, D), which is indicative for an enhanced movement of auxin originating from the shoot and/or primary root towards the lateral root apex. Auxin regulates both lateral root initiation and elongation, but there is increasing evidence that lateral root initiation primarily depends on basipetally transported auxin (Casimiro et al., 2001; De Smet et al., 2007), whereas lateral root emergence and elongation are controlled by acropetally transported auxin (Casimiro et al., 2001; Swarup et al., 2008). At which level auxin affects cell elongation is still unclear. One possibility is that basipetally transported auxin that ends up in the elongation zone is involved in the auxin-dependent inhibition of cell elongation (Swarup et al., 2005). Conversely, increased acropetal auxin transport within the lateral root could prevent that too much auxin accumulates at the cell elongation zone, thus allowing increased elongation. In line with this hypothesis, it has been shown that the loss of MDR1, a multidrug resistance-like ABC transporter, leads to significant reduction of acropetal auxin transport within lateral roots and decreased *DR5-GUS* activity specifically in the apices of lateral roots (Wu et al., 2007). As a consequence of defective acropetal auxin movement, *mdr1* mutants show impaired emergence and slower elongation of lateral roots (Wu et al., 2007), further highlighting the importance of acropetal auxin transport on lateral root elongation rather than initiation.

#### **4.4.4 Involvement of the putative DNA-binding protein GATA3 in the regulation of lateral root elongation under localized Fe**

Fe limitation evokes a series of physiological and morphological changes in plants, such as increased Fe mobilization and uptake (Briat et al., 2007; Kim and



Guerinot, 2007) and enhanced formation of root hairs (Schikora and Schmidt, 2001; Schmidt and Schikora, 2001). Genome-wide transcriptome analyses have revealed that many Fe deficiency-regulated responses are modulated at the transcriptional level (Dinney et al., 2008; Buckhout et al., 2009; Yang et al., 2010). However, up to now only few transcription factors have been demonstrated to play a role in the regulation of Fe starvation responses. Interestingly, in rice and Arabidopsis, most of the transcription factors belong to the basic helix-loop-helix (bHLH) family of DNA-binding proteins (Colangelo and Guerinot, 2004; Jakoby et al., 2004; Yuan et al., 2005; Ogo et al., 2006; Bauer et al., 2007; Ogo et al., 2007; Wang et al., 2007; Long et al., 2010). In Arabidopsis, FIT is important for the regulation of many Strategy I responses, such as the up-regulation of *IRT1* and *FRO2* under low Fe (Colangelo and Guerinot, 2004; Jakoby et al., 2004; Yuan et al., 2005). As a consequence of this role, *fit* mutants exhibit reduced Fe contents and are severely chlorotic when not supplied with generous amounts of highly soluble Fe (Colangelo and Guerinot, 2004). Despite of the central role of FIT in the modulation of many physiological responses to limited Fe, this transcription factor appears not to directly regulate the lateral root response to localized Fe. *fit* loss-of-function mutants failed to elongate their lateral roots in the Fe-containing compartment (Figure 10), most likely due to impaired Fe uptake by this mutant (Colangelo and Guerinot, 2004; Jakoby et al., 2004). In fact, the lateral root elongation of *fit1* plants under localized supply of Fe phenocopied the lateral root growth observed in *irt1* mutant plants (Figures 10 and 11). Moreover, the overexpression of *FIT* had no effect on lateral root development in response to localized Fe (Figure 10). Altogether, these observations indicate that FIT has no direct, Fe uptake-independent role in the regulation of architectural changes in response to localized Fe availability.

In order to identify novel regulatory components involved in the response of roots to localized Fe, a transposon-tagged collection of Arabidopsis was screened, consisting of lines harboring *Ds*-transposon insertions in putative DNA-binding proteins. In total, 302 lines were included in the screen, representing approximately 20% of the genes predicted to encode for transcription factors in the genome of *A. thaliana* (Riechmann et al., 2000; Riechmann and Ratcliffe, 2000; Qu and Zhu, 2006). The screen allowed the identification of one *Ds*-transposon

line – *gata3-1* – that did not display the typical stimulation of lateral root elongation when grown under localized supply of 25  $\mu$ M Fe (Figure 21A-E). In *gata3-1* plants, the expression of *GATA3* is completely abolished (Figure 21G). Interestingly, even the supply of higher Fe concentrations could not stimulate the elongation of lateral roots in *gata3-1* plants under localized Fe (Figure 22A, C). This phenotype was also confirmed by the analysis of a second independent mutant allele of *GATA3* (Figure 23A, B).

*GATA3* is a member of the type-IV zinc finger transcription factor family that binds to conserved GATA motifs (Teakle et al., 2002; Reyes et al., 2004). In plants, GATA factors have been implicated in the regulation of a multitude of processes such as light responses (Teakle et al., 2002), circadian regulation of gene expression (Teakle and Kay, 1995) and nitrogen metabolism (Bi et al., 2005). Moreover, functional analysis has revealed that some members of the GATA family play also a role in developmental processes, such as cell elongation (Nishii et al., 2000; Shikata et al., 2004) and the development of flowers and of the shoot apical meristem (Zhao et al., 2004). However, many GATA mutants do not display phenotypes or developmental defects under non-stressed conditions, indicating that there is a high level of redundancy among GATA members and/or that they primarily show conditional phenotypes (Manfield et al., 2007).

Under homogeneous Fe, lateral root length in *gata3-1* and *gata3-2* plants was almost indistinguishable from that of their respective wildtypes (No-0 and Col-0, respectively; Figures 22C and 23B). This indicates that rather than affecting the general program of lateral root development, *GATA3* is most likely involved in the modulation of elongation when Fe availability is spatially restricted. However, since the response of *gata3-1* plants was tested so far only under local Fe, one cannot rule out the possibility that this DNA-binding protein also affects lateral root development in response to the localized supply of other nutrients, such as nitrate or phosphate. In the case of nitrate, one member of the MADS-box family of transcription factor, *ANR1*, has been implicated in the signaling pathway that regulates lateral root elongation according to the external nitrate availability (Zhang and Forde, 1998).

One important observation in the present study was that the main components of the Fe uptake-machinery were not affected by the loss of *GATA3* (Figure 24). This strongly indicates that the decreased lateral elongation of *gata3-1* plants under localized Fe is not due to defective Fe uptake. In an earlier characterization of the expression pattern of GATA factors, it has been shown that *GATA3* belongs to the little clade of GATA genes that are preferentially expressed in roots (Manfield et al., 2007). In addition, a cell-type-specific transcriptome analyses indicated that *GATA3* expression is particularly increased in the root maturation zone (Birnbaum et al., 2003; Dinnyen et al., 2008). Although additional studies using the native *GATA3* promoter are required to confirm the predicted tissue localization, the possibility that *GATA3* is expressed more strongly in mature parts of the root is of particular interest, because the formation of lateral primordia and the subsequent lateral root emergence occur in the more distal parts of the root (Dubrovsky et al., 2000; Dubrovsky et al., 2001). Since lateral root elongation, but not lateral root number, was affected in *gata3-1* and *gata3-2* plants (Figures 21D, 22A,C and 23A), it is tempting to speculate that *GATA3* affects the emergence and the elongation of lateral roots, rather than their priming at the root meristem.

Additional evidence that *GATA3* plays a role in Fe signaling was provided by *GATA3* being significantly up-regulated in Fe-starved roots (Figure 25A, B). When grown in the separated agar plate system, *GATA3* expression was only up-regulated in roots grown under localized supply of 10  $\mu$ M Fe (Figure 25B). Under homogeneous supply of Fe, *GATA3* expression levels remained low. A genome-wide transcriptome analysis indicated that *GATA3* expression is induced by Fe in mature parts of the root (Dinnyen et al., 2008). Furthermore, since *GATA3* is restricted to roots (Manfield et al., 2007) and *gata3-1* and *gata3-2* mutants failed to elongate lateral roots into Fe-enriched agar plates, it is plausible to assume that *GATA3* functions in a root-endogenous regulatory circuit that controls lateral root development in response to Fe local availabilities. The comparison of *GATA3* expression levels in wildtype (*Col-gl*) and *frd3-1* mutant plants further supported this assumption, since *GATA3* expression was down-regulated in *frd3-1* roots (Figure 26A), although the shoots of this mutant were still chlorotic (Figure 15C). Importantly, this expression pattern differed greatly from that of *IRT1* and *FIT*. It was shown previously that both *IRT1* and *FIT* are under the control of local and

systemic signaling pathways (Vert et al., 2003; Wang et al., 2007). This is in line with the observations presented here, since *FIT* and *IRT1* transcript levels were still up-regulated in *frd3-1* roots supplied with 50  $\mu$ M Fe, whereas *GATA3* expression was already suppressed at 10  $\mu$ M Fe (Figure 26B, C).

Altogether, these expression analyses indicate that *GATA3* responds to Fe deficiency rather than to the local presence of Fe. Although these observations might go against the putative participation of *GATA3* in a signaling pathway controlled by the presence Fe, the following hypotheses may explain this apparent contradiction. (i) One hypothesis may suggest that *GATA3* acts as a Fe sensor. In this scenario, the absence of the metal (or substrate) - Fe or a chelated form of Fe - would induce the expression of the sensor. Conversely, the presence of Fe would trigger repression of *GATA3*. Such a metal-induced repression of sensors/receptors has been reported in the ethylene signaling pathway. When ethylene is present, the expression of the ethylene receptor *ETR2* is repressed in order to more precisely adjust the sensitivity of cells to this hormone (Chen et al., 2007). However, this hypothesis requires the existence of additional Fe sensors to regulate physiological Fe responses, such as the Fe acquisition machinery, since *IRT1* expression and the ferric-chelate reductase activity were not affected in *gata3-1* mutants (Figure 24). Interestingly, in fungi, GATA-type proteins have been shown to control Fe acquisition by negatively regulating the biosynthesis of siderophores (Zhou et al., 1998; Haas et al., 1999; Zhou and Marzluf, 1999; Oberegger et al., 2001; Oberegger et al., 2002; Chao et al., 2008; Schrettl et al., 2008). In *Schizosaccharomyces pombe* it has been shown that a GATA-type transcription factors similar to Fep1 down-regulates the Fe uptake machinery under sufficient Fe (reviewed in (Labbe et al., 2007). These GATA proteins possess a highly conserved region with four invariant cysteine residues that are located between two zinc finger domains, which are essential for DNA-binding (Pelletier et al., 2005; Chao et al., 2008). For a long time it was speculated that this region can bind Fe. Interestingly, it has recently been shown that ferric Fe is directly associated with the purified protein Sre1, which is the homolog of Fep1 in the fungal pathogen *Histoplasma capsulatum* (Chao et al., 2008). More importantly, when conserved cysteine residues located between the two zinc finger domains of Fep1 were mutated, the amount of Fe bound to the protein was

reduced and, as a consequence, the DNA-binding affinity of the transcription factor to its target genes was decreased (Chao et al., 2008). The current model suggests that after Fe depletion conditions, Fe binds to the GATA-type zinc finger Fep1 and, thus, allows Fep1 to bind to its target DNA sequence within the promoter of the regulated genes in order to repress transcription (Jbel et al., 2009). Once Fe is limited in the cell, less Fe is bound to Fep1 and the protein dissociates from the DNA, allowing transcription of the target genes to occur. However, all GATA-type transcription factors of plants have only one zinc finger (Reyes et al., 2004), and there is no evidence that a metal-binding domain similar to those of fungal GATA proteins is present in GATA3 from Arabidopsis.

(ii) A more straightforward explanation for the down-regulation of *GATA3* expression by Fe supply would be that *GATA3* is only one component of the Fe signaling pathway. This hypothesis would indicate that Fe deficiency sensitizes root cells by up-regulating one or more of the components of the pathway. This model could also explain why *GATA3* expression is down-regulated when sufficient Fe is present, since it would be reasonable for the cells to de-sensitize the system in order to avoid further lateral root elongation. A time-course expression of *GATA3* in response to Fe supply as well as the establishment of whether the protein is additionally regulated could be used to test this hypothesis. A similar regulatory process appears to be involved in the ANR1-dependent nitrate signaling. In fact, it has been shown that *ANR1* is specifically up-regulated by N starvation and rapidly down-regulated by nitrate re-supply (Gan et al., 2005).

Whether one of the aforementioned hypotheses holds true remains to be tested. The tissue-specific and subcellular localization of *GATA3* expression will certainly shed more light onto the role of *GATA3* in lateral root development in response to localized Fe. In addition, the comparison of genes being differentially regulated in *gata3-1* versus wildtype plants under localized Fe supply might allow the identification of downstream components of the Fe signaling cascade in roots, and thus to more precisely describe the position of *GATA3* therein.

Based on the results presented herein, a model for the Fe-dependent regulation of lateral root elongation is proposed (Figure 27). Root uptake of localized Fe is mediated by the Fe(II)-transporter IRT1 allowing to increase the symplastic Fe

pool. When Fe is applied to leaves, this symplastic pool can also be replenished by Fe derived from shoot-to-root translocation. This establishes a local gradient in tissue Fe concentrations in the primary root axis. AUX1 expression increases in response to the local symplastic Fe pool, thus facilitating the acropetal transport of auxin which then stimulates the emergence of initiated lateral root primordia and the elongation of emerged lateral roots; the latter being mainly the result of enhanced elongation of differentiated cells. It is assumed that GATA3 sensitizes the root to Fe by up-regulating the expression of one or more of the components involved in the root response to localized Fe supplies. *GATA3* expression is up-regulated in response to Fe deficiency. However, in contrast to *FIT*, *GATA3* responds only to a local, root-endogenous Fe signaling. Taken together, these findings provide an example on how the patchy availability of an essential microelement can re-program lateral root development to enable its spatially restricted exploitation from the growth substrate.

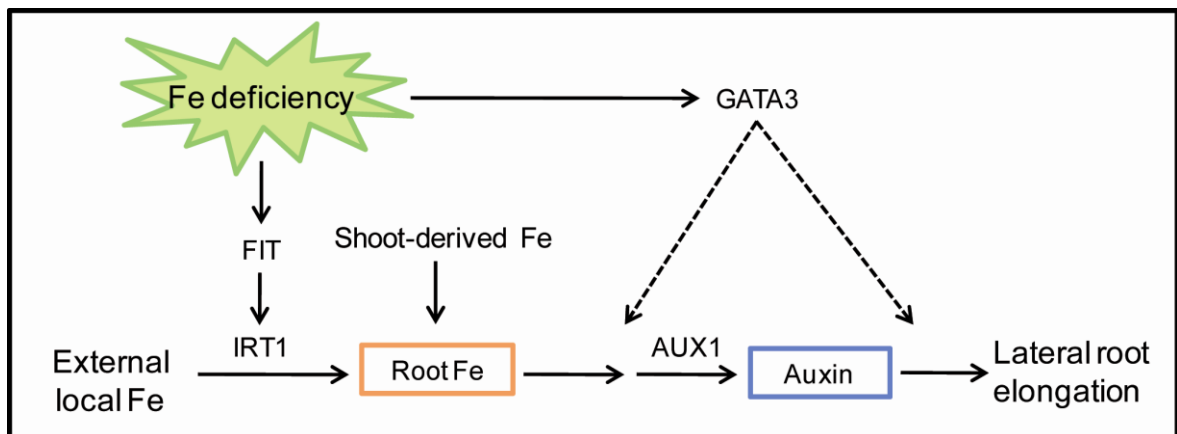


**Figure 27. Model for the Fe-dependent regulation of lateral root development.** Uptake of Fe via the high-affinity  $\text{Fe}^{2+}$  transporter IRT1 increases the symplastic root Fe pool. Additional Fe derived from the shoot and/or other parts of the root can contribute to this pool. Symplastic root Fe then changes auxin distribution in an AUX1-dependent manner by diverting more auxin towards the lateral root tip. Increased acropetal auxin movement in lateral roots is likely to increase the longitudinal elongation of mature cells, subsequently resulting in enhanced lateral root elongation. GATA3 probably sensitizes roots to Fe by regulating the expression of as yet unknown target genes.

## **5 Ionomics-based identification of a transcription factor involved in the signaling of P deficiency in Arabidopsis roots**

### **5.1 Introduction**

The accumulation of inorganic ions in plant tissues depends on genetic, developmental and environmental factors. Perturbations in any of these factors can result in significant changes in the ionome of different plants tissues. The term ionome was coined to describe the content of multiple inorganic ions measured in a certain sample at a given time (Lahner et al., 2003), even though not all measured elements are necessarily in an ionic form. It has been demonstrated that the ionome is sensitive to the physiological status of a plant (Baxter et al., 2008b) and might be significantly altered in genetically distinct plants (Rus et al., 2006; Baxter et al., 2008a; Baxter et al., 2009; Baxter et al., 2010). Ionomics-based screens have already been successfully employed for gene discovery purposes (Lahner et al., 2003; Rus et al., 2006; Baxter et al., 2008a; Baxter et al., 2008b; Baxter et al., 2009; Danku et al., 2009), leading for example to the identification of a novel allele of the Na<sup>+</sup> transporter HKT1 (Rus et al., 2006) and the molybdenum transporter MOT1 of Arabidopsis (Baxter et al., 2008a). However, in all these studies the ionomic profiling was used to screen natural accession lines and chemically or physically mutagenized plants. The main drawbacks from the screening of such populations are the subsequent laborious and time-consuming mapping steps to identify the underlying genetic components affecting the accumulation of a certain element.

Since a considerable amount of homozygous insertion lines has been made available, the screening of such collections of mutants may more rapidly allow discovering genes affecting a plant's ionome. Thus, in the present study, multi-element analysis was performed in a collection of homozygous *Ds*-transposon insertion lines from the RIKEN Institute (Kuromori et al., 2004; Ito et al., 2005). Selected were lines in which the *Ds*-transposon insertion was predicted to disrupt the expression of proteins with DNA-binding activity. The present analysis focused on transcription factor mutants because many biological processes in plants, such

as cell cycle, nutrient acquisition accumulation in plants are regulated at the level of gene expression (Century et al., 2008). The multi-elemental analysis of these lines allowed the identification of insertion mutants with significant alterations in the concentration of one or more elements in roots and shoots. One of the selected *Ds*-transposon lines showed a higher P accumulation in shoots and root phenotypes on low P supply, which made it attractive to investigate the role of the disrupted gene in more detail.

Because P is incorporated into nucleic acids, ATP and phospholipids, it is an essential element for the growth and development of plants, since it participates in many pivotal cellular processes such as energy conservation, photosynthesis and respiration (Marschner, 1995; Yuan and Liu, 2008). Although abundant in most soils, P availability is usually very limited, because P can be precipitated and bound by cations or converted into organic compounds (Marschner, 1995; Raghothama, 1999; Ticconi and Abel, 2004). Plants preferentially take up P as inorganic orthophosphate (Pi), the form of P which can be taken up and assimilated inside plant cells (Marschner, 1995; Raghothama, 1999). In order to cope with the frequently occurring limitation in available P forms, plants have evolved biochemical and morphological strategies to mobilize P. The main physiological responses are the up-regulation of high-affinity Pi transporters and the enhanced release of root exudates to mobilize Pi from otherwise unavailable pools in the soil (Raghothama, 1999; Rausch and Bucher, 2002; Ticconi and Abel, 2004). In addition, P starvation also triggers remarkable changes in root morphology and architecture. P-starved plants typically exhibit an increased length and density of root hairs (Bates and Lynch, 1996; Schmidt and Schikora, 2001), reduced primary root growth and stimulated lateral root development (Lopez-Bucio et al., 2003; Ticconi et al., 2004; Svistoonoff et al., 2007; Perez-Torres et al., 2008). All these morphological changes are thought to increase the explorative surface area of plant roots to counteract the limited diffusion of Pi in the soil solution.

It has been demonstrated that root architectural changes are controlled primarily by the external Pi availability rather than by systemic signals reporting the plant's internal P status. Indeed, the contact of the primary root tip with low Pi medium is



sufficient to trigger an inhibition of primary root growth (Svistoonoff et al., 2007), not only suggesting that this response is sensitive to the local availability of Pi, but also that the P deficiency sensing likely takes place at the root tip (Ticconi et al., 2004; Svistoonoff et al., 2007; Ticconi et al., 2009). The identification of mutants and their underlying genes further supported the existence of a local Pi sensing mechanism in roots. Phosphorous deficiency-induced primary root inhibition is reversed in *lpr1* and *lpr2* mutants, making them insensitive to external Pi concentrations (Svistoonoff et al., 2007). Since *lpr* mutants are defective in the expression of multicopper oxidases, it has been suggested that these proteins are involved in sensing Pi at the primary root tip (Svistoonoff et al., 2007). In contrast to *lpr1* and *lpr2*, *pdr2* mutants are overly sensitive to low P, exhibiting earlier loss of meristematic activity and marked inhibition of primary root elongation (Ticconi et al., 2004). More recently, it has been shown that *PDR2* encodes an ER-localized P<sub>5</sub>-type ATPase involved in the modulation of meristematic activity in response to P starvation (Ticconi et al., 2009). Under P starvation, *pdr2* mutant plants showed a lower accumulation of the root cell patterning proteins SCARECROW (SCR) and SHORT ROOT (SHR) in the primary root meristem, indicating that PDR2 is involved in maintaining SCR and SHR levels when P is limited. Interestingly, it has also been demonstrated that PDR2 and LPR1 likely act in the same P signaling pathway (Ticconi et al., 2009).

Although most P starvation-responsive genes are regulated at the transcriptional level (Wu et al., 2003; Misson et al., 2005), surprisingly few transcription factors have been found to be implicated in the regulation of this response. The MYB-factor PHR1 plays a major role in the regulation of many P starvation responses in Arabidopsis (Rubio et al., 2001). In agreement with its proposed regulatory function, a subset of P starvation-induced responses is deregulated in *phr1* mutants. Because *PHR1* itself is not transcriptionally regulated nor is its subcellular localization affected by P, the existence of another regulatory mechanism for PHR1 activation in response to P starvation has been proposed (Rubio et al., 2001). At least one level of post-translational regulation appears to be sumoylation, mediated by the stress-responsive SUMO E3 ligase SIZ1 (Miura et al., 2005; Miura et al., 2007). Besides PHR1, also MYB62, ZAT6 and WRKY75 have been implicated in the regulation of P starvation responses (Devaiah et al.,

2007b; Devaiah et al., 2007a; Devaiah et al., 2009). Conversely to *PHR1*, *ZAT6*, *WRKY75* and *MYB62* are up-regulated in response to low P (Misson et al., 2005; Devaiah et al., 2007b; Devaiah et al., 2007a; Devaiah et al., 2009). It appears, however, that these transcription factors play distinct roles during the adaptation to P shortage. Furthermore, whereas MYB62 and ZAT6 most likely act as repressors (Devaiah et al., 2007a; Devaiah et al., 2009), WRKY75 positively regulates a subset of P starvation-induced genes (Devaiah et al., 2007b). Besides modulating biochemical responses to low P, WRKY75 and ZAT6 also regulate some morphological traits in root architecture (Devaiah et al., 2007b; Devaiah et al., 2007a).

In the present study, an ionomics-based screening strategy was used to identify novel transcription factors involved in the regulation of nutrient accumulation in *A. thaliana*. It was observed that approximately 9% of the *Ds*-transposon-tagged lines screened showed a significant change in the accumulation of at least one element. Significant changes were observed for all elements measured, although at different frequencies. One of the pre-selected insertion mutants, which displayed greater accumulation of P and K in the shoots, showed multiple phenotypes when grown under restricted P supply. In these plants, the *Ds*-transposon disrupts the expression of *NGAL1* (At2g36080), which encodes a putative transcription factor from the plant-specific B3-type superfamily of DNA-binding proteins. Phenotypical analyses allowed proposing a role of NGAL1 in the regulation of root development under low P availability.

## 5.2 Material and methods

### 5.2.1 Screening of *Ds*-transposon lines

#### 5.2.1.1 Plant culture

In order to determine element concentrations in roots and shoots, wildtype (No-0) and *Ds*-transposon-tagged lines were grown hydroponically under nonsterile conditions in a growth cabinet. Seeds were germinated in darkness for 4 days and pre-cultured on moistened rock wool. After 1 week, tap water was replaced by a nutrient solution containing 2.0 mM  $\text{NH}_4\text{NO}_3$ , 1.0 mM  $\text{KH}_2\text{PO}_4$ , 1.0 mM  $\text{MgSO}_4$ ,

250  $\mu\text{M}$   $\text{K}_2\text{SO}_4$ , 250  $\mu\text{M}$   $\text{CaCl}_2$ , 100  $\mu\text{M}$  Na-Fe-EDTA, 50  $\mu\text{M}$  KCl, 30  $\mu\text{M}$   $\text{H}_3\text{BO}_3$ , 5  $\mu\text{M}$   $\text{MnSO}_4$ , 1.0  $\mu\text{M}$   $\text{ZnSO}_4$ , 1.0  $\mu\text{M}$   $\text{CuSO}_4$ , and 0.7  $\mu\text{M}$   $\text{NaMoO}_4$  (pH adjusted to 5.8 by KOH). The nutrient solution was replaced once a week during the first 3 weeks, twice in the 4<sup>th</sup> week, and every 2 days in the following weeks. During the last week of growth, sub-toxic levels of Cd (0.5  $\mu\text{M}$   $\text{CdCl}_2$ ), Ni (2.0  $\mu\text{M}$   $\text{NiCl}_2$ ), Co (2.0  $\mu\text{M}$   $\text{CoCl}_2$ ) and Na (500  $\mu\text{M}$  NaCl) were supplied to the nutrient solution. The conditions throughout the whole growth period were adjusted as follows: 10/14h light/dark; temperature 22°C/18°C (light/dark), 70% relative humidity at a light intensity of 280  $\mu\text{mol m}^{-2} \text{s}^{-1}$ . After 36 days, shoot and root tissues were harvested separately. Roots and shoots were rinsed in ddH<sub>2</sub>O for 1 minute and blotted dry with tissue paper. Fresh weights of entire rosettes (shoots) and roots were recorded. Samples were then dried at 65°C until constant weight.

### 5.2.1.2 Elemental analyses

Dry samples were wet-digested in a high pressure–digestion apparatus (UltraClave III, MLS, Leutkirch, Germany). Whole roots or shoots were weighed and placed into quartz vessels and digested using 2.5 mL concentrated  $\text{HNO}_3$ , 2 mL HCl and 1 mL ultrapure  $\text{H}_2\text{O}$ . All acids were of ultrapure quality. Elemental analysis was performed by ICP-OES (Varian Vista Pro) or, when necessary, by ICP-MS (ELAN 6000, Perkin Elmer). The concentrations of B, Ca, Cd, Co, Cu, Fe, K, Mo, Mg, Mn, Na, Ni, P, S and Zn were simultaneously measured. The ICP-MS was equipped with a standard Scott-type spray chamber and a cross-flow nebulizer. The internal standard rhodium (10  $\text{mg L}^{-1}$ ) was used to correct for the drift of the instrument. For quality control, the certified reference material SRM 1575a ('pine needles'; National Institute of Standards and Technology/NIST) was used. The recovery rate was >95%.

## 5.2.2 Phenotypical characterization of *ngal1* mutants

### 5.2.2.1 Plant material and growth conditions

The *Arabidopsis thaliana* ecotypes used in this study as wildtypes were Nossen-0 (No-0) and Columbia-0 (Col-0). For *in vitro* experiments, seeds were surface sterilized in 70% (v/v) ethanol and 0.05% (v/v) Triton X-100 and stratified at 4°C

for 2 days. Seeds were germinated in sterile petri dishes containing half-strength MS (Murashige and Skoog, 1962) medium. Seven-day-old seedlings were transferred to modified  $\frac{1}{2}$  MS medium containing 1.5 mM  $\text{KH}_2\text{PO}_4$  supplemented with 1.0% (w/v) Difco Agar (Becton Dickinson) and 0.5% sucrose. For P deficiency,  $\text{KH}_2\text{PO}_4$  was replaced by an equimolar concentration of KCl; for K starvation,  $\text{KH}_2\text{PO}_4$  and  $\text{KNO}_3$  were replaced by  $\text{NaH}_2\text{PO}_4$  and  $\text{Ca}(\text{NO}_3)_2$  and instead of agar, 0.8% (w/v) agarose was used; for N deficiency only 150  $\mu\text{M}$   $\text{NH}_4\text{NO}_3$  was added and 10 mM  $\text{KNO}_3$  was replaced by 10 mM KCl. For Fe treatments, Fe was either omitted (-Fe + 15  $\mu\text{M}$  ferrozine) or supplied as 75  $\mu\text{M}$  Fe-EDTA (+Fe) or 300  $\mu\text{M}$  Fe-EDTA (++Fe). The seedlings were grown in a 10-h-light/14-h-dark cycle at 22°C/19°C (light/dark) with 120  $\mu\text{mol photons m}^{-2} \text{ s}^{-1}$ . Plates were placed vertically to allow the roots to grow along the agar surface.

For P starvation experiments in hydroponic culture, wildtype and *ngal1-1* plants were grown under the conditions described in 4.2.1.1 for 5 weeks. In this case, 1.0 mM  $\text{KH}_2\text{PO}_4$  was replaced by an equimolar concentration of KCl.

### 5.2.2.2 Root growth measurements

After 10 days on treatments (depending on the experiment), root systems were scanned by an Epson Expression 10000XL scanner (Seiko, Epson) at 300 dpi resolution. Root growth measurements were taken from scanned images using WhinRHIZO version Pro2007d software (Regents Instruments Canada Inc.). Lateral root primordia were observed in a conventional light microscope (Axioskop, Zeiss, Germany) at 40-fold magnification. Developmental stages of lateral root initials were classified according to Zhang et al. (1999). Ten seedlings per genotype and treatment were assessed.

### 5.2.2.3 Plant transformation

The 2.025 bp promoter sequence of *NGAL1* was amplified from gDNA by PCR using specific primers (*pNGAL1-For*: 5'-CACCCATCACATCCAAATTTGAAG-3'; *pNGAL1-Rev*: 5'-ATAATACATCAAGTATGTATAAGATATG-3') and cloned into pENTR/D/TOPO entry vector, following to the manufacturer's instructions (Invitrogen). This construct was then sub-cloned either into pGWB3 (no promoter, C-GUS) or pGWB4 (no promoter, C-sGFP) binary vectors by the recombination of

attL and attR sites, according to the manufacturer's recommendations (Invitrogen). These vectors were obtained from Tsuyoshi Nakagawa (Research Institute of Molecular Genetics, Shimane University, Matsue, Japan). The binary vectors were then transferred to *Agrobacterium tumefaciens* (GV3101). Arabidopsis (Col-0) plants were transformed according to the floral dip method (Clough and Bent, 1998). Transgenic plants expressing *pNGAL1-GUS* or *pNGAL1-GFP* were selected on ½ MS agar media supplemented with 0.5% (w/v) sucrose and 40 mg L<sup>-1</sup> of kanamycin sulfate.

### 5.2.2.4 Histochemical analysis

For  $\beta$ -glucuronidase analysis, roots were incubated overnight at 37°C in a GUS reaction buffer containing 0.4 mg mL<sup>-1</sup> of 5-bromo-4-chloro-3-indolyl- $\beta$ -D-glucuronide, 50 mM sodium phosphate, pH 7.2, 0.5 mM ferricyanide, 0.5 mM ferrocyanide, 50 mM EDTA and 0.1 % (v/v) Triton-X. After 12 h, the roots were cleared and mounted as described in Malamy and Benfey (1997). Roots were photographed in a conventional light microscope (Axioskop, Zeiss, Germany) with a CCD camera (AxioCam HRc, Zeiss, Germany).

### 5.2.2.5 Propidium iodide staining of roots

Seven-day-old wildtype (No-0) and *ngal1-1* seedlings germinated on ½ MS were transferred to +P (1.5 mM Pi) or -P (15  $\mu$ M Pi) for additional 5 days of growth. Roots were stained with 10  $\mu$ g mL<sup>-1</sup> propidium iodide solution for 10-15 minutes. Stained roots were imaged with an LSM 510 META confocal microscope (Zeiss, Göttingen, Germany). The 488 nm excitation and 458-514 nm emission lines were used to image the propidium iodide-derived fluorescence. Images were assembled using Adobe Illustrator CS4.

### 5.2.2.6 Expression analysis

For quantitative real-time PCR, total RNA was extracted from roots of wildtype (No-0) or *ngal1-1* plants using the Trizol RNA extraction kit (Invitrogen). RNA was quantified and treated with DNase I (Invitrogen). One microgram of total RNA was reverse transcribed into cDNA using oligo(dT)<sub>24</sub> primers and the SuperScriptII Reverse Transcriptase Kit (Invitrogen). Quantitative real-time PCR analysis was performed using an Eppendorf mastercycler realplex (Eppendorf, Germany) and

QuantiTect SYBR Green qPCR Mix (Qiagen). Relative transcript abundance was calculated by the Mastercycler ep realplex software package version 2.0. Gene-specific primers were used to measure the relative expression of *UBIQUITIN2* (*UBQ2*) (*UBQ2*-For: 5'-CCAAGATCCAGGACAAAGAAGGA-3'; *UBQ2*-Rev: 5'-TGGAGACGAGCATAACACTTGC-3'); *NGAL1* (*NGAL1*-For: 5'-TCTGCTTTGAGGACGAGGAA-3'; *NGAL1*-Rev: 5'-AGCGAGGCATTGGATTGAAC-3'); *PHT1;1* (*PHT1;1*-For: 5'-GAGCTCTAGGAAATGGCCGAAC-3'; *PHT1;1*-Rev: 5'-TGACAATCGCCGTGAAATGA-3'); *PHT1;4* (*PHT1;4*-For: 5'-ACCCAATGCTACAACCTTCG-3'; *PHT1;4*-Rev: 5'-CTGGGTTCTGAGCCAAGTAC-3'); *IPS1* (*IPS1*-For: 5'-AGACTCGAGAAGGCTGATTCAGA-3'; *IPS1*-Rev: 5'-TTGCCCAATTCTAGAGGGAGA-3'); *SHR* (*SHR*-For: 5'-TCCTTCGCATTCTCAGCCAATG-3'; *SHR*-Rev: 5'-AGAGCTCGTTGAGCGTCCATAG-3'); *SCR* (*SCR*-For: 5'-ATTAGCGGTTGGAGG-3'; *SCR*-Rev: 5'-ACTAAGAACGAGGCGT-3'); *PDR2* (*PDR2*-For: 5'-CTTTTCACTACGTGGTCCGTGG-3'; *PDR2*-Rev: 5'-TGTCTCCCGAGGATGCTGAAT-3'); and *CYCB1;1* (*CYCB1;1*-For: CCTGGTGGAGTGGTTGATTGATG-3'; *CYCB1;1*-Rev: CGACATGAGAAGAGCACTGAGAC-3').

Semi-quantitative RT-PCR was used to measure the expression of *NGAL1* in *ngal1-1* (*Afor*: 5'-GGAGCAGATACGTCAAGGAGAA-3'; *Arev*: 5'-TGTGTGA GAACCGTCAGGTGTG-3') and *ngal1-2* (*Bfor*: 5'-TCTCTCTCAATTTTCACTCTCTTCC-3'; *Brev*: 5'-GCCCCATTAAGGTTCTGGTTTT-3') plants. As control, the expression of the housekeeping gene *ACTIN2* (*ACT2*-For: 5'-GACCTTGCTGACGTGACCTTAC-3'; *ACT2*-Rev: 5'-GTAGTCAACAGCAACAAAGGAGAGC-3') was assessed.

#### 5.2.2.7 Quantification of soluble Pi

Soluble Pi contents were determined according to (Chiou et al., 2006). Plant material from *in vitro* or hydroponic culture was frozen in liquid nitrogen and homogenized with extraction buffer containing 10 mM Tris, 1.0 mM EDTA, 100 mM NaCl, 1.0 mM  $\beta$ -mercaptoethanol, and 1.0 mM phenylmethylsulfonyl fluoride, pH 8.0 at a ratio of 1 mg sample (fresh weight) to 10  $\mu$ l extraction buffer. A total 100  $\mu$ l homogenized sample was mixed with 900  $\mu$ l 1% glacial acetic acid and incubated at 42°C for 30 min. The solution was then centrifuged at 13,000 *g* for 5

min, and 300 µl of the supernatant was used to measure the Pi concentration. 700 µl of assay solution (0.35% NH<sub>4</sub>MoO<sub>4</sub>, 0.86 N H<sub>2</sub>SO<sub>4</sub>, and 1.4% ascorbic acid) was added to 300 µl sample solution and incubated at 42°C for 30 min. The Pi concentration was measured by absorbance at 820 nm (Spectrophotometer, Genesys 10 Vis UV, Thermo). Results were expressed as mg Pi g<sup>-1</sup> fresh weight.

### **5.2.2.8 *In vivo* acid phosphatase staining**

The activity of acid phosphatases (APase) was monitored *in vivo* by transferring wildtype and *ngal1-1* plants grown for 7 days in +P or -P to an agar medium containing the APase stain 5-bromo-4-chloro-3-indolyl phosphate (BCIP; Trull and Deikman, 1998). The staining medium contained 50 mM Na-acetate (pH 4.9), 10 mM MgCl<sub>2</sub> and 0.04% of the APase substrate BCIP, as solidified by 0.8% agar. After overnight staining, plants were scanned at 600 dpi directly on the agar plate by using an Epson Expression 10000XL scanner (Seiko, Epson).

## **5.3 Results**

### **5.3.1 Element profiling of *Ds*-transposon insertion lines affected in the expression of transcription factors**

The elemental profiles were determined in 302 transgenic lines harboring *Ds*-transposon insertions in genes encoding for DNA-binding proteins (Kuromori et al., 2004; Ito et al., 2005). All lines along with the wildtype accession No-0 were grown under adequate nutrient supply with sub-toxic levels of Ni, Cd, Co and Na. Unfortunately, a considerable variation among samples from the same mutant line was observed for root concentrations, especially regarding the micronutrients (data not shown). Thus, unless indicated otherwise, the results presented here are the elemental profiles of shoots.

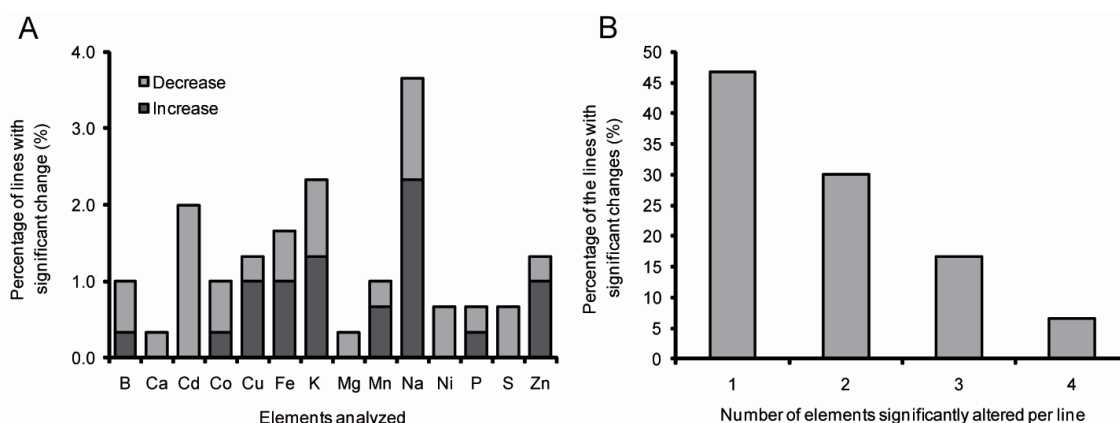


**Figure 28. Percentage of *Ds*-transposon-tagged lines with significant change in element accumulation in shoots.** (A) Percentage of lines with significantly increased or decreased accumulation of a particular element in the shoots. Considered as significant were those changes which were statistically different in relation to wildtype (No-0) by means of Student's *t* test ( $P < 0.05$ ). (B) Frequency of *Ds*-transposon mutants showing significant changes in the accumulation of one or more elements.

Approximately 9% of the lines screened showed statistically significant differences in the shoot concentration of at least one of the elements measured by ICP-OES or ICP-MS. Candidate lines were found for all elements analyzed (Figure 28A). Most of the lines showing significant changes in shoot ion concentrations were affected in the accumulation of Na, K and Cd. In fact, 3.6% of the lines screened showed significant changes in Na concentrations in the shoot (Figure 28A). By contrast, less than 0.4% of the lines exhibited significant changes in the accumulation of Ca and Mg in their shoots. The majority (~63%) of the significant changes observed were reductions in shoot concentrations (Figure 28A). However, some interesting patterns could be observed. For example, most of the lines with significant changes in shoot concentration of Cu, Fe, K, Mn, Na and Zn exhibited a higher accumulation than wildtype plants (Figure 28A). By contrast, all lines with altered accumulation of Ca, Cd, Mg, Ni and S showed significant reductions in shoot concentrations.

Another important result from this elemental profiling was that more than 50% of the lines identified showed significant changes in the shoot concentration of more than one element (Figure 28B). Table 3 lists all *Ds*-transposon lines showing significant changes in shoot concentrations of one or more elements. These lines showed distinct ion profiles. For example, four (i.e. 50%) of the lines with a



significant deviation in K accumulation exhibited also a concomitant significant change in Na levels (Table 3). This observation is most likely due to the fact that K and Na concentrations showed a significant positive correlation ( $r = 0.58$ ;  $P < 0.001$ ; Table 4). It is noteworthy, however, that only the minority (~37%) of the lines with altered Na concentrations showed simultaneously alterations in K concentrations (Table 3).

Correlations were calculated between the concentrations of elements in the shoots as well as between shoot ion concentrations and shoot or root biomass. As shown in Table 4, shoot and root fresh weight were strongly and significantly correlated ( $r = 0.86$ ;  $P < 0.001$ ). Single element concentrations had only low correlation coefficients with root and shoot fresh weights. As an exception, the shoot K concentration showed a significant correlation with shoot biomass ( $r = 0.41$ ;  $P < 0.001$ ; Table 4). Some significant correlations between element concentrations in shoots were observed. More noticeable were the positive correlations of Ca with Mg, Mn, P and Co; and Mg with Ca, P, Co and Ni (Table 4).

### 5.3.2 Isolation of a *Ds*-transposon-tagged line hypersensitive to low P

Based on the identification of *Ds*-transposon-tagged lines with altered shoot element concentrations (Table 3), those lines were selected which showed in addition a conditional growth phenotype for the corresponding element. For that purpose, pre-selected lines were grown *in vitro* under limiting or toxic concentrations of that particular element. A primary goal from this study was to identify transcription factors involved in the regulation of Fe homeostasis. However, none of the lines that showed significant changes in Fe accumulation exhibited distinct growth defects or improvements when subjected to low or toxic Fe concentrations (data not shown). Instead, one *Ds*-transposon line pre-selected based on altered accumulation of K and P showed altered root architecture when grown under low P. This line – RATM12-1961-1 – exhibited a significant 25% and 17% increase in the shoot accumulation of K and P, respectively (Figure 29A, D, E). The larger accumulation of P and K were not accompanied by significant changes in shoot or root biomass (Figure 29B, C). In these plants, the *Ds*-transposon is inserted into the first exon of the open reading frame of At2g36080,

a gene predicted to encode the putative B3-type transcription factor *NGAL1* (Figure 30A, B; Alvarez et al., 2009). Thus, RATM 12-1962-1 was renamed as *ngal1-1*. RT-PCR expression analysis revealed that *NGAL1* expression is completely disrupted in *ngal1-1* roots and shoots (Figure 30C). On P-deficient medium, *ngal1-1* plants showed visible root architectural changes when compared

**Table 3.** List of *Ds*-transposon insertion lines with a significant change in the shoot concentration of one or more elements. Shown are percent changes in relation to wild type (No-0) plants. These differences are statistically significant (*t*-test;  $P \leq 0.05$ ).

<i>Ds</i> line (RATM)	B	Ca	Cd	Co	Cu	Fe	K	Mg	Mn	Na	Ni	P	S	Zn
11-0797-1		-20.2	-36.7										-24	
11-1818-1	34.4													
12-0565-1										32.6				
12-1962-1							25.7					15.2		
12-2311-1						-26.2						-20.6		
12-2919-1										31.3				
12-3469-1			-39										-24.4	
12-3742-1										64.6				
12-4902-1					25.8									
12-5633-1										29.7				
13-1146-1			-27.3											
13-1214-1						31.3								
13-3072-1				-30.9							-38.2			
15-0256-1														-37.9
15-0871-1						25.3	-36		26.4	-25.7				
15-0881-1				-16.5				-20.3		-26.7	-30.8			
15-2971-1							25.1							
15-3163-1					-16		-31.6			-22.9				
15-4779-1			-25.9			-21.2								
15-5103-1			-27.8											
16-0043-1			-21				34.6							
16-0077-1					22.8				29.7					57.8
16-0188-1							31.4			12.8				
16-0292-1						36.4								42.5
16-0842-1	-19.3						-25.4							
16-0906-1										24.4				
16-1066-1					21.4					-18.8				31.7
16-2733-1				30										
16-2749-1	-26.5													
16-3040-1							37.8		-23.3	50.6				

**Table 4.** Correlation of all nutrient concentrations measured in the shoot. Pearson's correlation coefficients ( $r$ ) for the correlation of all shoot nutrient concentrations and rosette and root weight. Significant correlation coefficients ( $P < 0.01$ ) are highlighted in bold.

	Shoot	B_s	Ca_s	Cd_s	Co_s	Cu_s	Fe_s	K_s	Mg_s	Mn_s	Mo_s	Na_s	Ni_s	P_s	S_s	Zn_s
Root	<b>0.86</b>	-0.20	0.36	0.00	0.22	0.32	-0.19	0.23	0.25	0.08	0.23	0.14	0.08	0.22	-0.05	0.25
Shoot		-0.10	0.20	0.06	0.00	0.22	-0.14	<b>0.41</b>	0.13	-0.05	0.14	0.26	-0.04	0.23	0.03	0.15
B_s			-0.02	0.14	-0.19	-0.20	0.25	0.36	0.25	-0.25	-0.21	0.32	0.20	0.13	0.43	-0.44
Ca_s				-0.33	<b>0.52</b>	0.26	-0.19	-0.21	<b>0.67</b>	<b>0.59</b>	-0.10	-0.22	0.45	<b>0.59</b>	0.04	0.48
Cd_s					-0.19	0.40	0.21	0.43	-0.34	-0.17	0.28	0.28	-0.29	-0.39	<b>0.50</b>	-0.23
Co_s						0.36	-0.25	-0.14	<b>0.61</b>	0.32	0.13	-0.12	<b>0.68</b>	0.32	-0.02	<b>0.53</b>
Cu_s							0.15	0.02	0.08	0.31	0.35	0.10	0.08	0.07	0.25	0.43
Fe_s								0.03	-0.25	0.14	0.11	0.28	-0.25	0.04	0.10	0.00
K_s									0.20	<b>-0.52</b>	0.24	<b>0.58</b>	0.19	0.08	<b>0.54</b>	-0.45
Mg_s										0.13	-0.05	0.03	<b>0.80</b>	<b>0.61</b>	0.29	0.15
Mn_s											-0.09	-0.24	0.00	0.43	-0.15	<b>0.67</b>
Mo_s												0.44	-0.01	-0.18	0.07	0.00
Na_s													0.06	0.09	0.19	-0.25
Ni_s														0.44	0.24	0.09
P_s															0.09	0.34
S_s																-0.30

to the wildtype (Figure 30D). In fact, primary root elongation was significantly inhibited in *ngal1-1* plants subjected to low P (Figure 30D, E). In order to analyze the phenotype in a second mutant allele, one T-DNA insertion mutant of At2g36080, in another genetic background (Col-0), was selected (Figure 30B). Although *NGAL1* expression is not completely repressed in the *ngal1-2* T-DNA mutant (Figure 30G), these plants also showed a significant inhibition of primary root length under low P, even though to a lower extent than *ngal1-1* (Figure 30F, H).

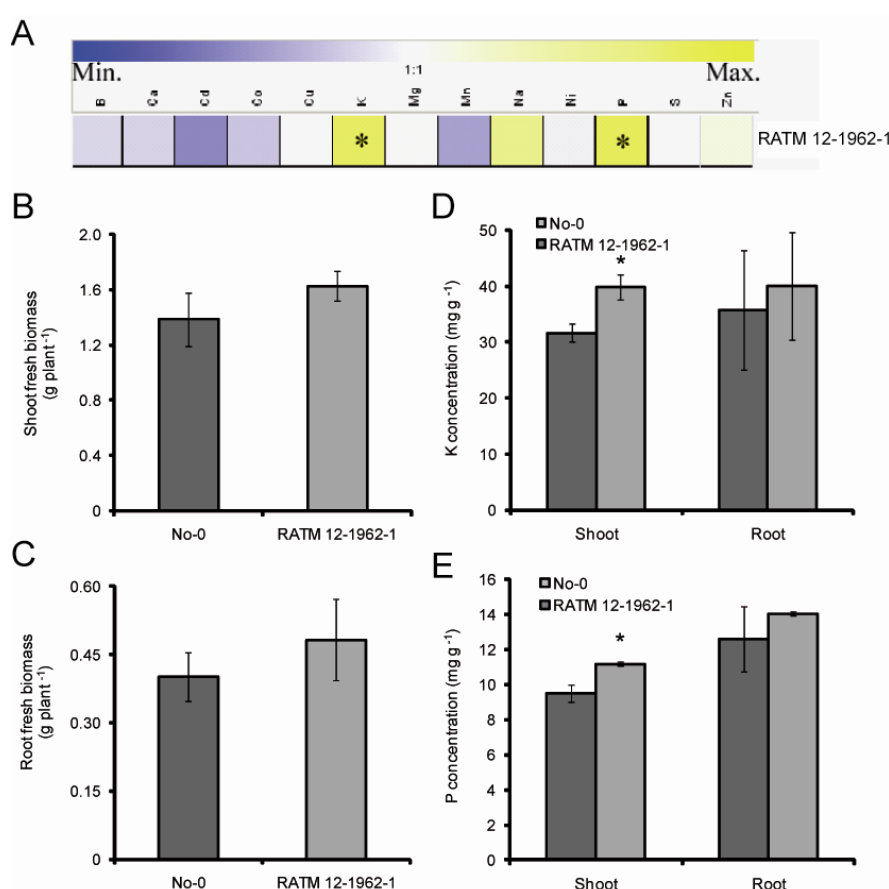


**Figure 29. Identification of one *Ds*-transposon insertion line with significant changes in the accumulation of K and P.** (A) Heat-map representation of the relative shoot elemental profile of the *Ds*-transposon insertion line RATM 12-1962-1. \* indicates significant change in relation to wildtype ( $t$  test;  $P < 0.05$ ). (B) Shoot and (C) root fresh biomass, and total shoot and root concentrations of (D) K and (E) P in wildtype (No-0) and RATM 12-1962-1 plants grown in hydroponic culture for 36 days. Bars indicate means  $\pm$  SD ( $n \geq 3$  replicates). \* denotes a significant difference to the wildtype by means of Student's  $t$  test ( $P < 0.05$ ).

**Table 5.** Correlation of all nutrient concentrations measured in the root. Pearson's correlation coefficients ( $r$ ) for the correlation of all root nutrient concentrations and rosette and root weight. Significant correlation coefficients ( $P < 0.01$ ) are highlighted in bold.

	shoot	B_r	Ca_r	Cd_r	Co_r	Cu_r	Fe_r	K_r	Mg_r	Mn_r	Mo_r	Na_r	Ni_r	P_r	S_r	Zn_r
Root	<b>0.85</b>	-0.15	-0.14	-0.17	0.01	-0.10	-0.14	0.15	-0.03	-0.21	0.07	0.00	0.06	0.01	0.09	-0.12
Shoot		-0.17	-0.16	-0.08	0.01	-0.05	-0.23	0.19	0.00	-0.11	0.07	0.04	0.06	0.04	0.16	-0.08
B_r			-0.08	0.08	-0.20	-0.01	0.14	-0.45	-0.19	-0.05	-0.18	0.25	-0.25	-0.36	-0.47	0.03
Ca_r				0.22	-0.16	0.33	<b>0.58</b>	-0.36	<b>0.71</b>	0.31	-0.35	0.26	-0.33	0.08	-0.24	0.35
Cd_r					0.22	<b>0.66</b>	0.00	-0.14	0.07	0.43	-0.17	0.18	-0.17	-0.01	-0.05	<b>0.89</b>
Co_r						-0.07	-0.12	0.44	0.05	0.07	0.30	0.18	<b>0.81</b>	0.46	<b>0.50</b>	0.32
Cu_r							0.06	-0.08	0.09	0.14	-0.10	0.18	-0.38	0.08	-0.02	<b>0.61</b>
Fe_r								-0.49	0.22	0.32	-0.43	0.04	-0.23	0.16	-0.47	0.19
K_r									0.02	-0.13	<b>0.61</b>	0.22	<b>0.61</b>	<b>0.66</b>	0.94	-0.24
Mg_r										0.18	-0.09	0.20	0.02	0.22	0.11	0.16
Mn_r											-0.32	0.14	-0.03	0.07	-0.08	0.47
Mo_r												0.16	0.41	0.43	<b>0.61</b>	-0.26
Na_r													0.11	0.37	0.28	0.11
Ni_r														0.48	<b>0.63</b>	-0.16
P_r															<b>0.63</b>	-0.01
S_r																-0.14



Primary root elongation of *ngal1-1* plants could be almost fully restored by the supply of  $\geq 50 \mu\text{M}$  Pi (Figure 31), indicating that the inhibition was restricted to very limited P availability. In a concentration range of 50 – 1000  $\mu\text{M}$  Pi, *ngal1-1* still showed a slight disadvantage in primary root elongation, but caught up wildtype levels at 1.5 mM Pi supply. The inhibition of primary root elongation is a typical root architectural change displayed by most *Arabidopsis* accessions when subjected to P-deficient growth conditions (Williamson et al., 2001; Lopez-Bucio et al., 2002; Lopez-Bucio et al., 2003). However, in *ngal1-1* plants this root architectural change appeared hypersensitive when they were grown under limited P availability. In addition, compared to wildtype (No-0) plants, P-starved *ngal1-1* plants not only exhibited significantly shorter primary roots (Figure 30E), but also increased lateral root length and density (Figure 32B, C). However, conversely to primary root inhibition, the increased lateral root length was independent of P supply, since *ngal1-1* lateral roots were also longer when grown under sufficient P (Figure 32C). The root/shoot ratio was not significantly altered in *ngal1-1* when compared to the wildtype (Figure 32D), indicating that the stronger inhibition of primary root elongation was compensated for by the increased development of lateral roots. Altogether, these results indicate that *NGAL1* plays a role in the modulation of root architectural changes in response to low P supply. Furthermore, the loss of *NGAL1* expression results in a hypersensitive reaction to the absence of P in the growth medium.

### 5.3.3 Role of *NGAL1* in lateral root development

In order to compare lateral root formation in a time-course between wildtype and *ngal1-1* plants, seven-day-old plants were transferred to  $\frac{1}{2}$  MS media supplemented with sufficient (1.5 mM Pi) or limited P ( $\sim 15 \mu\text{M}$  Pi) concentrations. After 2 and 4 days, the proportion of lateral root primordia at different developmental stages was determined according to the classification proposed by Zhang et al. (1999). Already after 2 days on treatment, *ngal1-1* plants showed an increased proportion of emerged lateral root primordia (Figure 33A). At this time point, the transfer to a P-deficient medium had almost no effect on the development of lateral root initials in wildtype plants (Figure 33A). In P-starved

*ngal1-1* plants, however, a significant increase in the frequency of lateral roots at developmental stage D (emerged,  $\geq 0.5$  mm long) could be observed. After 4 days on treatments, the effect of the loss of *NGAL1* on lateral root development was even more pronounced, since especially under low P more lateral roots were at stage D and less at stage A (Figure 33B). Altogether, these results indicate that *NGAL1* affects lateral root development mainly by negatively modulating the emergence of lateral root primordia. Since enhance lateral root initiation was also observed under sufficient P availability, it appears that *NGAL1* plays also a P-independent role on lateral root development.

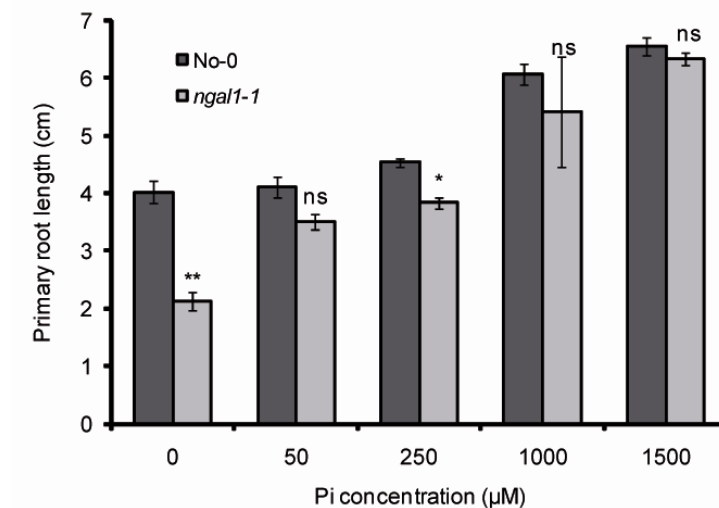


**Figure 31. The short-root phenotype of *ngal1-1* is reversed by an increasing supply of Pi.** Eight-day-old wild-type (No-0) and *ngal1-1* plants were transferred to  $\frac{1}{2}$  MS media supplemented with the indicated Pi concentrations and grown for 12 days. Bars represent means  $\pm$  SE ( $n = 10$ ). \* denotes significant and *ns* not significant differences by Student's *t* test ( $P < 0.05$ ).

#### 5.3.4 The short-root phenotype of *ngal1-1* is specific for P starvation

Besides low P availability, other nutritional deficiencies have also been demonstrated to trigger substantial changes in root architecture (Lopez-Bucio et al., 2003). Thus, primary root elongation of *ngal1-1* plants was also assessed under N, K and Fe starvation. As shown in Figure 34A, the primary root of *ngal1-1* plants was 50% shorter compared to the wildtype under low P, whereas no significant difference was observed under any other nutritional deficiency tested. These results indicated that the hypersensitive primary root inhibition observed in



*ngal1-1* plants is specific for P deficiency. Importantly, although *ngal1-1* plants accumulated more K in their shoots, no significant differences in terms of root growth, biomass production or chlorophyll concentrations were observed when these plants were grown under low K (Figure 34A, C, D).

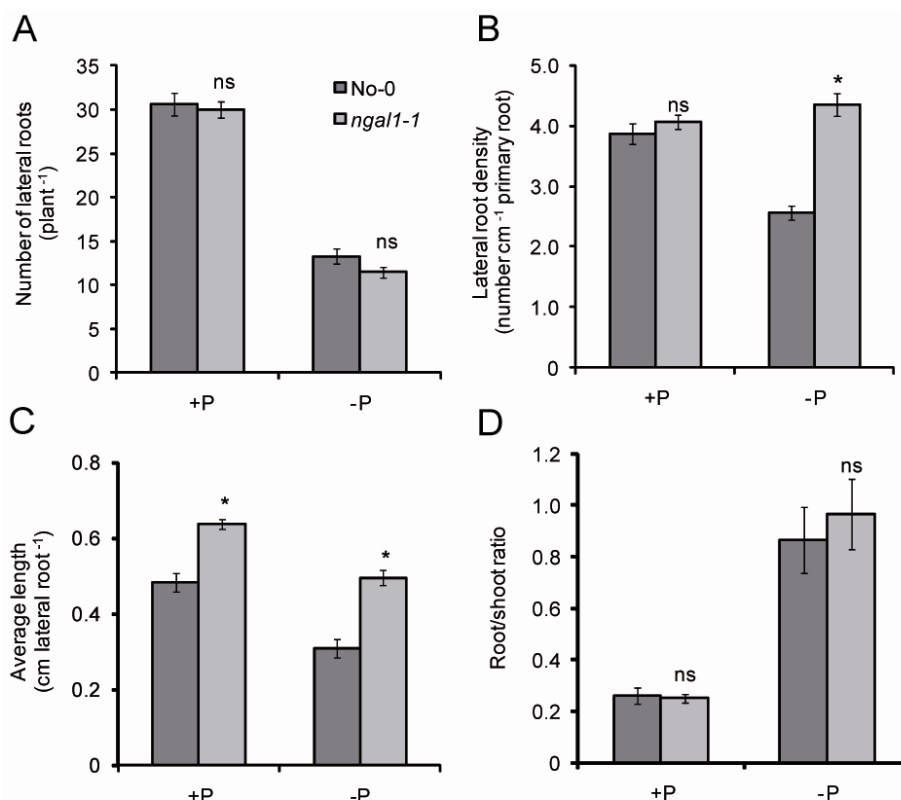


**Figure 32. The influence of NGAL1 on lateral root development.** (A) Total number of lateral roots, (B) lateral root density, (C) total lateral root length and (D) root/shoot fresh weight ratio of wildtype (No-0) and *ngal1-1* plants grown under +P (1.5 mM Pi) or -P (15  $\mu$ M Pi). Eight-day-old wildtype (No-0) and *ngal1-1* seedlings were transferred to the indicated treatments. After 10 days, plates were scanned. Bars represent means  $\pm$  SD ( $n = 10$ ). \* denotes significant and *ns* not significant difference by Student's *t* test ( $P < 0.05$ ).

Since the bioavailability of Fe is negatively affected in the presence of P, it has been proposed that under low P supplies the availability of Fe rises to even toxic levels in roots (Hirsch et al., 2006; Ward et al., 2008). Thus, primary root inhibition under low P may be a consequence of Fe toxicity (Ward et al., 2008). In fact, the supply of high Fe concentrations (300  $\mu$ M) caused a marked repression of shoot and root growth in both wildtype and *ngal1-1* plants, irrespective of the P supply (data not shown). Furthermore, high external Fe concentrations had a negative impact on primary root elongation (Figure 34B). However, when high Fe was

supplied together with sufficient P, the primary root inhibition of wildtype and *ngal1-1* plants occurred at a similar extent (Figure 34B). By contrast, a concomitant limitation of Fe and P alleviated the inhibition of primary root growth and partially restored the *ngal1-1* short-root phenotype. However, even under this condition *ngal1-1* plants still exhibited significantly shorter primary roots (Figure 34B). The supply of 75 $\mu$ M Fe to P-starved plants, in turn, reduced the elongation of the primary root in both wildtype and *ngal1-1* plants (Figure 34B). Thus, despite the negative effect of Fe on primary elongation of P-deficient plants, *ngal1-1* plants were already impaired in primary root elongation in the absence of Fe, indicating that the short-root phenotype of *ngal1-1* plants resulted primarily from a limited P availability rather than from an indirect effect of Fe toxicity.

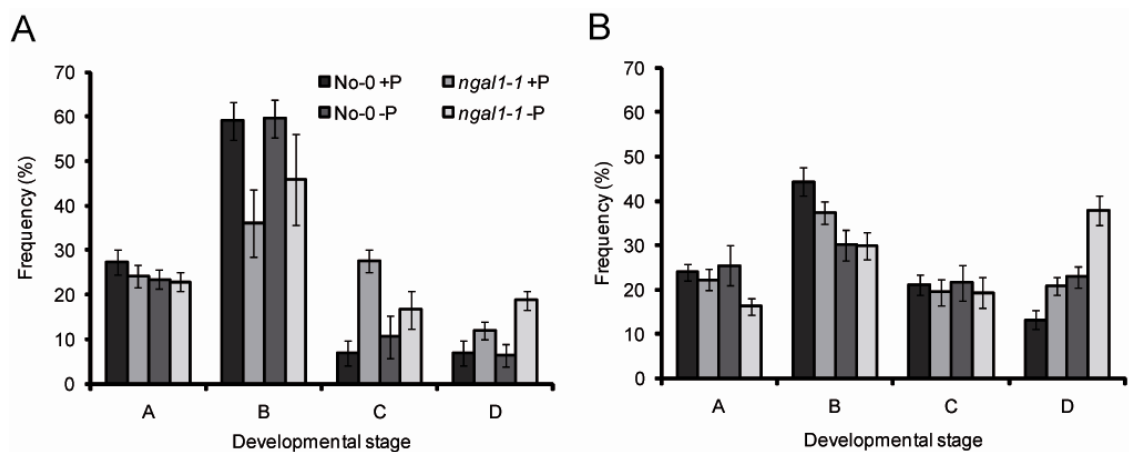


**Figure 33. Lateral root emergence is stimulated in *ngal1-1* plants.** (A,B) Lateral root development in wildtype (No-0) and *ngal1-1* plants in response to low Pi. Seven-day-old plants were transferred to either +P (1.5 mM Pi) or -P (15  $\mu$ M Pi). The developmental stage of lateral root initials was assessed after (A) 2 or (B) 4 days according to the classification proposed by (Zhang et al., 1999). Shown are means  $\pm$  SD (n = 10). Stage A, lateral root primordia with up to 3 cell layers; Stage B, unemerged lateral root, >3 cell layers; Stage C, emerged lateral root, <0.5 mm long; Stage D, emerged lateral root,  $\geq$ 0.5 mm long.

### 5.3.5 The effect of *NGAL1* on some P starvation-induced responses

Apart from root architectural changes, P starvation triggers also a series of biochemical responses in roots committed to increase Pi mobilization in the rhizosphere and subsequent Pi uptake (Raghothama, 1999; Ticconi and Abel, 2004). In order to investigate the involvement of *ngal1-1* in the regulation of P deficiency-induced responses, a subset of P deficiency-responsive genes was selected. Because AtPHT1;1 and AtPHT1;4 represent the two major high-affinity

Pi transporters in roots (Muchhal et al., 1996; Shin et al., 2004), their expression was measured in response to 5 days of P starvation in wildtype and *ngal1-1* roots. As expected, mRNA levels of *AtPHT1;1* and particularly *AtPHT1;4* were markedly up-regulated by P starvation. However, the loss of *NGAL1* did not significantly affect the expression levels of these genes (Figure 35A, B). Besides Pi transporters, genes involved in P signaling, such as *AtIPS1*, have also been shown to rapidly respond to P limitation (Franco-Zorrilla et al., 2007). In line with previous work, *AtIPS1* expression was strongly up-regulated by low P, even though its expression levels were reduced in *ngal1-1* roots when compared to wildtype (Figure 35C). Nevertheless, even in *ngal1-1* roots, *IPS1* transcription levels were still increased by more than 200-fold in response to P starvation.

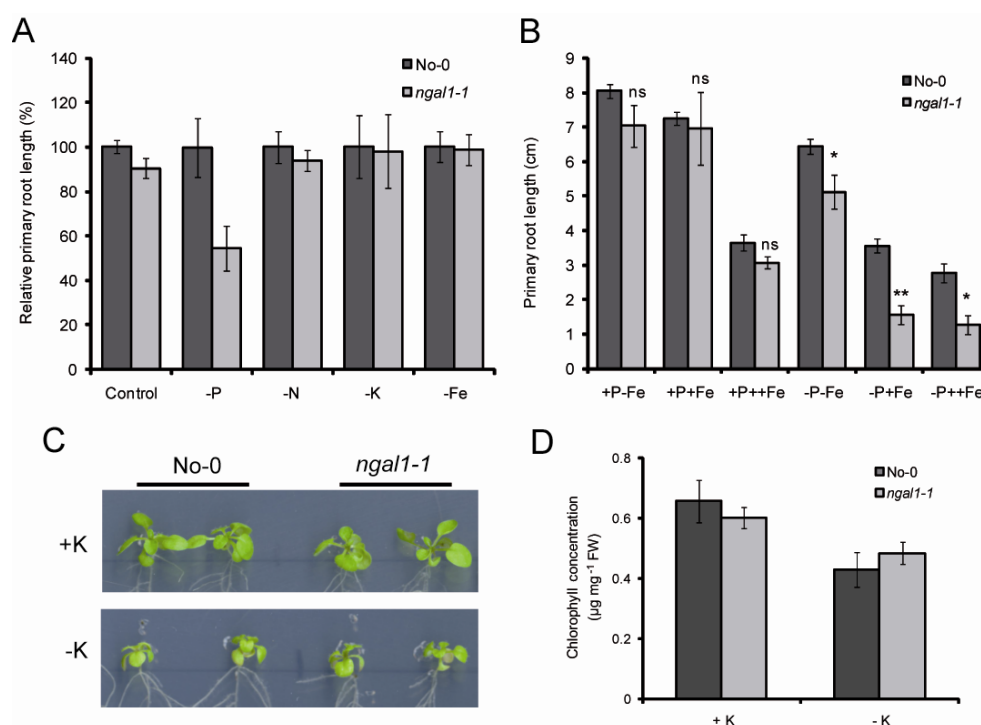


**Figure 34. Short-root phenotype of *ngal1-1* plants is specific for P limitation.** (A) Relative primary root length of *ngal1-1* plants grown on  $\frac{1}{2}$  MS media adequately supplied with all nutrients (control) or depleted in one of the indicated nutrients. Seven-day-old seedlings germinated on  $\frac{1}{2}$  MS were transferred to the indicated treatments for another 10 days. (B) Effect of combined P and Fe supplies on primary root elongation of wildtype (No-0) and *ngal1-1* plants. Eight-day-old wildtype (No-0) and *ngal1-1* seedlings were transferred to the indicated treatments. After 10 days, plates were scanned and primary root length was determined by image analysis. +P (1.5 mM Pi), -P (15 µM Pi), -Fe (no Fe added + 15 µM ferrozine) +Fe (75 µM Fe-EDTA) and ++Fe (300 µM Fe-EDTA). Bars represent means  $\pm$  SD ( $n = 10$ ). \* denotes significant and *ns* not significant difference by Student's *t* test ( $P < 0.05$ ). (C) Growth and (D) chlorophyll concentration of wildtype (No-0) and *ngal1-1* plants in response to K starvation. Seven-day-old seedlings were transferred either to +K (1.5 mM K) or -K (no K added) for 10 days. Bars represent mean  $\pm$  SD from 5 seedlings per replicate ( $n = 5$  replicates).

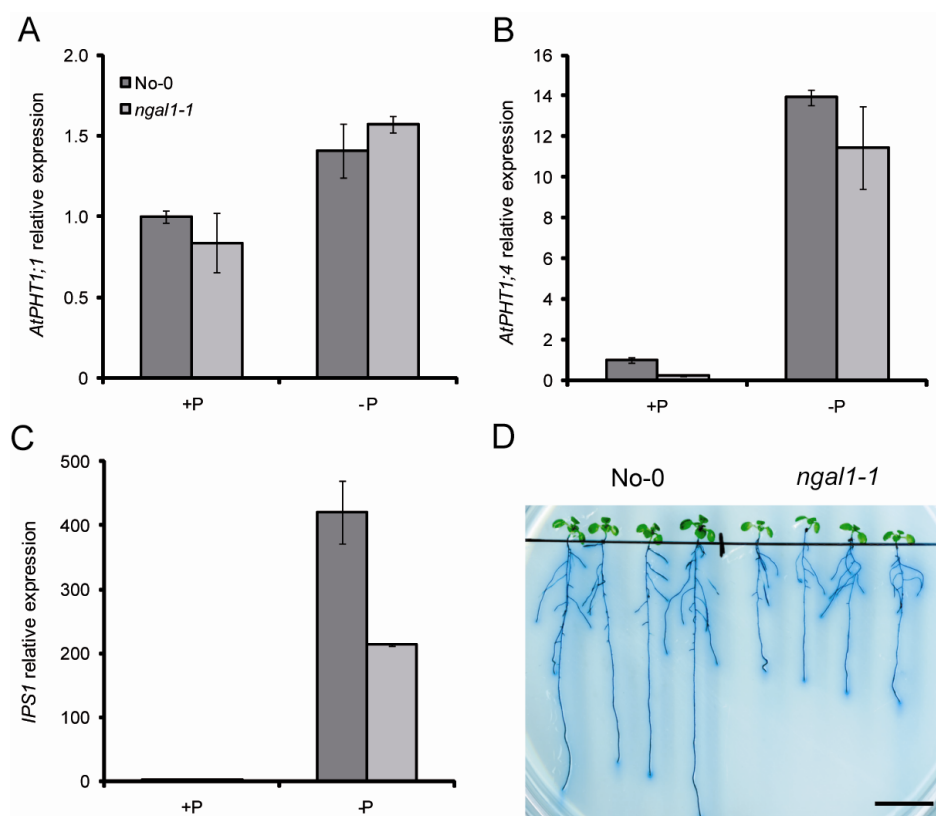


**Figure 35. Effect of NGAL1 on the activation of P deficiency-induced responses in roots.** (A–C) Relative expression levels of (A) *AtPHT1;1* (*AtPT1*), (B) *AtPHT1;4* (*AtPT2*) and (C) *IPS1* in roots of wildtype (No-0) and *ngal1-1* plants. Eight-day-old seedlings were transferred to  $\frac{1}{2}$  MS medium supplement with either +P (1.5 mM Pi) or –P (15  $\mu$ M Pi). After 5 days on treatments, root samples were collected for RNA extraction. Shown are relative levels of transcripts in roots as determined by quantitative RT-PCR (means  $\pm$  SE;  $n = 3$  replicates). (D) *In vivo* acid phosphatase (APase) activity. Eight-day-old seedlings were transferred to  $\frac{1}{2}$  MS medium with +P (1.5 mM Pi) or –P (15  $\mu$ M Pi). After 7 days on treatments, APase staining was performed. The experiment was repeated twice and yielded similar results. Shown are representative plants. Scale bar = 1 cm.

Phosphorous starvation also increases the secretion of extracellular acid phosphatases (APases), as a strategy to mobilize more Pi from the rhizosphere (Abel et al., 2002; Tran et al., 2010a; Tran et al., 2010b). To test whether *NGAL1* is required for the induction of this response, roots of wildtype and *ngal1-1* seedlings grown for 7 days under +P or –P conditions were transferred to agar media containing the APase stain BCPI (Trull and Deikman, 1998). The action of root-released APases on the substrate BCIP generates a blue precipitate, and this intensity is indicative for the amount of APases present at the root surface. As expected, *in vivo* APase staining was almost absent in plants grown under +P (data not shown). When exposed for 7 days to –P, APase staining was strongly induced, but not affected by the loss of *NGAL1* (Figure 35D).

Although only a subset of P deficiency-induced responses was tested, the results presented here indicate that the loss of *NGAL1* does most likely not significantly affect the induction of P-mobilizing root responses.

### 5.3.6 The short-root phenotype of *ngal1-1* is not due to a nutritional defect

The analysis of P deficiency-regulated responses revealed that *ngal1-1* plants are not impaired in the activation of major components of Pi mobilization (Figure 35). Thus, a defect in Pi acquisition is probably not the cause for the hypersensitive inhibition of primary root elongation in *ngal1-1* plants when grown under low P availability (Figures 30D, E). One could envisage two hypotheses to explain the hypersensitive primary root of *ngal1-1* plants under low P observed: (1) the shorter primary root of *ngal1-1* plants grown under low P could reflect a nutritional effect; or (2) this phenotype could be the consequence of a defect in P signaling. In order to test the first hypothesis, soluble Pi contents were measured in shoots and roots of wildtype and *ngal1-1* plants. A higher accumulation of Pi was observed in roots and shoots of *ngal1-1* plants when grown on P-sufficient medium (Figure 36A). The same tendency held true for plants grown on hydroponic solution (Figure 36B, C). These observations went along with the increased P accumulation measured in *ngal1-1* plants during the ionomics-based screen reported before (Figure 29). As expected, the transfer of plants to P-deficient medium decreased markedly the Pi concentrations in roots and shoots. Under P deficiency, Pi levels measured in *ngal1-1* plants were similar to those of the wildtype irrespective of whether plants were grown on agar (Figure 36A) or in nutrient solution (Figure 36B, C). According to these observations, the short-root phenotype of *ngal1-1* plants is highly unlikely to result from a lower P nutritional status.

The time-dependent assessment of primary root elongation revealed that *ngal1-1* plants suffer from an earlier inhibition of primary root growth (Figure 37A). Indeed, whereas the primary root elongation rate in wildtype plants was significantly decreased only after 8 days on  $-P$ , in *ngal1-1* plants the elongation rate was markedly reduced already after 4 days (Figure 37A). These results indicate that the loss of *ngal1-1* results in an earlier inhibition of primary root elongation under P-limited conditions.

Thus, in order to test the alternative hypothesis, i.e. that the hypersensitive primary root inhibition of *ngal1-1* plants reflected a defect in P signaling pathway, plants were grown on a horizontal split-root setup, in which seven-day-old seedlings were transferred to horizontally-split agar plates, so that the primary root apex was placed on the lower segment.

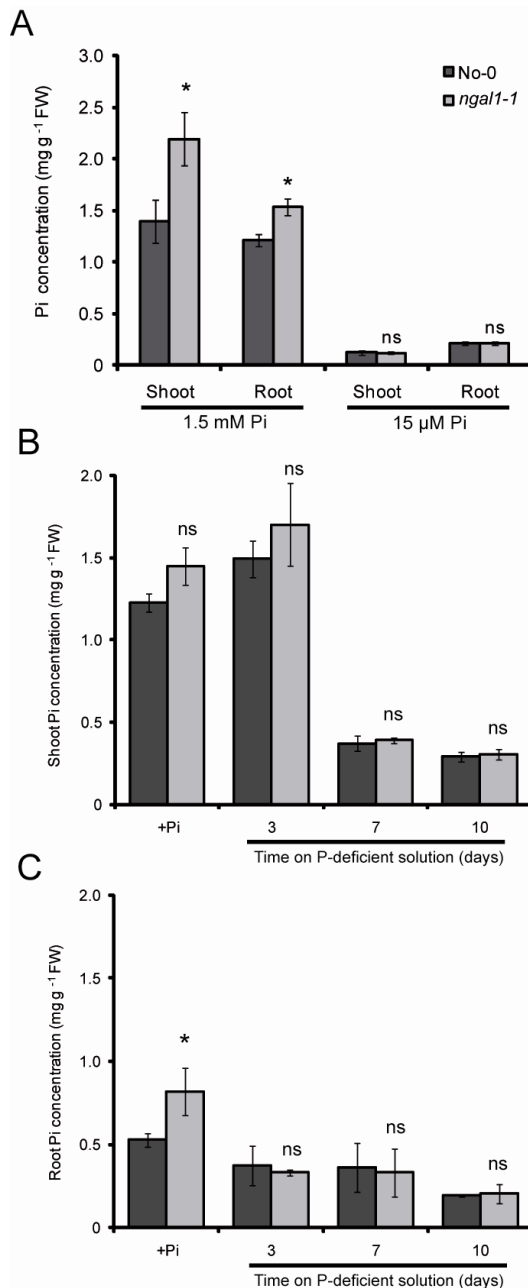


**Figure 36. Effect of NGAL1 on the P nutritional status of plants.** (A) Soluble Pi concentrations in shoots and roots of wildtype (No-0) and *ngal1-1* plants grown under sufficient P (1.5 mM Pi) or limited P (15 μM) supply. Eight-day-old seedlings were transferred to half-strength MS media in the presence or absence of Pi. Bars represent means  $\pm$  SE from 5 plants per replicate (n = 6 replicates). (B, C) Soluble Pi concentrations in (B) shoots and (C) roots of wildtype and *ngal1-1* plants grown in hydroponic culture. Plants pre-cultivated in nutrient solution containing 1.0 mM Pi for 36 days were transferred to P-sufficient or P-deficient solution for the indicated time. Bars represent means  $\pm$  SE from 10 plants per replicate (n = 5 replicates). \* denotes significant and ns not significant differences by Student's *t* test ( $P < 0.05$ ).

The upper or lower agar segments were supplied with contrasting amounts of P (Figure 37B). In control treatments, plants were grown on plates adequately supplied with P (1.25 mM Pi) or limited in P (15 μM Pi) in both compartments. After

7 days, it was observed that primary roots of *ngal1-1* plants were significantly shorter when the root tip was in contact with the  $-P$  medium, even when the rest of the root and the shoot were placed on a P-sufficient agar segment (Figure 37B). By contrast, primary root elongation was almost completely restored to wildtype levels when  $P_i$  was available in the lower agar segment, even though shoots were grown in the absence of P.

These results strongly suggested that the hypersensitive inhibition of primary root elongation observed in *ngal1-1* plants under low P resulted from a defective local, root-endogenous P signaling in the primary root tip.

### **5.3.7 *NGAL1* is expressed in root tips and is up-regulated by P-starvation**

In order to determine whether the expression of *NGAL1* is regulated by P, its expression levels were measured by means of quantitative RT-PCR in roots of plants grown *in vitro* under low P for 3 or 5 days. As shown in Figure 38, *NGAL1* expression was significantly up-regulated in response to low P. This indicates that *NGAL1* itself is also subjected to the regulation by upstream components of the P deficiency signaling cascade. Next, the localization of *NGAL1* expression was studied. Thus, transgenic lines in which the expression of *GUS* (*uidA*) or *GFP* is driven by the native 2025 bp upstream sequence of the *NGAL1* coding gene were generated. First, *pNGAL1-GUS* lines revealed that *NGAL1* is mainly expressed in roots (Figure 39A, B). *pNGAL1*-driven GUS activity was observed along the whole primary root axis as well as in lateral roots (Figure 39A-J). Importantly, *NGAL1* expression was stronger in the meristems of primary roots, especially when plants were subjected to P starvation (Figure 39C, D-F). In lateral roots, *NGAL1* was also mainly localized in the meristems (Figure 39I, J). In addition, the analysis of *pNGAL1-GFP* revealed that *NGAL1* is expressed mainly in endodermal and cortical cells (Figure 39G, H). Thus, these results indicate that *NGAL1* expression is significantly up-regulated in response to low external  $P_i$  concentrations. Furthermore, *NGAL1* is preferentially expressed in roots and particularly in the meristems of primary and lateral roots.

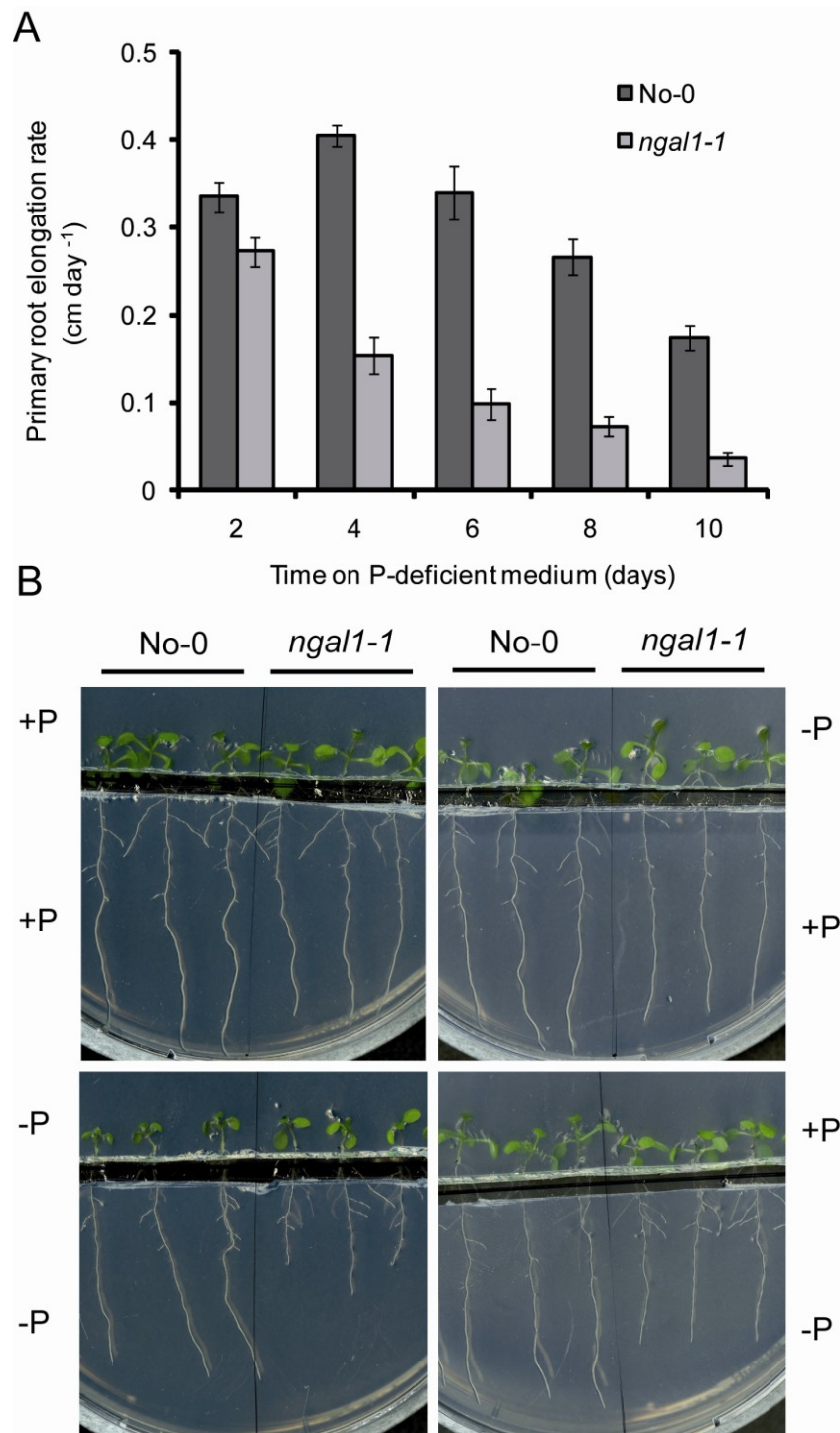


**Figure 37. *ngal1-1* plants are defective in local P signaling.** (A) Time-dependent elongation rate of primary roots of wildtype (No-0) and *ngal1-1* plants transferred to  $-P$ . Eight-day-old seedlings were transferred to half-strength MS medium without the supplementation of  $P_i$ . Primary root length was measured every two days and the rate of elongation was calculated. Shown are means  $\pm$  SE from 3 plants per replicate ( $n = 6$  replicates). (B) Horizontal-split root setup with compartments containing similar or distinct P supply. The primary root of eight-day-old wildtype (No-0) and *ngal1-1* seedlings was placed in the lower compartment (1 cm below the upper segment). Plants were continued to grow for another 7 days. The P treatment for each compartment is indicated by +P = 1.5 mM  $NaH_2PO_4$ ; and  $-P$  = no  $P_i$  added. The experiment was repeated twice and yielded similar results.



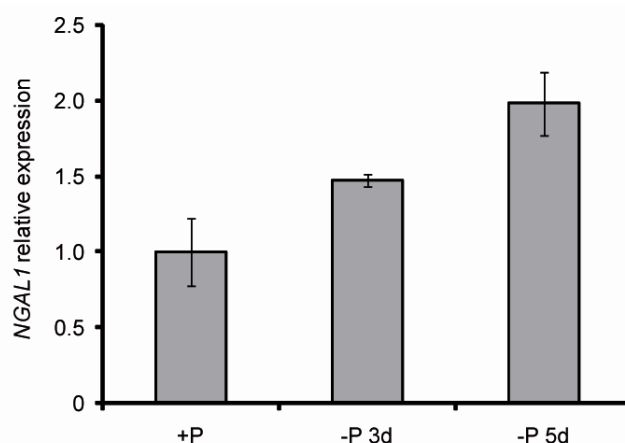


**Figure 38. *NGAL1* expression is induced by P starvation.** Relative transcript levels of *NGAL1* in roots of wildtype (No-0) plants growing under sufficient or limited P supply. Eight-day-old seedlings were transferred to half-strength MS medium either with +P (1.5 mM Pi) or –P (15  $\mu$ M Pi). After 3 and 5 days on treatments, root samples were collected for RNA extraction. Shown are relative levels of expression in roots as determined by quantitative RT-PCR (means  $\pm$  SE;  $n = 3$  replicates).

### 5.3.8 *NGAL1* modulates stem-cell maintenance under low P

The previous results presented herein showed that *ngal1-1* plants displayed an earlier inhibition of primary root elongation when grown under low P (Figure 37A) and, as a consequence, *ngal1-1* plants had markedly shorter primary roots than the wildtype (Figure 30D, E). It was also shown that *NGAL1* is expressed in roots, including root meristems, particularly when plants were grown under P limitation (Figure 39). These observations indicated that *NGAL1* is involved in the modulation of root growth under low P. Root elongation results from the interplay of cell division activity in the meristem and the rate of differentiation and elongation of cells that leave the meristem (Scheres et al., 2002). In order to determine meristematic activity, the expression levels of the cell division regulator *CYCB1;1* were measured by means of quantitative RT-PCR in roots of wildtype and *ngal1-1* plants exposed to low P for 5 days. *ngal1-1* roots exhibited significantly lower *CYCB1;1* transcript levels, even when not challenged by P starvation (Figure 40A). However, when transferred to –P for 5 days, *CYCB1;1* expression levels were more strongly down-regulated in *ngal1-1* roots than in wildtype. This observation suggested that cell division activity was markedly impaired in *ngal1-1* roots.



**Figure 39. Tissue-specific expression of *NGAL1*.** (A, B) *pNGAL1::GUS* expression in five-day-old seedlings germinated under (A) sufficient or (B) limited P. (C) Histochemical staining of *pNGAL1::GUS* expression in primary roots of plants grown under +P or -P for 5 days. (D-H) *pNGAL1::GFP* expression in primary root tips of plants grown under (D) sufficient or (E-F) deficient P availability for 7 days. (G, H) *pNGAL1*-driven GFP expression in the root hair zone of primary roots under low P. (I, J) *pNGAL1::GUS* expression on (I) emerging and (J) elongating lateral roots of plants grown under P limitation for 5 days. In (C, J), scale bars indicate 500  $\mu$ m.

To demonstrate the effect of reduced meristematic activity on primary root elongation, wildtype and *ngal1-1* plants grown in the absence of P for 12 days were transferred back to P-sufficient medium to assess their ability in restoring primary root growth. Whereas wildtype plants were able to recover primary root elongation as soon as they were exposed to the P-supplied medium, *ngal1-1*

plants showed very limited root elongation in response to restored P supply (Figure 40B, C). These results further supported that the loss of *NGAL1* leads to reduced meristematic activity. To explore the cause of meristem exhaustion in *ngal1-1*, the integrity of root meristems was analysed upon transfer to low P. Propidium iodide staining of cell walls was used to reveal the overall structure of root meristems. Whereas under sufficient P both wildtype and *ngal1-1* roots exhibited similar meristem organization, the transfer to P starvation for 5 days resulted in major changes in *ngal1-1* primary root meristems (Figure 41). In fact, P deficiency led to a severe disorganization of the stem cell niche in P-deficient *ngal1-1* roots. The quiescent center (QC) apparently got lost in these plants and, consequently, meristematic cells started to differentiate (Figure 41). Moreover, columella cells were partially fused and the root cap was degraded.

Recently, it was shown that the P<sub>5</sub>-type ATPase *PDR2* is involved in the modulation of stem-cell maintenance under low P (Ticconi et al., 2009). Furthermore, it has been demonstrated that *PDR2* regulates the proper localization of the root patterning regulators *SCARECROW* (*SCR*) and *SHORT ROOT* (*SHR*). Since *ngal1-1* plants also exhibited major defects in meristem organization, the expression levels of *PDR2*, *SCR* and *SHR* were assessed in this mutant in response to –P. As shown in Figure 42A, despite the slightly reduced *PDR2* expression under +P, the expression levels of this gene were not affected by either P starvation or *NGAL1* mutation. This result was expected, since *PDR2* transcript levels are not significantly regulated by P availability (Ticconi et al., 2009). Conversely to *PDR2*, *SHR* expression was markedly down-regulated in *ngal1-1* roots, particularly in the absence of P (Figure 42C). In addition, *SCR* expression was down-regulated in *ngal1-1* roots under low P (Figure 42B). Altogether, these results indicate that *NGAL1* is involved in the modulation of root meristematic activity under P deficiency by maintaining *SCR* and *SHR* expression.

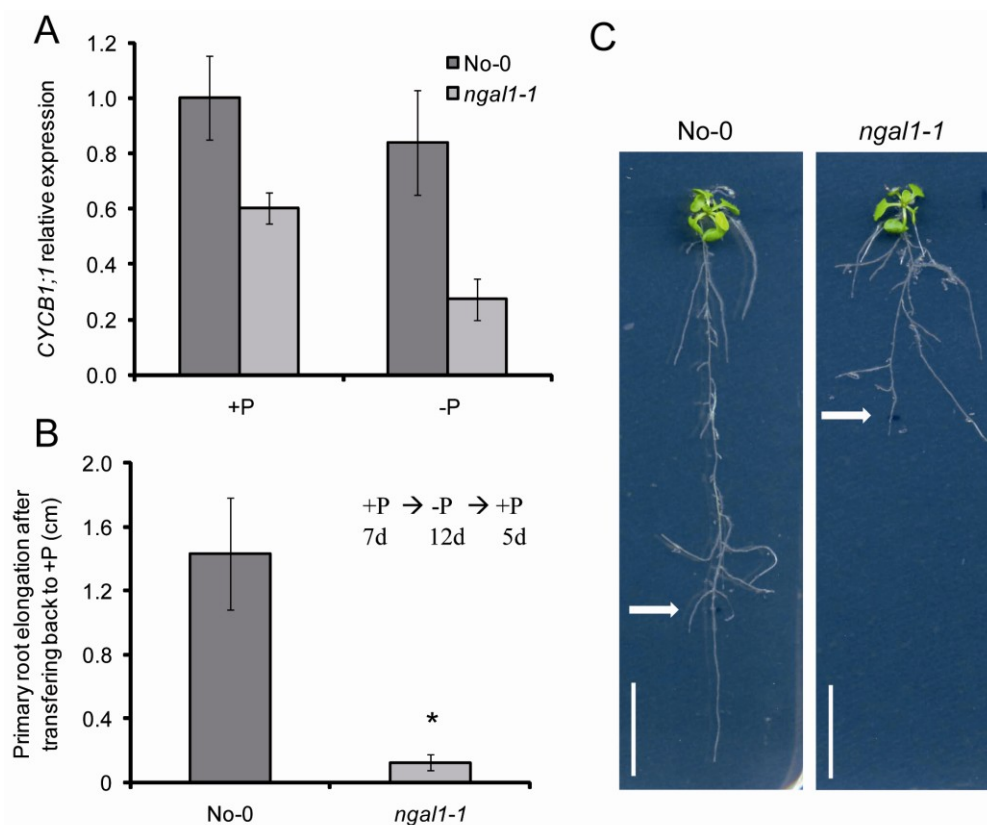


**Figure 40. NGAL1 is necessary for maintaining meristematic activity under low P.** (A) Relative expression levels of the cell division regulator *CYCB1;1* in wildtype (No-0) and *ngal1-1* roots in response to low P. Eight-day-old seedlings were transferred to  $\frac{1}{2}$  MS medium supplemented with sufficient P (1.5 mM Pi; +P) or low P (15  $\mu$ M Pi; -P). After 5 d on treatments, root samples were collected for RNA extraction. Shown are relative transcript levels in roots as determined by quantitative RT-PCR (means  $\pm$  SE;  $n = 3$  replicates). (B, C) Effect of Pi re-supply to P-starved plants on primary root elongation. Seven-day-old wildtype (No-0) and *ngal1-1* seedlings germinated under  $\frac{1}{2}$  MS medium, were transferred to -P. After 12 days, plants were transferred back to +P. (B) Primary root length after 5 days in +P (means  $\pm$  SE of 3 plants per replicate;  $n = 5$  replicates). (C) Phenotype of representative plants in response to the re-supply of P. Arrows indicate the length of primary roots at the time when plants were transferred from P-deficient to P-sufficient medium. \* denotes significant difference by Student's *t* test ( $P < 0.05$ ).

## 5.4 DISCUSSION

### 5.4.1 Ionomics-based screen of *Ds*-transposon-tagged lines allowed the identification of transcription factors involved in the regulation of ion homeostasis

With the aim of identifying novel regulatory components involved in the control of element accumulation in plants, elemental profiling was performed in insertion mutants grown in hydroponic solution. Thus, 302 *Ds*-transposon-tagged lines

affected in the expression of genes predicted to encode for transcription regulators were screened. It has been estimated that in the genome of *A. thaliana* at least 1,500 genes (~5.9% of the genome) code for transcription factors (Riechmann et al., 2000; Riechmann and Ratcliffe, 2000; Qu and Zhu, 2006). In the present study, the *Ds*-transposon insertion lines included approximately 20% of these genes. Because the phenotypic characterization was not limited to one single condition, since the concentrations of 15 elements were simultaneously assessed in these lines, one could expect that the probability of finding relevant candidates was considerably enhanced.

The results presented herein (Figure 28; Table 3) indicate that the loss of transcription factors has a great impact on the ionome of Arabidopsis plants. Based on the number of *Ds*-transposon-tagged lines that showed significant changes in the accumulation of at least one element, almost 10% of transcription factors are directly or indirectly involved in the regulation of the leaf ionome under adequate nutrient supply. Since in many of these cases, a single gene intervention resulted in the alteration of a complex trait, the results presented here also indicate that the manipulation of the expression of transcription factors represents an attractive strategy to influence element accumulation in plant organs, such as for biofortification purposes.

Another important observation from the nutrient profiling presented here is that more than 50% of the lines identified showed significant changes in the shoot concentration of more than one element (Figure 28B). This result is not surprising, because ion homeostasis is highly interconnected and thus the change of one nutrient commonly affects the accumulation of other nutrients (Lahner et al., 2003; Baxter, 2009). In addition, this observation indicates that the accumulation of different elements might be controlled by common regulatory factors. In a genome-wide ionomic profiling of fast-neutron-mutagenized Arabidopsis plants, it was observed that only 11% of the mutants with significant changes in leaf ion concentrations were affected in only one element (Lahner et al., 2003). This lower number might be due to the fact that fast neutron-mediated mutagenesis often leads to multiple mutations and genomic re-arrangements, thus affecting potentially more gene loci. Although not further explored in the present study,

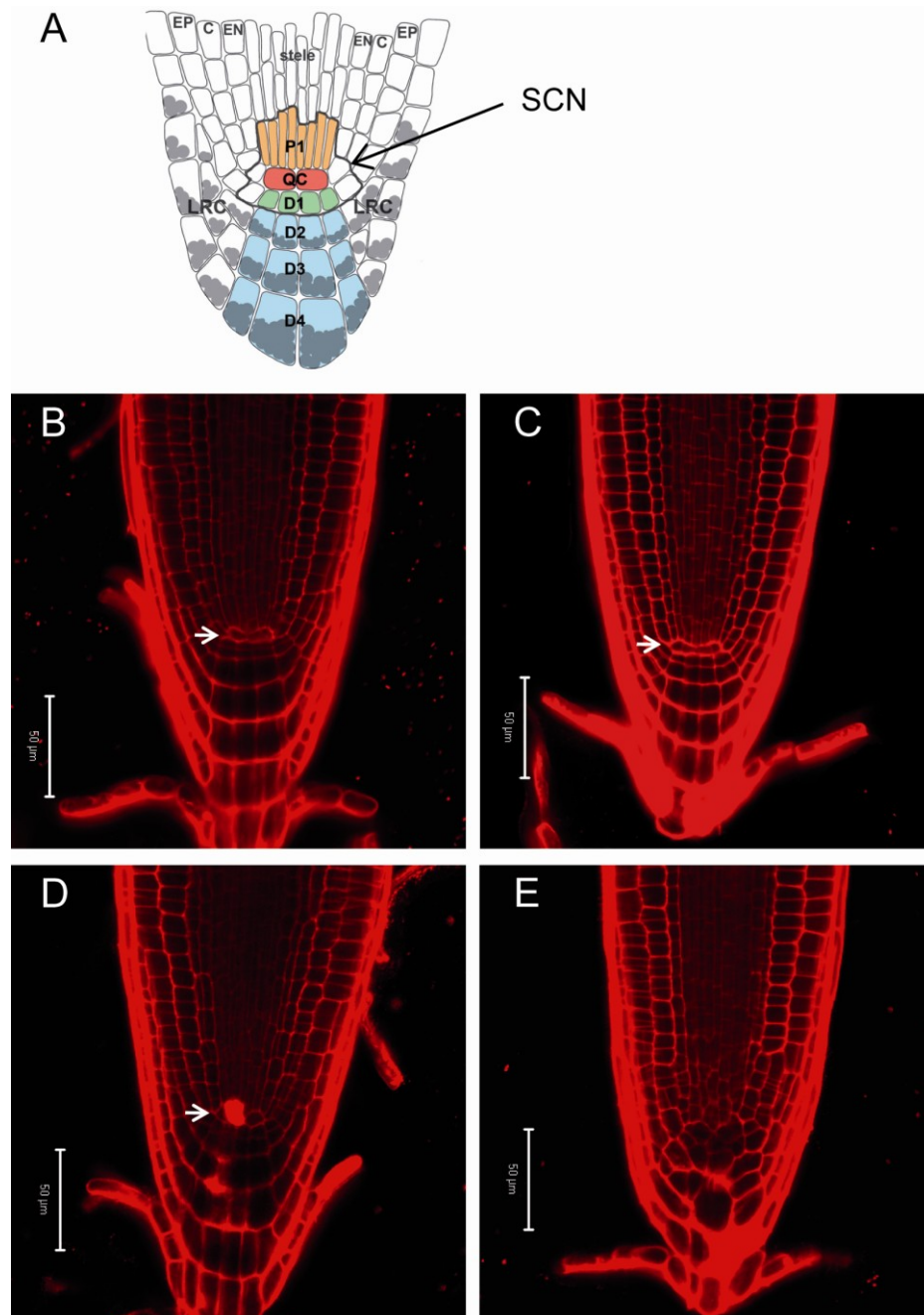


**Figure 41. Primary root meristem organization under low P.** (A) Schematic representation of a primary root meristem according to Stahl et al. (2009). QC = quiescent center; SCN = stem cell niche; P1 = stele initials; LRC = lateral root cap; D1 = columela stem cells; D2-D4 = columela cells; EN = endodermis; C = cortex; EP = epidermis. (B-E) Optical sections of propidium iodide-stained primary root tips of wildtype (B, D) and *ngal1-1* (C, E) grown under +P (B, D) or -P (C, E) for 5 days. The experiment was repeated twice and yielded similar results. Shown are representative sections. Scale bars = 50  $\mu$ m. Arrows indicate the position of the QC.

additional bioinformatic tools and strategies could be employed to establish those transcription factors that regulate simultaneously the accumulation of more than one element.



In addition, the multi-elemental analysis performed in the present study revealed interesting correlations between the concentrations of different elements (Table 4 and 5). As an example, Ca and Mg concentrations showed a strong positive correlation in shoots ( $r = 0.67$ ;  $P < 0.001$ ) and roots ( $r = 0.71$ ;  $P < 0.001$ ). The positive correlation between these two macronutrients is well reported in the literature (Marschner, 1995; Watanabe et al., 2007; Broadley et al., 2010) and there is evidence that, at least in some tissues, the accumulation of Ca and Mg is partially controlled by common regulatory networks (Broadley et al., 2008). One exception for that is the accumulation of these macronutrients in seeds, where distinct QTLs have been found for Ca and Mg (Vreugdenhil et al., 2004). In this regard, it has been reported that most significant correlations were tissue-specific, indicating that the accumulation of a particular element is differently regulated in different organs of the plant (Ghandilyan et al., 2009a; Ghandilyan et al., 2009b). Also in the present study only few significant correlations were found to occur in both shoots and roots (Table 4 and 5).

Finally, the elemental profiling of *Ds*-transposon insertion lines allowed the identification of one transcription factor involved in the modulation of root architecture under low P. In addition, other lines, which were selected based on their significant altered elemental composition, also showed minor phenotypes in subsequent *in vitro* phenotypical analyses (data not shown). This demonstrates that the elemental profiling represents an unbiased strategy for the identification of novel processes and molecular players relevant for the element accumulation in plants. Considering the relatively large number of transposon insertion lines with significantly altered elemental profiles, an independent phenotyping strategy was chosen to confirm the relevance for the altered ionome. Growing pre-selected lines on high or low supplies of those nutrients which were significantly altered under adequate supply, allowed selecting 5 out of 25 lines. However, not all lines could be subjected to this additional phenotypical screening yet. This combined approach provided a solid basis for an in-detail analysis of 5 lines, out of which only one was followed up.

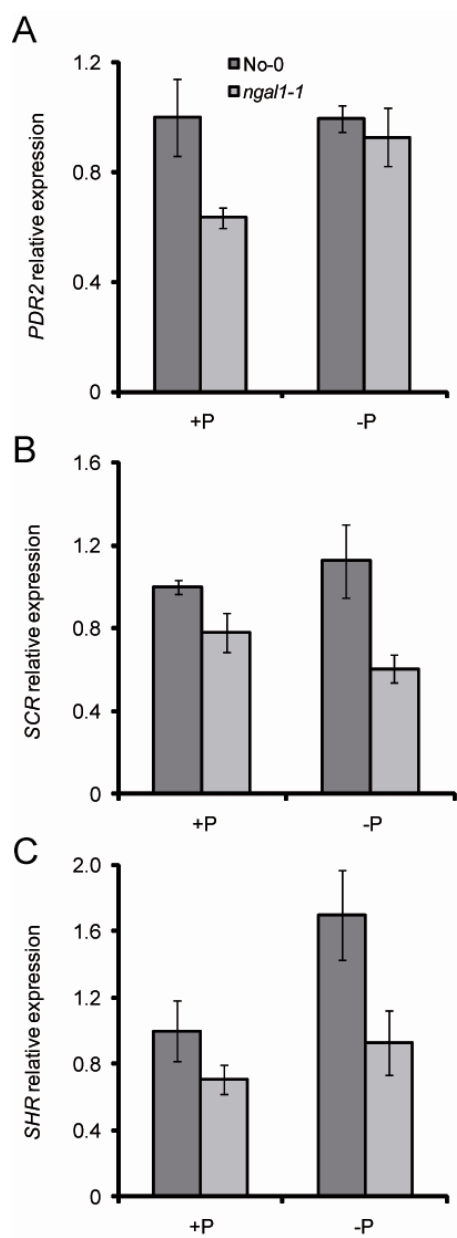


**Figure 42. Expression of *PDR2* and root patterning genes.** (A-C) Relative expression levels of (A) *PDR2*, (B) *SCR* and (C) *SHR* in roots of wildtype (No-0) and *ngal1-1* plants. Eight-day-old seedlings were transferred to half-strength MS medium containing +P (1.5 mM Pi) or -P (15 μM Pi). After 5 days on treatments, root samples were collected for RNA extraction. Shown are relative transcript levels in roots as determined by quantitative RT-PCR (means  $\pm$  SE; n = 3 replicates).

#### 5.4.2 Involvement of NGAL1 in P and K accumulation

P starvation represents a major limiting factor for plant productivity worldwide. When P is limited, plants activate a series of biochemical and morphological responses to improve Pi mobilization and uptake. Although most of these responses are regulated at the transcriptional level (Wu et al., 2003; Franco-Zorrilla et al., 2004; Misson et al., 2005), upstream regulators in particular of morphological adaptations to P deficiency are not yet fully understood. In this study, one putative transcription factor from the B3 superfamily was identified as



one component of the regulatory pathway of P deficiency responses in Arabidopsis roots. The suppression of *NGAL1* transcription in *ngal1-1* knockout mutants resulted in an altered root architecture (Figure 30D, E) and in an increased accumulation of K and P, especially in the shoot (Figure 29). However, the increase in shoot P concentrations was quite moderate compared to that of P over-accumulator mutants, such as *pho2* (Delhaize and Randall, 1995; Dong et al., 1998; Aung et al., 2006), and no visual symptoms of P toxicity in *ngal1-1* leaves were observed (Figure 30D). This situation was different in the case of K, where *ngal1-1* plants were phenotypically undistinguishable from the wildtype when grown under low K supply (Figure 34A, B-D). The fact that K accumulation in shoots was also increased in *ngal1-1* plants, could be due to a direct effect of *NGAL1* on K homeostasis or an indirect effect, since the homeostasis of many nutrients is interlinked (Baxter, 2009, 2010). In support of this, it was previously demonstrated that shoot K concentrations decrease markedly when plants are grown under low P (Misson et al., 2005), indicating that P deficiency negatively affects K accumulation. However, the elemental analysis performed in the present study revealed that K and P concentrations show a significant positive correlation only in roots ( $r = 0.66$ ;  $P < 0.001$ ), whereas no such correlation was found in shoots ( $r = 0.08$ ;  $P > 0.05$ ).

The enhanced P accumulation in *ngal1-1* was confirmed in an independent experiment, in which soluble Pi levels were measured (Figure 36). Interestingly, enhanced Pi accumulation in *ngal1-1* shoots and roots was restricted to P-sufficient growth conditions (Figure 36). For comparison, the over-accumulation of Pi in *pho2* mutants is mainly due to a de-regulated activity of some PHT1-type Pi transporters which are not properly down-regulated when Pi is supplied at sufficient levels (Aung et al., 2006; Bari et al., 2006). By contrast, in the present study the expression of *PHT1;1* and *PHT1;4* was regulated in a comparable manner in wildtype and *ngal1-1* plants under sufficient or low P supply (Figure 35A, B). In addition, the activity of APases in *ngal1-1* roots was indistinguishable from wildtype (Figure 35D), indicating that these Pi starvation-regulated responses were not affected by *NGAL1*. It has been shown that many Pi transporters are negatively regulated by the shoot P status (Miura et al., 2005; Aung et al., 2006; Bari et al., 2006). In fact, the mutation of *SIZ1*, a small ubiquitin-like modifier E3

ligase, leads to higher expression of *PHT1;4* and *AtPS2* (acid phosphatase) specifically under P supply (Miura et al., 2005). As a consequence, *siz1* mutants accumulate more Pi in shoots when grown under adequate P supply. Therefore, it is plausible that also in *ngal1-1* plants some components contributing to the uptake of Pi are de-regulated. Since there are many Pi transporters predicted to be expressed in Arabidopsis (Raghothama and Karthikeyan, 2005), their expression analysis should be completed before solid conclusions are drawn. Another possibility is that the increased surface area of *ngal1-1* plants because of the enhanced lateral root elongation (Figure 32C) increased root Pi uptake and thus represented an advantage for P acquisition.

#### 5.4.3 Impact of NGAL1 on root architecture

When transferred to low P media *ngal1-1* plants showed a remarkable reduction of primary root elongation (Figure 30D, E). These observations indicated that *ngal1-1* plants are more sensitive to low P. The hypersensitive inhibition of primary root growth was accompanied by an increased lateral root density and length (Figure 32B, C). Inhibition of primary root elongation and increased lateral root density are typical root architectural changes observed in response to P limitation (Linkohr et al., 2002; Lopez-Bucio et al., 2002; Lopez-Bucio et al., 2003; Perez-Torres et al., 2008). These morphological responses are likely to increase the explorative capacity of plant roots, especially in the top soil horizon, where Pi concentrations are usually higher (Lynch and Brown, 2001). The short-root phenotype of *ngal1-1* was specific to P starvation (Figure 34A) and could be largely recovered to wildtype levels by the supply of  $> 50 \mu\text{M}$  Pi (Figure 31). Similar to *ngal1-1*, also *pdr2* plants exhibit an overly sensitive primary root inhibition when grown under low Pi (Ticconi et al., 2004). In *pdr2* mutants, primary root growth arrest under limited P availability is due to an earlier reduction of cell division in the root apical meristems. As a result of the decreased meristematic activity, *pdr2* mutants show a rapid meristem exhaustion and stem-cell differentiation (Ticconi et al., 2009). In the present study, the loss of *NGAL1* expression significantly reduced the expression of the cell cycle regulator *CYCB1;1* (Figure 40A). Furthermore, *ngal1-1* primary root meristems showed major structural defects when grown under low P,

(Figure 41). Indeed, as soon as 5 days after transfer to  $-P$ , the quiescent center integrity in *ngal1-1* roots was extensively compromised and primary root meristems exhibited a strong disorganization and a loss of stem-cell identity (Figure 41). It has been shown that following the inhibition of cell elongation in P-deficient primary root tips, meristematic activity markedly decreases and unrestricted cell differentiation is induced (Sanchez-Calderon et al., 2005). As a consequence, the root developmental program shifts from indeterminate to determinate growth. The quiescent center is responsible for maintaining the indeterminate growth of roots. An experimental removal of the quiescent center by laser ablation triggered unrestricted differentiation of the surrounding stem-cell initials (van den Berg et al., 1997). Thus, the apparent loss of meristem identity in *ngal1-1* plants was most likely responsible for the earlier shift to determinate growth exhibited by these plants under low P (Figure 37A). Furthermore, because *ngal1-1* plants showed only limited recovery of primary root elongation when transferred back to  $+P_i$  after 12 days of growth in the absence of P (Figure 40B, C), NGAL1 most likely helps to maintain the meristematic activity under low P, thereby allowing plants to recover root growth whenever  $P_i$  becomes available again.

Recently, it was demonstrated that the root patterning regulators SCR and SHR were mis-localized in the root meristems of *pdr2* mutants (Ticconi et al., 2009). However, it is still not clear whether this was a consequence or the cause of the meristematic repression observed in P-starved *pdr2* plants. Here, it is shown that *SHR* was up-regulated in roots of wildtype plants after 5 days of growth in the absence of P (Figure 42C). By contrast, in *ngal1-1* roots the expression levels of *SCR* and *SHR* were lower (Figure 42B, C). Together with two PLETHORA (*PLT1/2*) transcription factors, SCR and SHR regulate the proper function and activity of the stem-cell niche in the root apical meristem (Petricka and Benfey, 2008; Iyer-Pascuzzi and Benfey, 2009). In *scr* and *shr* mutants stem-cell initials differentiate because the quiescent center loses its identity (DiLaurenzio et al., 1996; Helariutta et al., 2000; Sabatini et al., 2003). Thus, the defective up-regulation of *SCR* and *SHR* in *ngal1-1* roots in response to P deficiency might have compromised stem-cell identity, leading to differentiation and subsequent loss of meristematic activity.

Evidence is accumulating that P and Fe homeostasis are linked in plants (Ward et al., 2008; Zheng et al., 2009). In solution, P and Fe form precipitates, thus reducing the bioavailability of either nutrient (Dalton et al., 1983). It has been suggested that root architectural changes observed under P starvation are the consequence of an increasing Fe availability in the medium, and that the removal of Fe from a P-depleted medium restores primary root elongation (Ward et al., 2008). However, the short-root phenotype of *ngal1-1* plants is very likely independent of an interaction with Fe, since *ngal1-1* roots were significantly shorter under low P even when Fe was absent (Figure 34B). In addition, the supply of high Fe concentrations to Pi-sufficient medium inhibited the primary root of wildtype and *ngal1-1* plants to almost the same extent.

Besides its impact on primary root growth, the loss of *NGAL1* expression also severely affected lateral root development. Although the number of lateral roots was not significantly altered in *ngal1-1* mutants (Figure 32B), lateral root density, specifically under low P, was enhanced in these plants (Figure 32C). Lateral root elongation was also stimulated in *ngal1-1* plants, although this phenotype was not restricted to P deficiency (Figure 32D). Phosphorous starvation triggers major changes in lateral root development, such as lateral root initiation and elongation (Williamson et al., 2001; Lopez-Bucio et al., 2002; Perez-Torres et al., 2008). Evidence has been provided that auxin plays a major role in the regulation of these responses, since the sensitivity towards exogenously applied auxin is increased in P-starved roots (Lopez-Bucio et al., 2002; Perez-Torres et al., 2008). It has been shown that the expression of the auxin receptor *TIR1* is up-regulated when plants are grown under low P (Perez-Torres et al., 2008). As a consequence, the AUX/IAA auxin repressors are degraded, allowing the ARF19-mediated stimulation of lateral root formation to occur. Importantly, the stimulation of lateral root development under low P starts before the primary root is inhibited (Williamson et al., 2001; Lopez-Bucio et al., 2002; Perez-Torres et al., 2008). Here, it is shown that relative to the wildtype, lateral root initials in *ngal1-1* plants were more advanced in their development (Figure 33). This observation was not restricted to, but slightly stimulated under low P, since P-starved *ngal1-1* plants showed a higher number of emerged lateral roots (stage D). Furthermore, this response appeared to be largely independent of the primary root inhibition, since it

was observed in *ngal1-1* plants already after 2 days in  $-P$  (Figure 33), whereas a significant primary root reduction occurred only after 4 days (Figure 37A). Therefore, these observations indicate that NGAL1 has a negative impact on lateral root initiation and elongation that is independent of its action on the primary root meristem.

#### **5.4.4 The local regulation of root architectural changes in response to P is dependent on a functional NGAL1**

When grown under low P, *ngal1-1* plants showed a hypersensitive inhibition of primary root elongation (Figure 30D, E; 34A and 37A). This phenotype could be due to: (1) a nutritional effect, in which  $P_i$  concentrations in *ngal1-1* roots were more depleted than in the wildtype, leading to an earlier inhibition of primary root elongation; or (2) a defective P signaling, in which *ngal1-1* plants are not able to properly sense and/or transduce the information on the external  $P_i$  availability. In order to test the first hypothesis,  $P_i$  concentrations in shoots and roots of wildtype and *ngal1-1* plants were measured (Figure 36). However,  $P_i$  levels in *ngal1-1* roots were not significantly different from the wildtype. It is important to take into account that these observations cannot completely rule out the possibility that also the meristems of *ngal1-1* plants were more P-depleted. However, the observation that the expression of the two major root-expressed  $P_i$  transporters and the acid phosphatase activity were not significantly affected in *ngal1-1* roots (Figure 35) further supported that *ngal1-1* plants were not more starved than wildtype plants. Altogether, these observations strongly suggest that the short-root phenotype of *ngal1-1* plants in P-depleted medium was not due to a nutritional defect. Instead, primary roots of *ngal1-1* plants were shorter than the wildtype only when their primary root tips were placed in contact with a P-deficient medium, even though their shoots and basal root parts were still in contact with P-sufficient medium (Figure 37B). In addition, the short-root phenotype of *ngal1-1* plants could be almost fully recovered by exposing only the primary root tips to adequate supply of  $P_i$ . This is reminiscent from studies showing that roots are able to sense the local availability of  $P_i$  (Svistoonoff et al., 2007). The contact of the root tip to P-deficient medium is enough to trigger growth inhibition, independently of the P nutritional

status of the shoot, indicating that this response is largely under the control of a local signaling circuit (Linkohr et al., 2002; Ticconi et al., 2004; Svistoonoff et al., 2007). The findings reported in the present study further reinforce this view and indicate that *NGAL1* is necessary to maintain the local P signaling in root tips. In agreement with this putative role, *NGAL1* promoter activity strongly localizes to the root meristems (Figure 39). However, since *NGAL1* expression is also regulated by P (Figure 38), *NGAL1* itself is most likely located downstream of the P sensing event.

In conclusion, the data presented in this work indicates that *NGAL1* functions in the local, root-endogenous P signaling that modulates root architectural changes in response to limited P availability. In the primary root, *NGAL1* expression in the meristems maintains meristematic activity under low P by up-regulating *SHR* and *SCR*. In lateral roots, *NGAL1* appears to repress lateral root development, irrespectively of the P availability.

## 6 General discussion

Roots are essential for the adaptation of plants to a continuously changing environment, since they explore the underground in the search for often limited water and essential minerals. Not surprisingly, plants endowed with larger root systems are more tolerant to abiotic stresses (Ekanayake et al., 1985b; Ekanayake et al., 1985a; Price and Tomos, 1997; Werner et al., 2010). In this regard, it has been shown that the majority of drought stress-tolerant rice plants exhibit a highly branched and deep root system (Price et al., 1997). On the other hand, improved root extension and root size correlate positively with increased P acquisition efficiency in *A. thaliana* (Narang et al., 2000) or P use efficiency in *Brassica oleracea* (Hammond et al., 2009). Besides the intrinsic, genetically-programmed properties of root systems, environmental stimuli have a profound impact on the overall shape and structure of roots. The ability to integrate external signals into the internal default program is a major component of root plasticity, representing a crucial adaptive advantage, e.g. when nutrients are sparingly available.

Although roots have a massive impact on plant growth and adaptation to stresses, most studies and breeding efforts have been concentrated on the improvement of above-ground parts of plants. In fact, the difficulty of accessing intact root systems for analysis hinders a more extensive exploration of root development for breeding purposes (Gewin, 2010). Nonetheless, the improvement of root systems is a promising strategy to enhance tolerance against stresses and to increase yield in crop plants (de Dorlodot et al., 2007). Thus, the understanding of the intrinsic and responsive factors involved in root development is fundamental to more successfully exploit the potential of root activities in breeding programs. In the present thesis, the major aim was to characterize novel signaling processes involved in root development and nutrient acquisition. The results presented here demonstrate that roots respond directly to nutrient signals, thereby activating signaling cascades that alter hormone distribution and/or developmental programs. These architectural changes ultimately impact on nutrient acquisition and plant performances under challenging growth conditions.

## 6.1 Nutrients as signals for root development

The plasticity of roots represents a remarkable feature, since it allows the intrinsic developmental program to respond to environmental stimuli. Among those, nutrients act as signals that can induce profound alterations on root morphology and architecture (Lopez-Bucio et al., 2003; Malamy, 2005)). These root responses strongly indicate that roots are able to monitor external fluctuations in nutrient availability. Indeed, when nitrate availability is locally restricted, plant roots preferentially colonize the nitrate-enriched soil patches (Drew, 1975; Zhang and Forde, 1998; Zhang et al., 1999; Remans et al., 2006b). This response is mainly achieved by an increased elongation of pre-existing lateral roots. Recently, it was reported that lateral roots also respond to a localized supply of ammonium (Lima et al., 2010). In contrast to nitrate, ammonium stimulates mainly lateral root initiation. In the present work, it is shown that modifications in root architecture are not elicited only by macronutrients, but also by micronutrients, such as Fe (Figure 6). Plant roots respond to a localized supply of Fe mainly by increasing lateral root elongation. Although many nutrients affect root architecture, it is becoming evident that they generate signals which are integrated into the root developmental program at different levels. For instance, the local supply of nitrate stimulates the elongation of lateral roots (Zhang and Forde, 1998; Zhang et al., 1999; Remans et al., 2006b), whereas local ammonium increases the initiation of new lateral roots (Lima et al., 2010). Furthermore, although localized nitrate or localized Fe stimulate lateral root elongation, they affect different cellular processes, since nitrate induces cell division in the meristem (Zhang et al., 1999), whereas Fe increases the elongation of differentiated cells (Figure 16).

Perhaps the best characterized example of a nutrient affecting root development is the effect of nitrate in lateral root elongation (Zhang and Forde, 1998; Zhang et al., 1999; Linkohr et al., 2002; Remans et al., 2006b). Rather than reflecting a nutritional effect, this response appears to be primarily the outcome of a signaling cascade activated by nitrate sensing (Zhang and Forde, 1998; Zhang et al., 1999). The possibility that nitrate acts as a signal molecule has been inferred from the observation that it regulates many aspects of plant development (Crawford, 1995; Stitt, 1999; Krouk et al., 2010a). A key role in nitrate signaling responses is taken



in by the nitrate transporter NRT1.1 (Munos et al., 2004; Krouk et al., 2006; Remans et al., 2006b; Walch-Liu and Forde, 2008; Krouk et al., 2010b). This conclusion is largely based on the observation that expression of NRT2.1, the major high-affinity transporter of nitrate (Cerezo et al., 2001; Filleur et al., 2001), is not up-regulated in response to N starvation in the NRT1.1-deficient mutant *chl1* (Munos et al., 2004; Krouk et al., 2006). In addition, NRT1.1 plays also a major role on the nitrate signaling cascade responsible for changing root architecture according to the external nitrate supply (Remans et al., 2006b; Walch-Liu and Forde, 2008; Krouk et al., 2010b). Expression of the MADS-box transcription factor *ANR1*, which is also involved in nitrate-dependent lateral root development (Zhang and Forde, 1998), is markedly down-regulated in *chl1* mutants (Remans et al., 2006b). This indicates that NRT1.1 acts upstream of ANR1 in this signaling cascade. It is noteworthy that most nitrate signaling defects observed in *chl1* mutants were largely uncoupled from nitrate uptake (Krouk et al., 2006; Remans et al., 2006b; Ho et al., 2009; Wang et al., 2009). Thus, it is likely that besides facilitating nitrate transport, NRT1.1 also functions as a nitrate sensor in plant roots (Ho et al., 2009; Krouk et al., 2010b). In this case, NRT1.1 may represent the first example of plant transceptor, a membrane protein that functions in nutrient transport and sensing (Ho and Tsay, 2010; Gojon et al., 2011).

The present study shows that the stimulation of lateral root growth by Fe as well as its inhibition by excessive Fe supplies is largely controlled by local, shoot-independent signals (Figure 15). The Fe(II) transporter IRT1 is required for the differential response of Fe on lateral root initiation and elongation (Figure 11A,B). However, since Fe uptake is severely impaired in *irt1* mutants (Colangelo and Guerinot, 2004), this response is most likely due to reduced internal Fe concentrations. Thus, it is not yet clear whether IRT1 functions as a Fe transceptor. To more precisely address this possibility, it is necessary to uncouple the transport from the sensing function, as shown in the case of NRT1.1, where a point mutation resulted in impaired nitrate transport but did not affect the NRT1.1-dependent signaling function (Ho et al., 2009). The results presented herein indicate that, in addition to nitrate, also Fe may act as a signal that modulates root development. This assumption is based on the observation that the elongation of lateral roots was stimulated or inhibited depending on the concentration of Fe

present in the agar segment with which the roots were in contact (Figure 6). In addition, it is shown that symplastic Fe can alter auxin distribution in the apices of lateral roots (Figure 17). Finally, the observation that the loss of *GATA3* impairs the lateral root response to local Fe (Figures 21, 22, 23) without affecting the Fe uptake machinery (Figure 24) further reinforces the existence of a Fe-dependent signaling mechanism regulating lateral root development.

In other organisms, the existence of Fe sensing mechanisms has been demonstrated (Beinert and Kennedy, 1993; Klausner et al., 1993; Hentze and Kuhn, 1996; Iwai et al., 1998; Pelletier et al., 2005; Jbel et al., 2009; Salahudeen et al., 2009; Vashisht et al., 2009). One well documented system that functions in mammalian cells is controlled by the bifunctional protein IRP1. When cellular levels are low, IRP1 loses its 4Fe-4S cluster and is then able to repress ferritin translation (Klausner et al., 1993; Hentze and Kuhn, 1996). By contrast, high levels of Fe re-establish the 4Fe-4S cluster and the protein regains its aconitase activity. De-repressed ferritin translation then allows ferritin accumulation to capture excessive Fe before it reaches toxic levels. In plants, however, such a mechanism appears not to exist (Arnaud et al., 2007). Thus, alternative Fe sensing mechanisms remain to be uncovered in plants.

## **6.2 Nutrient signals differentially modulate the development of primary and lateral roots**

One important aspect of root plasticity is that the availability of different nutrients triggers distinct changes in morphology and architecture. For instance, P deficiency typically inhibits primary root elongation and increases lateral root formation (Williamson et al., 2001; Linkohr et al., 2002; Lopez-Bucio et al., 2002), whereas the limitation of N stimulates lateral root elongation and has almost no impact on primary root growth (Linkohr et al., 2002). Thus, N primarily acts at the lateral root tips, while Pi has opposite effects on primary and lateral root meristems. Since N and Pi are released from organic matter and thus are usually more available in the top soil (Lynch and Brown, 2001), a shallower and more horizontal distribution of roots may offer plants an adaptive advantage to forage the nutrient reservoir. The present work adds to this by showing that Fe deficiency

has a greater impact on lateral root development than in primary root elongation (Figure 5). However, under excessive Fe both primary and lateral root growth are inhibited (Figure 6). These responses are in contrast to those triggered by nitrate, since both N deficiency and high nitrate affect mainly lateral root development (Zhang et al., 1999). These differences in the responsiveness of roots of different order to nutrient deficiency or local nutrient availabilities could indicate the action of distinct mechanisms or that nutrient signals are integrated into developmental processes at different levels.

The developmental stage at which the meristems are exposed to nutrients appears relevant for the quality of the response. It has been reported that under high nitrate supply (>10 mM), the development of lateral roots is strongly inhibited, whereas primary root growth remains largely unaffected (Zhang et al., 1999; Tian et al., 2009). A closer inspection revealed that lateral root growth was arrested at earlier stages of development, so that lateral root initials failed to elongate (Zhang et al., 1999). Interestingly, when mature lateral roots were exposed to high external nitrate concentrations they were largely insensitive to the nitrate-mediated inhibition of elongation (Zhang et al., 1999), indicating that the nitrate-sensitive checkpoint takes place at an earlier developmental stage. In addition, under low P availability, the meristematic activity in primary root tips is rapidly inhibited, whereas it is still maintained in lateral roots (Sanchez-Calderon et al., 2005; Jain et al., 2007). If the exposition to low P is prolonged, then the elongation of mature lateral roots is also inhibited (Sanchez-Calderon et al., 2005). This may be indicative for a dynamically changing sensitivity towards nutrients during root development. Such a developmental stage-specific change could indicate that sensitive checkpoints are differently expressed during the development of roots.

Time-course expression analyses have been indicating that different sets of genes are induced or repressed during lateral development (Vanneste et al., 2005; De Smet et al., 2008). In this context, an important observation is that hormones act at specific stages during the initiation and emergence of lateral roots (Fukaki and Tasaka, 2009b). Thus, hormones might contribute to the distinct responsiveness of roots of different order to nutrient signals. Since ABA synthesis mutants (*abi4* and *abi5*) displayed longer lateral roots under high nitrate supply (Signora et al.,

2001), ABA is likely involved in the nitrate-dependent inhibition of lateral roots. In agreement with the preferential action of nitrate on lateral roots, these *abi* mutants did not exhibit significant changes in primary root growth (Signora et al., 2001). Importantly, the treatment of *Arabidopsis* seedlings with ABA phenocopies the effect of high nitrate, i.e. unchanged primary root elongation but a dose-dependent inhibition of lateral root development (De Smet et al., 2003). More recently, it has been shown that the ABA-regulated AP2 domain transcription factor ABI4 controls specifically lateral root formation by reducing polar auxin transport in roots (Shkolnik-Inbar and Bar-Zvi, 2010). Thus, environmental cues that perturb ABA synthesis are likely to more profoundly affect lateral root growth. In the case of P, it appears that the inhibition of primary root growth in response to low P is auxin-independent, although auxin is required for the low P-induced lateral root formation (Williamson et al., 2001; Lopez-Bucio et al., 2002; Lopez-Bucio et al., 2005; Jain et al., 2007). This view has been further corroborated by the observation that increased TIR1-mediated auxin sensitivity in pericycle cells enhances lateral root formation and emergence without significantly affecting primary root growth (Perez-Torres et al., 2008). In addition, although P deficiency-induced lateral root development was markedly affected by suppressing or over-expressing *TIR1*, these perturbations had only minor effects on primary root elongation (Perez-Torres et al., 2008). Although contrasting reports on the effect of auxin in primary root elongation have been published (Lopez-Bucio et al., 2005; Nacry et al., 2005), it is very likely that during P starvation auxin mainly targets lateral root initiation.

The ontogenically distinct entity of primary roots and lateral roots could also affect the way they respond to nutrients. Since lateral roots develop post-embryonically from the embryonic primary root, it is plausible to assume that lateral root growth depends on the development of the primary root. Such a dependency could explain the apparently contrasting effect of P availability on the growth of primary and lateral roots. It has been speculated that the P starvation-induced inhibition of the parental root reflects a loss of apical dominance, which is responsible for triggering the enhanced formation of lateral roots (Nacry et al., 2005; Sanchez-Calderon et al., 2005). However, several lines of evidence suggest that increased lateral root formation in response to limited P is largely independent from the

primary root (Perez-Torres et al., 2008). First, the formation and emergence of lateral root initials was observed before any change in primary root growth could be detected (Perez-Torres et al., 2008). Actually, the present study reinforces this view, since lateral root development was induced in P-starved plants before any change in primary root elongation could be detected (Figure 33 and 37A). Second, lateral root formation in P-starved *lpi3* mutants, which are largely insensitive to primary root inhibition by low P (Sanchez-Calderon et al., 2006), was indistinguishable from wildtype (Perez-Torres et al., 2008). In addition, it is shown here that NGAL1 plays a dual role in the regulation of root development in response to low P. On the one hand, NGAL1 positively maintains the meristematic activity in the primary root meristem whenever P is limiting. On the other hand, it negatively affects lateral root development under P sufficient conditions. Third, *pdr2* mutants exhibit simultaneously reduced growth of primary and lateral roots (Ticconi et al., 2004). Since this phenotype is distinct from that of wildtype plants, it has been suggested that lateral roots of *pdr2* mutants lack a protective mechanism against low P (Malamy, 2005). Such a mechanism is maintained in *ngal1-1* plants (Figure 32). Finally, it is also likely that distinct pathways are active in primary and lateral roots or even in roots of different order. Since the post-transcriptional activation of ANR1 by a synthetic promoter altered only lateral root development without affecting primary root growth (Filleur et al., 2005), the nitrate signalling in primary roots likely involves different components from that of lateral roots.

In the case of P, it appears that primary root elongation is controlled by local P availability (Figure 37B; Ticconi et al., 2004; Svistoonoff et al., 2007), whereas lateral root growth is additionally under systemic control by shoot-derived signals (Jain et al., 2007; Karthikeyan et al., 2007). Phosphorus-starved plants usually accumulate more starch and sugars (Ciereszko and Barbachowska, 2000; Morcuende et al., 2007; Müller et al., 2007) and sucrose is involved in the systemic regulation of P starvation-induced root responses (Liu et al., 2005; Jain et al., 2007; Karthikeyan et al., 2007; Hammond and White, 2008). Interestingly, the supply of sucrose to P-starved plants further increased lateral root density, while it had no effect on primary root length (Jain et al., 2007; Karthikeyan et al., 2007). The distinct effect of sucrose appears to be related to its interference on the transport of auxin from shoots to roots, as shown by increased acropetal transport

of auxin in the presence of sucrose (Jain et al., 2007). Thus, in contrast to primary root growth, lateral root development is not only controlled by the local P status, but also by systemic signaling cascades, as those mediated by sucrose delivered by the shoot.

In the present study, it is shown that Fe availability primarily targets lateral root development, as shown by the reduced number and length of lateral roots and the largely unaffected primary root elongation under Fe deficiency (Figure 5). In addition, the loss of GATA3 affected specifically lateral root development in response to localized Fe supply (Figure 21B, C). Since under Fe deficiency the number of lateral roots was significantly reduced (Figure 5D), Fe likely affects lateral root development at very early stages. In addition, the presence of Fe stimulates lateral root emergence (Table 2) and the elongation of emerged lateral roots (Figure 6E) by redirecting auxin in lateral root apices (Figure 17A, B). However, excessive supply of Fe results in a concomitant repression of the elongation of primary and lateral roots (Figure 6A, E and I). This repressive effect of Fe on root elongation is most likely local, since only roots in contact with high Fe were inhibited (Figure 6C, E and G). In contrast to Fe, high nitrate inhibits specifically lateral root development in a systemic manner (Zhang et al., 1999).

### **6.3 Role of transcription factors in the signaling cascades affecting root development**

Transcription factors regulate many plant processes as diverse as development, responses to abiotic or biotic stresses, cell fate and identity and regulation of metabolism (Century et al., 2008; Swaminathan et al., 2008; Dubos et al., 2010; Rushton et al., 2010). As transcription factors usually regulate a set of genes, they are interesting candidates for the genetic manipulation of complex traits (Century et al., 2008; Grotewold, 2008). In *Arabidopsis*, many transcription factors have been shown to affect root development (Sabatini et al., 2003; Aida et al., 2004; Hardtke et al., 2004; Wilmoth et al., 2005; Okushima et al., 2007; Lucas et al., 2010; Sozzani et al., 2010). However, since the mis-expression of most of these transcription factors results in major phenotypical defects in the development of primary and/or lateral roots, they most likely regulate intrinsic processes of

development. Nevertheless, it still remained to be tested to which extent they are also important for environmentally-regulated changes in root architecture. To date, only a few transcription factors have been shown to affect root development in a nutrient-specific manner. The first one to be identified was the MADS-box transcription factor ANR1. ANR1 is necessary for the preferential lateral root growth in nitrate-rich patches (Zhang and Forde, 1998). WRKY75 has been shown to negatively regulate root development, while positively controlling the expression of P starvation-induced responses in roots (Devaiah et al., 2007b). However, since the target genes of ANR1 or WRKY75 are not yet known it is still unclear at which level they act on the lateral root development.

The present study, adds two additional uncharacterized transcription factors to the list of nutrient-responsive transcription factors that modulate root morphology. NGAL1 is involved in the maintenance of the meristematic activity under low P by affecting the expression of *SHR*, which is up-regulated in response to low P supply (Figure 42B, C). Both *SHR* and *SCR*, which are members of the GRAS family of transcription factors (DiLaurenzio et al., 1996; Helariutta et al., 2000), are essential for maintenance the root apical meristem (Benfey et al., 1993; Scheres et al., 1995; DiLaurenzio et al., 1996; Helariutta et al., 2000; Sabatini et al., 2003). Since *SHR* and *SCR* expression were down-regulated in *ngal1-1* roots under low P (Figure 42B, C), these plants suffered an earlier meristematic exhaustion (Figure 40), mainly due to structural defects in the cellular organization of the root apical meristem (Figure 41). These observations indicate that the NGAL1-dependent activation of *SCR* and especially *SHR* is necessary to maintain stem cell identity in the primary root meristems in response to low P, thus delaying the onset of the determinate phase of growth. Altogether, these results exemplify how a cascade of transcription factors transfers the signals of nutrient availability into the intrinsic root developmental program. The identification of upstream components as well as additional targets of NGAL1 definitely merits future attention.

The transcription factor GATA3 appears to be a regulatory component required for the lateral root elongation into Fe-enriched patches (Figure 21). Although the molecular targets of GATA3 are yet to be determined, the present results anticipate that *AUX1* represents a promising candidate for a target gene

downstream of GATA3 (Figure 19). In addition, also other components of the auxin transport and signaling pathway might be regulated by GATA3. One important observation from this study is that conversely to *FIT*, which regulates the Fe acquisition machinery in roots, the expression of *GATA3* is primarily regulated by a root-endogenous signaling pathway (Figure 26). This result is particularly exciting because it is shown here that lateral root elongation in response to Fe is mainly controlled by the local presence of Fe (Figure 15).

The Fe-dependent lateral root elongation under localized Fe supply as well as the lacking lateral root response in *gata3* mutant plants, which were isolated in a screen that was designed for the identification of regulatory components in Fe-responsive lateral root architecture, added Fe to the list of nutrients that modulate root architecture. Besides N and P, Fe is now the third nutrient that appears to be sensed by plant roots. So far, it is unclear how many of the 17 essential elements provoke targeted responses of the lateral root system. The early study of Drew (1975) could not identify a stimulated lateral root formation by local supply of K, thus indicating that roots did not evolve this morphological adaptation to each of the nutrients. Current investigations on lateral root responses to other nutrients indicate that these responses are weaker or more difficult to identify and quantify (B. Gruber and N. von Wirén, *personal communication*). Looking at the final list of nutrients that elicit lateral root responses will not only be interesting in terms of understanding the selection pressure exerted by nutrient supplies on root architecture, but also which nutrients may be useful to direct root growth of plants growing under challenging environmental conditions.



## 7 References

- Abdel-Ghany, S.E., and Pilon, M. (2008). MicroRNA-mediated systemic down-regulation of copper protein expression in response to low copper availability in arabidopsis. *J Biol Chem* 283, 15932-15945.
- Abel, S., Ticconi, C.A., and Delatorre, C.A. (2002). Phosphate sensing in higher plants. *Physiol Plantarum* 115, 1-8.
- Aida, M., Beis, D., Heidstra, R., Willemsen, V., Blilou, I., Galinha, C., Nussaume, L., Noh, Y.S., Amasino, R., and Scheres, B. (2004). The PLETHORA genes mediate patterning of the Arabidopsis root stem cell niche. *Cell* 119, 109-120.
- Alvarez, J.P., Goldshmidt, A., Efroni, I., Bowman, J.L., and Eshed, Y. (2009). The NGATHA distal organ development genes are essential for style specification in Arabidopsis. *Plant Cell*, 21, 1373-1393.
- Amtmann, A., and Blatt, M.R. (2009). Regulation of macronutrient transport. *New Phytol* 181, 35-52.
- Amtmann, A., Hammond, J.P., Armengaud, P., and White, P.J. (2006). Nutrient sensing and signalling in plants: Potassium and phosphorus. *Adv Bot Research*, 43, 209-257.
- Arnaud, N., Murgia, I., Boucherez, J., Briat, J.F., Cellier, F., and Gaymard, F. (2006). An iron-induced nitric oxide burst precedes ubiquitin-dependent protein degradation for Arabidopsis AtFer1 ferritin gene expression. *J Biol Chem* 281, 23579-23588.
- Arnaud, N., Ravet, K., Borlotti, A., Touraine, B., Boucherez, J., Fizames, C., Briat, J.F., Cellier, F., and Gaymard, F. (2007). The iron-responsive element (IRE)/iron-regulatory protein 1 (IRP1)-cytosolic aconitase iron-regulatory switch does not operate in plants. *Biochem J* 405, 523-531.
- Aung, K., Lin, S.I., Wu, C.C., Huang, Y.T., Su, C.L., and Chiou, T.J. (2006). pho2, a phosphate overaccumulator, is caused by a nonsense mutation in a MicroRNA399 target gene. *Plant Physiol* 141, 1000-1011.
- Bari, R., Pant, B.D., Stitt, M., and Scheible, W.R. (2006). PHO2, microRNA399, and PHR1 define a phosphate-signaling pathway in plants. *Plant Physiol* 141, 988-999.
- Bates, T.R., and Lynch, J.P. (1996). Stimulation of root hair elongation in *Arabidopsis thaliana* by low phosphorus availability. *Plant Cell Environ* 19, 529-538.
- Bates, T.R., and Lynch, J.P. (2001). Root hairs confer a competitive advantage under low phosphorus availability. *Plant Soil* 236, 243-250.
- Bauer, P., Ling, H.Q., and Gueriot, M.L. (2007). FIT, the FER-LIKE IRON DEFICIENCY INDUCED TRANSCRIPTION FACTOR in Arabidopsis. *Plant Physiol Bioch* 45, 260-261.
- Baxter, I. (2009). Ionomics: studying the social network of mineral nutrients. *Curr Opin Plant Biol* 12, 381-386.

- Baxter, I. (2010). Ionomics: The functional genomics of elements. *Brief Funct Genomics* 9, 149-156.
- Baxter, I., Hosmani, P.S., Rus, A., Lahner, B., Borevitz, J.O., Muthukumar, B., Mickelbart, M.V., Schreiber, L., Franke, R.B., and Salt, D.E. (2009). Root suberin forms an extracellular barrier that affects water relations and mineral nutrition in *Arabidopsis*. *Plos Genet* 5, 1-12.
- Baxter, I., Muthukumar, B., Park, H.C., Buchner, P., Lahner, B., Danku, J., Zhao, K., Lee, J., Hawkesford, M.J., Guerinot, M.L., and Salt, D.E. (2008a). Variation in molybdenum content across broadly distributed populations of *Arabidopsis thaliana* is controlled by a mitochondrial molybdenum transporter (MOT1). *Plos Genet* 4, 1-12.
- Baxter, I., Brazelton, J.N., Yu, D.N., Huang, Y.S., Lahner, B., Yakubova, E., Li, Y., Bergelson, J., Borevitz, J.O., Nordborg, M., Vitek, O., and Salt, D.E. (2010). A coastal cline in sodium accumulation in *Arabidopsis thaliana* is driven by natural variation of the sodium transporter AtHKT1;1. *Plos Genet* 6, 1-8.
- Baxter, I.R., Vitek, O., Lahner, B., Muthukumar, B., Borghi, M., Morrissey, J., Guerinot, M.L., and Salt, D.E. (2008b). The leaf ionome as a multivariable system to detect a plant's physiological status. *Proc Natl Acad Sci USA* 105, 12081-12086.
- Beinert, H., and Kennedy, M.C. (1993). Aconitase, a two-faced protein: enzyme and iron regulatory factor. *Faseb J* 7, 1442-1449.
- Benfey, P.N., Linstead, P.J., Roberts, K., Schiefelbein, J.W., Hauser, M.T., and Aeschbacher, R.A. (1993). Root development in *Arabidopsis*: four mutants with dramatically altered root morphogenesis. *Development* 119, 57-70.
- Benkova, E., Michniewicz, M., Sauer, M., Teichmann, T., Seifertova, D., Jurgens, G., and Friml, J. (2003). Local, efflux-dependent auxin gradients as a common module for plant organ formation. *Cell* 115, 591-602.
- Bi, Y.M., Zhang, Y., Signorelli, T., Zhao, R., Zhu, T., and Rothstein, S. (2005). Genetic analysis of *Arabidopsis* GATA transcription factor gene family reveals a nitrate-inducible member important for chlorophyll synthesis and glucose sensitivity. *Plant J* 44, 680-692.
- Birnbaum, K., Shasha, D.E., Wang, J.Y., Jung, J.W., Lambert, G.M., Galbraith, D.W., and Benfey, P.N. (2003). A gene expression map of the *Arabidopsis* root. *Science* 302, 1956-1960.
- Briat, J.F., Curie, C., and Gaymard, F. (2007). Iron utilization and metabolism in plants. *Curr Opin Plant Biol* 10, 276-282.
- Broadley, M.R., Hammond, J.P., White, P.J., and Salt, D.E. (2010). An efficient procedure for normalizing ionomics data for *Arabidopsis thaliana*. *New Phytol* 186, 270-274.
- Broadley, M.R., Hammond, J.P., King, G.J., Astley, D., Bowen, H.C., Meacham, M.C., Mead, A., Pink, D.A.C., Teakle, G.R., Hayden, R.M., Spracklen, W.P., and White, P.J. (2008). Shoot calcium and magnesium concentrations differ between subtaxa, are highly heritable, and associate with potentially pleiotropic loci in *Brassica oleracea*. *Plant Physiol* 146, 1707-1720.

- Brumbarova, T., and Bauer, P. (2005). Iron-mediated control of the basic helix-loop-helix protein FER, a regulator of iron uptake in tomato. *Plant Physiol* 137, 1018-1026.
- Buckhout, T.J., Yang, T.J.W., and Schmidt, W. (2009). Early iron-deficiency-induced transcriptional changes in Arabidopsis roots as revealed by microarray analyses. *BMC Genomics* 10, 1-16.
- Burleigh, S.H., and Harrison, M.J. (1999). The down-regulation of *Mt4*-like genes by phosphate fertilization occurs systemically and involves phosphate translocation to the shoots. *Plant Physiol* 119, 241-248.
- Carswell, C., Grant, B.R., Theodorou, M.E., Harris, L., Niere, J.O., and Plaxton, W.C. (1996). The fungicide phosphonate disrupts the phosphate-starvation response in *Brassica nigra* seedlings. *Plant Physiol* 110, 105-110.
- Carswell, M.C., Grant, B.R., and Plaxton, W.C. (1997). Disruption of the phosphate-starvation response of oilseed rape suspension cells by the fungicide phosphonate. *Planta* 203, 67-74.
- Casimiro, I., Beeckman, T., Graham, N., Bhalerao, R., Zhang, H., Casero, P., Sandberg, G., and Bennett, M.J. (2003). Dissecting Arabidopsis lateral root development. *Trends Plant Sci* 8, 165-171.
- Casimiro, I., Marchant, A., Bhalerao, R.P., Beeckman, T., Dhooge, S., Swarup, R., Graham, N., Inze, D., Sandberg, G., Casero, P.J., and Bennett, M. (2001). Auxin transport promotes Arabidopsis lateral root initiation. *Plant Cell* 13, 843-852.
- Century, K., Reuber, T.L., and Ratcliffe, O.J. (2008). Regulating the regulators: The future prospects for transcription-factor-based agricultural biotechnology products. *Plant Physiol* 147, 20-29.
- Cerezo, M., Tillard, P., Filleur, S., Munos, S., Daniel-Vedele, F., and Gojon, A. (2001). Major alterations of the regulation of root NO<sub>3</sub><sup>-</sup> uptake are associated with the mutation of *Nrt2.1* and *Nrt2.2* genes in arabidopsis. *Plant Physiol* 127, 262-271.
- Chaney, R.L. (1988). Plants can utilize iron from Fe-N,N'-Di-(2-Hydroxybenzoyl)-Ethylenediamine-N,N'-Diacetic acid, a ferric chelate with 106 greater formation constant than Fe-EDDHA. *J Plant Nutr* 11, 1033-1050.
- Chao, L.Y., Marletta, M.A., and Rine, J. (2008). Sre1, an iron-modulated GATA DNA-binding protein of iron-uptake genes in the fungal pathogen *Histoplasma capsulatum*. *Biochemistry-Us* 47, 7274-7283.
- Chen, O.S., Crisp, R.J., Valachovic, M., Bard, M., Winge, D.R., and Kaplan, J. (2004). Transcription of the yeast iron regulon does not respond directly to iron but rather to iron-sulfur cluster biosynthesis. *J Biol Chem* 279, 29513-29518.
- Chen, W.W., Yang, J.L., Qin, C., Jin, C.W., Mo, J.H., Ye, T., and Zheng, S.J. (2010a). Nitric oxide acts downstream of auxin to trigger root ferric-chelate reductase activity in response to iron deficiency in Arabidopsis. *Plant Physiol* 154, 810-819.
- Chen, W.W., Yang, J.L., Qin, C., Jin, C.W., Mo, J.H., Ye, T., and Zheng, S.J. (2010b). Nitric oxide acts downstream of auxin to trigger root ferric-chelate

- reductase activity in response to iron deficiency in Arabidopsis. *Plant Physiol* 154, 810-819.
- Chen, Y.F., Shakeel, S.N., Bowers, J., Zhao, X.C., Etheridge, N., and Schaller, G.E. (2007). Ligand-induced degradation of the ethylene receptor ETR2 through a proteasome-dependent pathway in Arabidopsis. *J Biol Chem* 282, 24752-24758.
- Chevalier, F., Pata, M., Nacry, P., Doumas, P., and Rossignol, M. (2003). Effects of phosphate availability on the root system architecture: large-scale analysis of the natural variation between Arabidopsis accessions. *Plant Cell Environ* 26, 1839-1850.
- Chiou, T.J., Aung, K., Lin, S.I., Wu, C.C., Chiang, S.F., and Su, C.L. (2006). Regulation of phosphate homeostasis by microRNA in Arabidopsis. *Plant Cell* 18, 412-421.
- Ciereszko, I., and Barbachowska, A. (2000). Sucrose metabolism in leaves and roots of bean (*Phaseolus vulgaris* L.) during phosphate deficiency. *J Plant Physiol* 156, 640-644.
- Ciereszko, I., Johansson, H., and Kleczkowski, L.A. (2005). Interactive effects of phosphate deficiency, sucrose and light/dark conditions on gene expression of UDP-glucose pyrophosphorylase in Arabidopsis. *J Plant Physiol* 162, 343-353.
- Clough, S.J., and Bent, A.F. (1998). Floral dip: a simplified method for *Agrobacterium*-mediated transformation of *Arabidopsis thaliana*. *Plant J* 16, 735-743.
- Colangelo, E.P., and Guerinot, M.L. (2004). The essential basic helix-loop-helix protein FIT1 is required for the iron deficiency response. *Plant Cell* 16, 3400-3412.
- Crawford, N.M. (1995). Nitrate - Nutrient and signal for plant-growth. *Plant Cell* 7, 859-868.
- Dalton, C.C., Iqbal, K., and Turner, D.A. (1983). Iron phosphate precipitation in Murashige and Skoog media. *Physiol Plantarum* 57, 472-476.
- Danku, J.M.C., Gumaelius, L., Baxter, I., and Salt, D.E. (2009). A high-throughput method for *Saccharomyces cerevisiae* (yeast) ionomics. *J Anal Atom Spectrom* 24, 103-107.
- de Dorlodot, S., Forster, B., Pages, L., Price, A., Tuberosa, R., and Draye, X. (2007). Root system architecture: opportunities and constraints for genetic improvement of crops. *Trends Plant Sci* 12, 474-481.
- De Smet, I., Signora, L., Beeckman, T., Inze, D., Foyer, C.H., and Zhang, H. (2003). An abscisic acid-sensitive checkpoint in lateral root development of Arabidopsis. *Plant J* 33, 543-555.
- De Smet, I., Tetsumura, T., De Rybel, B., Frey, N.F.D., Laplace, L., Casimiro, I., Swarup, R., Naudts, M., Vanneste, S., Audenaert, D., Inze, D., Bennett, M.J., and Beeckman, T. (2007). Auxin-dependent regulation of lateral root positioning in the basal meristem of Arabidopsis. *Development* 134, 681-690.
- De Smet, I., Vassileva, V., De Rybel, B., Levesque, M.P., Grunewald, W., Van Damme, D., Van Noorden, G., Naudts, M., Van Isterdael, G., De Clercq, R., Wang, J.Y., Meuli, N., Vanneste, S., Friml, J., Hilson, P., Jurgens, G., Ingram, G.C., Inze,

- D., Benfey, P.N., and Beeckman, T. (2008). Receptor-like kinase ACR4 restricts formative cell divisions in the Arabidopsis root. *Science* 322, 594-597.
- Delhaize, E. (1996). A metal-accumulator mutant of *Arabidopsis thaliana*. *Plant Physiol* 111, 849-855.
- Delhaize, E., and Randall, P.J. (1995). Characterization of a phosphate-accumulator mutant of *Arabidopsis thaliana*. *Plant Physiol* 107, 207-213.
- Dello Ioio, R., Linhares, F.S., Scacchi, E., Casamitjana-Martinez, E., Heidstra, R., Costantino, P., and Sabatini, S. (2007). Cytokinins determine Arabidopsis root-meristem size by controlling cell differentiation. *Curr Biol* 17, 678-682.
- Devaiah, B.N., Nagarajan, V.K., and Raghothama, K.G. (2007a). Phosphate homeostasis and root development in Arabidopsis are synchronized by the zinc finger transcription factor ZAT6. *Plant Physiol* 145, 147-159.
- Devaiah, B.N., Karthikeyan, A.S., and Raghothama, K.G. (2007b). WRKY75 transcription factor is a modulator of phosphate acquisition and root development in arabidopsis. *Plant Physiol* 143, 1789-1801.
- Devaiah, B.N., Madhuvanthi, R., Karthikeyan, A.S., and Raghothama, K.G. (2009). Phosphate starvation responses and gibberellic acid biosynthesis are regulated by the MYB62 transcription factor in Arabidopsis. *Mol Plant* 2, 43-58.
- DiLaurenzio, L., WysockaDiller, J., Malamy, J.E., Pysh, L., Helariutta, Y., Freshour, G., Hahn, M.G., Feldmann, K.A., and Benfey, P.N. (1996). The SCARECROW gene regulates an asymmetric cell division that is essential for generating the radial organization of the Arabidopsis root. *Cell* 86, 423-433.
- Dinnyen, J.R., Long, T.A., Wang, J.Y., Jung, J.W., Mace, D., Pointer, S., Barron, C., Brady, S.M., Schiefelbein, J., and Benfey, P.N. (2008). Cell identity mediates the response of Arabidopsis roots to abiotic stress. *Science* 320, 942-945.
- Doerner, P. (2008). Phosphate starvation signaling: a threesome controls systemic Pi homeostasis. *Curr Opin Plant Biol* 11, 536-540.
- Dong, B., Rengel, Z., and Delhaize, E. (1998). Uptake and translocation of phosphate by *pho2* mutant and wild-type seedlings of *Arabidopsis thaliana*. *Planta* 205, 251-256.
- Drew, M.C. (1975). Comparison of effects of a localized supply of phosphate, nitrate, ammonium and potassium on growth of seminal root system, and shoot, in barley. *New Phytol* 75, 479-490.
- Drew, M.C., and Saker, L.R. (1975). Nutrient supply and growth of seminal root system in barley. 2. Localized, compensatory increases in lateral root growth and rates of nitrate uptake when nitrate supply is restricted to only part of root system. *J Exp Bot* 26, 79-90.
- Dubos, C., Stracke, R., Grotewold, E., Weisshaar, B., Martin, C., and Lepiniec, L. (2010). MYB transcription factors in Arabidopsis. *Trends Plant Sci* 15, 573-581.
- Dubrovsky, J.G., Doerner, P.W., Colon-Carmona, A., and Rost, T.L. (2000). Pericycle cell proliferation and lateral root initiation in Arabidopsis. *Plant Physiol* 124, 1648-1657.

- Dubrovsky, J.G., Rost, T.L., Colon-Carmona, A., and Doerner, P. (2001). Early primordium morphogenesis during lateral root initiation in *Arabidopsis thaliana*. *Planta* 214, 30-36.
- Durrett, T.P., Gassmann, W., and Rogers, E.E. (2007). The FRD3-mediated efflux of citrate into the root vasculature is necessary for efficient iron translocation. *Plant Physiol* 144, 197-205.
- Duy, D., Wanner, G., Meda, A.R., von Wirén, N., Soll, J., and Philippar, K. (2007). PIC1, an ancient permease in *Arabidopsis* chloroplasts, mediates iron transport. *Plant Cell* 19, 986-1006.
- Ekanayake, I.J., Otoole, J.C., Garrity, D.P., and Masajo, T.M. (1985a). Inheritance of root characters and their relations to drought resistance in rice. *Crop Sci* 25, 927-933.
- Ekanayake, I.J., Garrity, D.P., Masajo, T.M., and Otoole, J.C. (1985b). Root pulling resistance in rice - inheritance and association with drought tolerance. *Euphytica* 34, 905-913.
- Enomoto, Y., Hodoshima, H., Shimada, H., Shoji, K., Yoshihara, T., and Goto, F. (2007). Long-distance signals positively regulate the expression of iron uptake genes in tobacco roots. *Planta* 227, 81-89.
- Ferreira, P.C.G., Hemerly, A.S., Engler, J.D., Vanmontagu, M., Engler, G., and Inze, D. (1994). Developmental expression of the *Arabidopsis* cyclin gene *Cyc1at*. *Plant Cell* 6, 1763-1774.
- Filleur, S., Walch-Liu, P., Gan, Y., and Forde, B.G. (2005). Nitrate and glutamate sensing by plant roots. *Biochem Soc T* 33, 283-286.
- Filleur, S., Dorbe, M.F., Cerezo, M., Orsel, M., Granier, F., Gojon, A., and Daniel-Vedele, F. (2001). An *Arabidopsis* T-DNA mutant affected in *Nrt2* genes is impaired in nitrate uptake. *Febs Lett* 489, 220-224.
- Fischer, U., Ikeda, Y., Ljung, K., Serralbo, O., Singh, M., Heidstra, R., Palme, K., Scheres, B., and Grebe, M. (2006). Vectorial information for *Arabidopsis* planar polarity is mediated by combined AUX1, EIN2, and GNOM activity. *Curr Biol* 16, 2143-2149.
- Forde, B.G., and Walch-Liu, P. (2009). Nitrate and glutamate as environmental cues for behavioural responses in plant roots. *Plant Cell Environ* 32, 682-693.
- Franco-Zorrilla, J.M., Martin, A.C., Solano, R., Rubio, V., Leyva, A., and Paz-Ares, J. (2002). Mutations at CRE1 impair cytokinin-induced repression of phosphate starvation responses in *Arabidopsis*. *Plant J* 32, 353-360.
- Franco-Zorrilla, J.M., Gonzalez, E., Bustos, R., Linhares, F., Leyva, A., and Paz-Ares, J. (2004). The transcriptional control of plant responses to phosphate limitation. *J Exp Bot* 55, 285-293.
- Franco-Zorrilla, J.M., Valli, A., Todesco, M., Mateos, I., Puga, M.I., Rubio-Somoza, I., Leyva, A., Weigel, D., Garcia, J.A., and Paz-Ares, J. (2007). Target mimicry provides a new mechanism for regulation of microRNA activity. *Nat Genet* 39, 1033-1037.
- Fujii, H., Chiou, T.J., Lin, S.I., Aung, K., and Zhu, J.K. (2005). A miRNA involved in phosphate-starvation response in *Arabidopsis*. *Curr Biol* 15, 2038-2043.

- Fukaki, H., and Tasaka, M. (2009a). Hormone interactions during lateral root formation. *Plant Mol Biol* 69, 437-449.
- Fukaki, H., and Tasaka, M. (2009b). Hormone interactions during lateral root formation. *Plant Mol Biol* 69, 437-449.
- Fukaki, H., Tameda, S., Masuda, H., and Tasaka, M. (2002). Lateral root formation is blocked by a gain-of-function mutation in the SOLITARY-ROOT/IAA14 gene of *Arabidopsis*. *Plant J* 29, 153-168.
- Gan, Y.B., Filleur, S., Rahman, A., Gotensparre, S., and Forde, B.G. (2005). Nutritional regulation of ANR1 and other root-expressed MADS-box genes in *Arabidopsis thaliana*. *Planta* 222, 730-742.
- Gansel, X., Munos, S., Tillard, P., and Gojon, A. (2001). Differential regulation of the  $\text{NO}_3^-$  and  $\text{NH}_4^+$  transporter genes *AtNrt2.1* and *AtAmt1.1* in *Arabidopsis*: relation with long-distance and local controls by N status of the plant. *Plant J* 26, 143-155.
- Garcia, M.J., Lucena, C., Romera, F.J., Alcantara, E., and Perez-Vicente, R. (2010). Ethylene and nitric oxide involvement in the up-regulation of key genes related to iron acquisition and homeostasis in *Arabidopsis*. *J Exp Bot* 61, 3885-3899.
- Geldner, N., Richter, S., Vieten, A., Marquardt, S., Torres-Ruiz, R.A., Mayer, U., and Jurgens, G. (2004). Partial loss-of-function alleles reveal a role for GNOM in auxin transport-related, post-embryonic development of *Arabidopsis*. *Development* 131, 389-400.
- Gewin, V. (2010). Food: an underground revolution. *Nature* 466, 552-553.
- Ghandilyan, A., Barboza, L., Tisne, S., Granier, C., Reymond, M., Koornneef, M., Schat, H., and Aarts, M.G.M. (2009a). Genetic analysis identifies quantitative trait loci controlling rosette mineral concentrations in *Arabidopsis thaliana* under drought. *New Phytol* 184, 180-192.
- Ghandilyan, A., Ilk, N., Hanhart, C., Mbengue, M., Barboza, L., Schat, H., Koornneef, M., El-Lithy, M., Vreugdenhil, D., Reymond, M., and Aarts, M.G.M. (2009b). A strong effect of growth medium and organ type on the identification of QTLs for phytate and mineral concentrations in three *Arabidopsis thaliana* RIL populations. *J Exp Bot* 60, 1409-1425.
- Giehl, R.F.H., Meda, A.R., and von Wirén, N. (2009). Moving up, down, and everywhere: signaling of micronutrients in plants. *Curr Opin Plant Biol* 12, 320-327.
- Gojon, A., Nacry, P., and Davidian, J.C. (2009). Root uptake regulation: a central process for NPS homeostasis in plants. *Curr Opin Plant Biol* 12, 328-338.
- Gojon, A., Krouk, G., Perrine-Walker, F., Laugier, E. (2011). Nitrate transceptor(s) in plants. *J Exp Bot* 62, 2299-2308.
- Graziano, M., and Lamattina, L. (2007). Nitric oxide accumulation is required for molecular and physiological responses to iron deficiency in tomato roots. *Plant J* 52, 949-960.
- Graziano, M., Beligni, M.V., and Lamattina, L. (2002). Nitric oxide improves internal iron availability in plants. *Plant Physiol* 130, 1852-1859.

- Green, L.S., and Rogers, E.E. (2004). FRD3 controls iron localization in Arabidopsis. *Plant Physiol* 136, 2523-2531.
- Grotewold, E. (2008). Transcription factors for predictive plant metabolic engineering: are we there yet? *Curr Opin Biotechnol* 19, 138-144.
- Grusak, M.A., and Pezeshgi, S. (1996). Shoot-to-root signal transmission regulates root Fe(III) reductase activity in the *dgl* mutant of pea. *Plant Physiol* 110, 329-334.
- Gustin, J.L., Loureiro, M.E., Kim, D., Na, G., Tikhonova, M., and Salt, D.E. (2009). MTP1-dependent Zn sequestration into shoot vacuoles suggests dual roles in Zn tolerance and accumulation in Zn-hyperaccumulating plants. *Plant J* 57, 1116-1127.
- Haas, H., Zadra, I., Stoffler, G., and Angermayr, K. (1999). The *Aspergillus nidulans* GATA factor SREA is involved in regulation of siderophore biosynthesis and control of iron uptake. *J Biol Chem* 274, 4613-4619.
- Hammond, J.P., and White, P.J. (2008). Sucrose transport in the phloem: integrating root responses to phosphorus starvation. *J Exp Bot* 59, 93-109.
- Hammond, J.P., Broadley, M.R., White, P.J., King, G.J., Bowen, H.C., Hayden, R., Meacham, M.C., Mead, A., Overs, T., Spracklen, W.P., and Greenwood, D.J. (2009). Shoot yield drives phosphorus use efficiency in *Brassica oleracea* and correlates with root architecture traits. *J Exp Bot* 60, 1953-1968.
- Hardtke, C.S., Ckurshumova, W., Vidaurre, D.P., Singh, S.A., Stamatiou, G., Tiwari, S.B., Hagen, G., Guilfoyle, T.J., and Berleth, T. (2004). Overlapping and non-redundant functions of the Arabidopsis auxin response factors MONOPTEROS and NONPHOTOTROPIC HYPOCOTYL 4. *Development* 131, 1089-1100.
- Helariutta, Y., Fukaki, H., Wysocka-Diller, J., Nakajima, K., Jung, J., Sena, G., Hauser, M.T., and Benfey, P.N. (2000). The SHORT-ROOT gene controls radial patterning of the Arabidopsis root through radial signaling. *Cell* 101, 555-567.
- Hentze, M.W., and Kuhn, L.C. (1996). Molecular control of vertebrate iron metabolism: mRNA-based regulatory circuits operated by iron, nitric oxide, and oxidative stress. *Proc Natl Acad Sci U S A* 93, 8175-8182.
- Hinsinger, P., Gobran, G.R., Gregory, P.J., and Wenzel, W.W. (2005). Rhizosphere geometry and heterogeneity arising from root-mediated physical and chemical processes. *New Phytol* 168, 293-303.
- Hirsch, J., Marin, E., Floriani, M., Chiarenza, S., Richaud, P., Nussaume, L., and Thibaud, M.C. (2006). Phosphate deficiency promotes modification of iron distribution in Arabidopsis plants. *Biochimie* 88, 1767-1771.
- Ho, C.H., and Tsay, Y.F. (2010). Nitrate, ammonium, and potassium sensing and signaling. *Curr Opin Plant Biol* 13, 604-610.
- Ho, C.H., Lin, S.H., Hu, H.C., and Tsay, Y.F. (2009). CHL1 Functions as a Nitrate Sensor in Plants. *Cell* 138, 1184-1194.
- Hodge, A. (2006). Plastic plants and patchy soils. *J Exp Bot* 57, 401-411.



- Hsieh, L.C., Lin, S.I., Shih, A.C.C., Chen, J.W., Lin, W.Y., Tseng, C.Y., Li, W.H., and Chiou, T.J. (2009). Uncovering small RNA-mediated responses to phosphate deficiency in *Arabidopsis* by deep sequencing. *Plant Physiol* 151, 2120-2132.
- Ito, T., Motohashi, R., Kuromori, T., Noutoshi, Y., Seki, M., Kamiya, A., Mizukado, S., Sakurai, T., and Shinozaki, K. (2005). A resource of 5,814 Dissociation transposon-tagged and sequence-indexed lines of *Arabidopsis* transposed from start loci on chromosome 5. *Plant Cell Physiol* 46, 1149-1153.
- Iwai, K., Drake, S.K., Wehr, N.B., Weissman, A.M., LaVaute, T., Minato, N., Klausner, R.D., Levine, R.L., and Rouault, T.A. (1998). Iron-dependent oxidation, ubiquitination, and degradation of iron regulatory protein 2: implications for degradation of oxidized proteins. *Proc Natl Acad Sci U S A* 95, 4924-4928.
- Iyer-Pascuzzi, A.S., and Benfey, P.N. (2009). Transcriptional networks in root cell fate specification. *BBA-Gene Regul Mech* 1789, 315-325.
- Jain, A., Poling, M.D., Smith, A.P., Nagarajan, V.K., Lahner, B., Meagher, R.B., and Raghothama, K.G. (2009). Variations in the composition of gelling agents affect morphophysiological and molecular responses to deficiencies of phosphate and other nutrients. *Plant Physiol* 150, 1033-1049.
- Jain, A., Poling, M.D., Karthikeyan, A.S., Blakeslee, J.J., Peer, W.A., Titapiwatanakun, B., Murphy, A.S., and Raghothama, K.G. (2007). Differential effects of sucrose and auxin on localized phosphate deficiency-induced modulation of different traits of root system architecture in *Arabidopsis*. *Plant Physiol* 144, 232-247.
- Jakoby, M., Wang, H.Y., Reidt, W., Weisshaar, B., and Bauer, P. (2004). FRU (BHLH029) is required for induction of iron mobilization genes in *Arabidopsis thaliana*. *Febs Lett* 577, 528-534.
- Jbel, M., Mercier, A., Pelletier, B., Beaudoin, J., and Labbe, S. (2009). Iron activates in vivo DNA binding of *Schizosaccharomyces pombe* transcription factor Fep1 through its amino-terminal region. *Eukaryot Cell* 8, 649-664.
- Karthikeyan, A.S., Varadarajan, D.K., Jain, A., Held, M.A., Carpita, N.C., and Raghothama, K.G. (2007). Phosphate starvation responses are mediated by sugar signaling in *Arabidopsis*. *Planta* 225, 907-918.
- Kim, S.A., and Guerinot, M.L. (2007). Mining iron: Iron uptake and transport in plants. *Febs Lett* 581, 2273-2280.
- Klausner, R.D., Rouault, T.A., and Harford, J.B. (1993). Regulating the fate of mRNA: the control of cellular iron metabolism. *Cell* 72, 19-28.
- Kobayashi, T., Nakayama, Y., Itai, R.N., Nakanishi, H., Yoshihara, T., Mori, S., and Nishizawa, N.K. (2003). Identification of novel cis-acting elements, IDE1 and IDE2, of the barley IDS2 gene promoter conferring iron-deficiency-inducible, root-specific expression in heterogeneous tobacco plants. *Plant J* 36, 780-793.
- Kobayashi, T., Ogo, Y., Itai, R.N., Nakanishi, H., Takahashi, M., Mori, S., and Nishizawa, N.K. (2007). The transcription factor IDEF1 regulates the response to and tolerance of iron deficiency in plants. *Proc Natl Acad Sci USA* 104, 19150-19155.

- Koike, S., Inoue, H., Mizuno, D., Takahashi, M., Nakanishi, H., Mori, S., and Nishizawa, N.K. (2004). OsYSL2 is a rice metal-nicotianamine transporter that is regulated by iron and expressed in the phloem. *Plant J* 39, 415-424.
- Konno, M., Ooishi, M., and Inoue, Y. (2006). Temporal and positional relationships between Mn uptake and low-pH-induced root hair formation in *Lactuca sativa* cv. Grand Rapids seedlings. *J Plant Research* 119, 439-447.
- Korshunova, Y.O., Eide, D., Clark, W.G., Guerinot, M.L., and Pakrasi, H.B. (1999). The IRT1 protein from *Arabidopsis thaliana* is a metal transporter with a broad substrate range. *Plant Mol Biol* 40, 37-44.
- Krouk, G., Tillard, P., and Gojon, A. (2006). Regulation of the high-affinity NO<sub>3</sub><sup>-</sup> uptake system by NRT1.1-mediated NO<sub>3</sub><sup>-</sup> demand signaling in *Arabidopsis*. *Plant Physiol* 142, 1075-1086.
- Krouk, G., Crawford, N.M., Coruzzi, G.M., and Tsay, Y.F. (2010a). Nitrate signaling: adaptation to fluctuating environments. *Curr Opin Plant Biol* 13, 266-273.
- Krouk, G., Lacombe, B., Bielach, A., Perrine-Walker, F., Malinska, K., Mounier, E., Hoyerova, K., Tillard, P., Leon, S., Ljung, K., Zazimalova, E., Benkova, E., Nacry, P., and Gojon, A. (2010b). Nitrate-regulated auxin transport by NRT1.1 defines a mechanism for nutrient sensing in plants. *Dev Cell* 18, 927-937.
- Krüger, C., Berkowitz, O., Stephan, U.W., and Hell, R. (2002). A metal-binding member of the late embryogenesis abundant protein family transports iron in the phloem of *Ricinus communis* L. *J Biol Chem* 277, 25062-25069.
- Kumanovics, A., Chen, O.S., Li, L.T., Bagley, D., Adkins, E.M., Lin, H.L., Dingra, N.N., Outten, C.E., Keller, G., Winge, D., Ward, D.M., and Kaplan, J. (2008). Identification of FRA1 and FRA2 as genes involved in regulating the yeast iron regulon in response to decreased mitochondrial iron-sulfur cluster synthesis. *J Biol Chem* 283, 10276-10286.
- Kuromori, T., Hirayama, T., Kiyosue, Y., Takabe, H., Mizukado, S., Sakurai, T., Akiyama, K., Kamiya, A., Ito, T., and Shinozaki, K. (2004). A collection of 11,800 single-copy *Ds* transposon insertion lines in *Arabidopsis*. *Plant J* 37, 897-905.
- Labbe, S., Pelletier, B., and Mercier, A. (2007). Iron homeostasis in the fission yeast *Schizosaccharomyces pombe*. *Biometals* 20, 523-537.
- Lahner, B., Gong, J.M., Mahmoudian, M., Smith, E.L., Abid, K.B., Rogers, E.E., Guerinot, M.L., Harper, J.F., Ward, J.M., McIntyre, L., Schroeder, J.I., and Salt, D.E. (2003). Genomic scale profiling of nutrient and trace elements in *Arabidopsis thaliana*. *Nat Biotechnol* 21, 1215-1221.
- Laine, P., Ourry, A., and Boucaud, J. (1995). Shoot control of nitrate uptake rates by roots of *Brassica napus* L - Effects of localized nitrate supply. *Planta* 196, 77-83.
- Landsberg, E.C. (1986). Function of rhizodermal transfer cells in the Fe stress response mechanism of *Capsicum annuum* L. *Plant Physiol* 82, 511-517.
- Lanquar, V., Lelievre, F., Bolte, S., Hames, C., Alcon, C., Neumann, D., Vansuyt, G., Curie, C., Schroder, A., Kramer, U., Barbier-Brygoo, H., and Thomine, S.

- (2005). Mobilization of vacuolar iron by AtNRAMP3 and AtNRAMP4 is essential for seed germination on low iron. *EMBO J* 24, 4041-4051.
- Li, W.F., Perry, P.J., Prafulla, N.N., and Schmidt, W. (2010). Ubiquitin-specific Protease 14 (UBP14) is involved in root responses to phosphate deficiency in Arabidopsis. *Mol Plant* 3, 212-223.
- Li, X.X., and Li, C.J. (2004). Is ethylene involved in regulation of root ferric reductase activity of dicotyledonous species under iron deficiency? *Plant Soil* 261, 147-153.
- Lima, J.E., Kojima, S., Takahashi, H., and von Wirén, N. (2010). Ammonium triggers lateral root branching in Arabidopsis in an AMMONIUM TRANSPORTER1;3-dependent manner. *Plant Cell* 22, 3621-3633.
- Lin, S.I., Chiang, S.F., Lin, W.Y., Chen, J.W., Tseng, C.Y., Wu, P.C., and Chiou, T.J. (2008). Regulatory network of *microRNA399* and PHO2 by systemic signaling. *Plant Physiol* 147, 732-746.
- Lin, W.Y., Lin, S.I., and Chiou, T.J. (2009). Molecular regulators of phosphate homeostasis in plants. *J Exp Bot* 60, 1427-1438.
- Lincoln, C., Britton, J.H., and Estelle, M. (1990). Growth and development of the *Axr1* mutants of Arabidopsis. *Plant Cell* 2, 1071-1080.
- Ling, H.Q., Koch, G., Baumlein, H., and Ganai, M.W. (1999). Map-based cloning of chloronerva, a gene involved in iron uptake of higher plants encoding nicotianamine synthase. *Proc Natl Acad Sci U S A* 96, 7098-7103.
- Ling, H.Q., Bauer, P., Bereczky, Z., Keller, B., and Ganai, M. (2002). The tomato fer gene encoding a bHLH protein controls iron-uptake responses in roots. *Proc Natl Acad Sci USA* 99, 13938-13943.
- Linkohr, B.I., Williamson, L.C., Fitter, A.H., and Leyser, H.M. (2002). Nitrate and phosphate availability and distribution have different effects on root system architecture of Arabidopsis. *Plant J* 29, 751-760.
- Liu, J.Q., Samac, D.A., Bucciarelli, B., Allan, D.L., and Vance, C.P. (2005). Signaling of phosphorus deficiency-induced gene expression in white lupin requires sugar and phloem transport. *Plant J* 41, 257-268.
- Lloyd, J.C., and Zakhleniuk, O.V. (2004). Responses of primary and secondary metabolism to sugar accumulation revealed by microarray expression analysis of the Arabidopsis mutant, pho3. *J Exp Bot* 55, 1221-1230.
- Lobreaux, S., Thoiron, S., and Briat, J.F. (1995). Induction of ferritin synthesis in maize leaves by an iron-mediated oxidative stress. *Plant J* 8, 443-449.
- Long, T.A., Tsukagoshi, H., Busch, W., Lahner, B., Salt, D.E., and Benfey, P.N. (2010). The bHLH transcription factor POPEYE regulates response to iron deficiency in Arabidopsis roots. *Plant Cell* 22, 2219-2236.
- Lopez-Bucio, J., Cruz-Ramirez, A., and Herrera-Estrella, L. (2003). The role of nutrient availability in regulating root architecture. *Curr Opin Plant Biol* 6, 280-287.
- Lopez-Bucio, J., Hernandez-Abreu, E., Sanchez-Calderon, L., Nieto-Jacobo, M.F., Simpson, J., and Herrera-Estrella, L. (2002). Phosphate availability alters

architecture and causes changes in hormone sensitivity in the Arabidopsis root system. *Plant Physiol* 129, 244-256.

Lopez-Bucio, J., Hernandez-Abreu, E., Sanchez-Calderon, L., Perez-Torres, A., Rampey, R.A., Bartel, B., and Herrera-Estrella, L. (2005). An auxin transport independent pathway is involved in phosphate stress-induced root architectural alterations in arabidopsis. Identification of BIG as a mediator of auxin in pericycle cell activation. *Plant Physiol* 137, 681-691.

Lucas, M., Swarup, R., Paponov, I.A., Swarup, K., Casimiro, I., Lake, D., Peret, B., Zappala, S., Mairhofer, S., Whitworth, M., Wang, J.H., Ljung, K., Marchant, A., Sandberg, G., Holdsworth, M.J., Palme, K., Pridmore, T., Mooney, S., and Bennett, M.J. (2010). SHORT-ROOT regulates primary, lateral and adventitious root development in Arabidopsis. *Plant Physiol* 155, 384-398.

Lucena, C., Waters, B.M., Romera, F.J., Garcia, M.J., Morales, M., Alcantara, E., and Perez-Vicente, R. (2006). Ethylene could influence ferric reductase, iron transporter, and H<sup>+</sup>-ATPase gene expression by affecting FER (or FER-like) gene activity. *J Exp Bot* 57, 4145-4154.

Lynch, J.P., and Brown, K.M. (2001). Topsoil foraging – an architectural adaptation of plants to low phosphorus availability. *Plant Soil* 237, 13.

Ma, Z., Bielenberg, D.G., Brown, K.M., and Lynch, J.P. (2001). Regulation of root hair density by phosphorus availability in *Arabidopsis thaliana*. *Plant Cell Environ* 24, 459-467.

Maas, F.M., Vandewetering, D.A.M., Vanbeusichem, M.L., and Bienfait, H.F. (1988). Characterization of phloem iron and its possible role in the regulation of Fe-efficiency reactions. *Plant Physiol* 87, 167-171.

Malamy, J.E. (2005). Intrinsic and environmental response pathways that regulate root system architecture. *Plant Cell Environ* 28, 67-77.

Malamy, J.E., and Benfey, P.N. (1997). Organization and cell differentiation in lateral roots of *Arabidopsis thaliana*. *Development* 124, 33-44.

Manfield, I.W., Devlin, P.F., Jen, C.H., Westhead, D.R., and Gilmartin, P.M. (2007). Conservation, convergence, and divergence of light-responsive, circadian-regulated, and tissue-specific expression patterns during evolution of the Arabidopsis GATA gene family. *Plant Physiol* 143, 941-958.

Marchant, A., Bhalerao, R., Casimiro, I., Eklof, J., Casero, P.J., Bennett, M., and Sandberg, G. (2002). AUX1 promotes lateral root formation by facilitating indole-3-acetic acid distribution between sink and source tissues in the Arabidopsis seedling. *Plant Cell* 14, 589-597.

Marschner, H. (1995). Mineral Nutrition of Higher Plants. Academic Press Limited, London.

Men, S.Z., Boutte, Y., Ikeda, Y., Li, X.G., Palme, K., Stierhof, Y.D., Hartmann, M.A., Moritz, T., and Grebe, M. (2008). Sterol-dependent endocytosis mediates post-cytokinetic acquisition of PIN2 auxin efflux carrier polarity. *Nat Cell Biol* 10, 237-U124.

Miller, A.J., Shen, Q.R., and Xu, G.H. (2009). Freeways in the plant: transporters for N, P and S and their regulation. *Curr Opin Plant Biol* 12, 284-290.

- Misson, J., Raghothama, K.G., Jain, A., Jouhet, J., Block, M.A., Bligny, R., Ortet, P., Creff, A., Somerville, S., Rolland, N., Doumas, P., Nacry, P., Herrerra-Estrella, L., Nussaume, L., and Thibaud, M.C. (2005). A genome-wide transcriptional analysis using *Arabidopsis thaliana* Affymetrix gene chips determined plant responses to phosphate deprivation. *Proc Natl Acad Sci USA* 102, 11934-11939.
- Miura, K., Jin, J.B., and Hasegawa, P.M. (2007). Sumoylation, a post-translational regulatory-process in plants. *Curr Opin Plant Biol* 10, 495-502.
- Miura, K., Rus, A., Sharkhuu, A., Yokoi, S., Karthikeyan, A.S., Raghothama, K.G., Baek, D., Koo, Y.D., Jin, J.B., Bressan, R.A., Yun, D.J., and Hasegawa, P.M. (2005). The *Arabidopsis* SUMO E3 ligase SIZ1 controls phosphate deficiency responses. *Proc Natl Acad Sci USA* 102, 7760-7765.
- Miwa, K., Takano, J., Omori, H., Seki, M., Shinozaki, K., and Fujiwara, T. (2007). Plants tolerant of high boron levels. *Science* 318, 1417-1417.
- Morales, F., Abadia, A., and Abadia, J. (1990). Characterization of the xanthophyll cycle and other photosynthetic pigment changes induced by iron-deficiency in sugar-beet (*Beta vulgaris* L). *Plant Physiol* 94, 607-613.
- Morcuende, R., Bari, R., Gibon, Y., Zheng, W.M., Pant, B.D., Blasing, O., Usadel, B., Czechowski, T., Udvardi, M.K., Stitt, M., and Scheible, W.R. (2007). Genome-wide reprogramming of metabolism and regulatory networks of *Arabidopsis* in response to phosphorus. *Plant Cell Environ* 30, 85-112.
- Muchhal, U.S., Pardo, J.M., and Raghothama, K.G. (1996). Phosphate transporters from the higher plant *Arabidopsis thaliana*. *Proc Natl Acad Sci USA* 93, 10519-10523.
- Müller, M., and Schmidt, W. (2004). Environmentally induced plasticity of root hair development in *Arabidopsis*. *Plant Physiol* 134, 409-419.
- Müller, R., Nilsson, L., Krintel, C., and Nielsen, T.H. (2004). Gene expression during recovery from phosphate starvation in roots and shoots of *Arabidopsis thaliana*. *Physiol Plantarum* 122, 233-243.
- Müller, R., Nilsson, L., Nielsen, L.K., and Nielsen, T.H. (2005). Interaction between phosphate starvation signalling and hexokinase-independent sugar sensing in *Arabidopsis* leaves. *Physiol Plantarum* 124, 81-90.
- Müller, R., Morant, M., Jarmer, H., Nilsson, L., and Nielsen, T.H. (2007). Genome-wide analysis of the *Arabidopsis* leaf transcriptome reveals interaction of phosphate and sugar metabolism. *Plant Physiol* 143, 156-171.
- Munos, S., Cazettes, C., Fizames, C., Gaymard, F., Tillard, P., Lepetit, M., Lejay, L., and Gojon, A. (2004). Transcript profiling in the *chl1-5* mutant of *Arabidopsis* reveals a role of the nitrate transporter NRT1.1 in the regulation of another nitrate transporter, NRT2.1. *Plant Cell* 16, 2433-2447.
- Murashige, T., and Skoog, F. (1962). A revised medium for rapid growth and bio assays with tobacco tissue cultures. *Physiol Plantarum* 15, 473-&.
- Murgia, I., Delledonne, M., and Soave, C. (2002). Nitric oxide mediates iron-induced ferritin accumulation in *Arabidopsis*. *Plant J* 30, 521-528.
- Nacry, P., Canivenc, G., Müller, B., Azmi, A., Van Onckelen, H., Rossignol, M., and Doumas, P. (2005). A role for auxin redistribution in the responses of the root

- system architecture to phosphate starvation in *Arabidopsis*. *Plant Physiol* 138, 2061-2074.
- Narang, R.A., Bruene, A., and Altmann, T. (2000). Analysis of phosphate acquisition efficiency in different *Arabidopsis* accessions. *Plant Physiol* 124, 1786-1799.
- Navari-Izzo, F., Cestone, B., Cavallini, A., Natali, L., Giordani, T., and Quartacci, M.F. (2006). Copper excess triggers phospholipase D activity in wheat roots. *Phytochem* 67, 1232-1242.
- Nilsson, L., Müller, R., and Nielsen, T.H. (2007). Increased expression of the MYB-related transcription factor, PHR1, leads to enhanced phosphate uptake in *Arabidopsis thaliana*. *Plant Cell Environ* 30, 1499-1512.
- Nishii, A., Takemura, M., Fujita, H., Shikata, M., Yokota, A., and Kohchi, T. (2000). Characterization of a novel gene encoding a putative single zinc-finger protein, ZIM, expressed during the reproductive phase in *Arabidopsis thaliana*. *Biosci Biotech Bioch* 64, 1402-1409.
- Normanly, J., Grisafi, P., Fink, G.R., and Bartel, B. (1997). *Arabidopsis* mutants resistant to the auxin effects of indole-3-acetonitrile are defective in the nitrilase encoded by the *NIT1* gene. *Plant Cell* 9, 1781-1790.
- Norwell, W.A. (1991). Reactions of metal chelates in soils and nutrient solutions. In *Micronutrients in Agriculture* (Madison, WI: Soil Sci. Am. Book series), pp. 187-227.
- Oberegger, H., Schoeser, M., Zadra, I., Abt, B., and Haas, H. (2001). SREA is involved in regulation of siderophore biosynthesis, utilization and uptake in *Aspergillus nidulans*. *Mol Microbiol* 41, 1077-1089.
- Oberegger, H., Zadra, I., Schoeser, M., Abt, B., Parson, W., and Haas, H. (2002). Identification of members of the *Aspergillus nidulans* SREA regulon: genes involved in siderophore biosynthesis and utilization. *Biochem Soc T* 30, 781-783.
- Ogo, Y., Itail, R.N., Nakanishi, H., Kobayashi, T., Takahashi, M., Mori, S., and Nishizawa, N.K. (2007). The rice bHLH protein OsiRO2 is an essential regulator of the genes involved in Fe uptake under Fe-deficient conditions. *Plant J* 51, 366-377.
- Ogo, Y., Itai, R.N., Inoue, H., Kobayashi, T., Suzuki, M., Takahashi, M., Mori, S., Nishizawa, N.K., and Nishizawa, N.K. (2006). Isolation and characterization of IRO2, a novel iron-regulated bHLH transcription factor in graminaceous plants. *J Exp Bot* 57, 2867-2878.
- Ogo, Y., Kobayashi, T., Itai, R.N., Nakanishi, H., Kakei, Y., Takahashi, M., Toki, S., Mori, S., and Nishizawa, N.K. (2008). A novel NAC transcription factor, IDEF2, that recognizes the iron deficiency-responsive element 2 regulates the genes involved in iron homeostasis in plants. *J Biol Chem* 283, 13407-13417.
- Okushima, Y., Fukaki, H., Onoda, M., Theologis, A., and Tasaka, M. (2007). ARF7 and ARF19 regulate lateral root formation via direct activation of LBD/ASL genes in *Arabidopsis*. *Plant Cell* 19, 118-130.

- Pant, B.D., Buhtz, A., Kehr, J., and Scheible, W.R. (2008). *MicroRNA399* is a long-distance signal for the regulation of plant phosphate homeostasis. *Plant J* 53, 731-738.
- Pelletier, B., Trott, A., Morano, K.A., and Labbe, S. (2005). Functional characterization of the iron-regulatory transcription factor Fep1 from *Schizosaccharomyces pombe*. *J Biol Chem* 280, 25146-25161.
- Peret, B., De Rybel, B., Casimiro, I., Benkova, E., Swarup, R., Laplaze, L., Beeckman, T., and Bennett, M.J. (2009). Arabidopsis lateral root development: an emerging story. *Trends Plant Sci* 14, 399-408.
- Perez-Torres, C.A., Lopez-Bucio, J., Cruz-Ramirez, A., Ibarra-Laclette, E., Dharmasiri, S., Estelle, M., and Herrera-Estrella, L. (2008a). Phosphate availability alters lateral root development in Arabidopsis by modulating auxin sensitivity via a mechanism involving the TIR1 auxin receptor. *Plant Cell* 20, 3258-3272.
- Perry, P., Linke, B., and Schmidt, W. (2007). Reprogramming of root epidermal cells in response to nutrient deficiency. *Biochem Soc T* 35, 161-163.
- Petricka, J.J., and Benfey, P.N. (2008). Root layers: complex regulation of developmental patterning. *Curr Opin Genet Dev* 18, 354-361.
- Pilon, M., Cohu, C.M., Ravet, K., Abdel-Ghany, S.E., and Gaymard, F. (2009). Essential transition metal homeostasis in plants. *Curr Opin Plant Biol* 12, 347-357.
- Porra, R.J., Thompson, W.A., and Kriedemann, P.E. (1989). Determination of accurate extinction coefficients and simultaneous equations for assaying chlorophyll-a and chlorophyll-b extracted with 4 different solvents - Verification of the concentration of chlorophyll standards by atomic-absorption spectroscopy. *Biochimica et Biophysica Acta* 975, 384-394.
- Price, A.H., and Tomos, A.D. (1997). Genetic dissection of root growth in rice (*Oryza sativa* L). 2. mapping quantitative trait loci using molecular markers. *Theor Appl Gen* 95, 143-152.
- Price, A.H., Tomos, A.D., and Virk, D.S. (1997). Genetic dissection of root growth in rice (*Oryza sativa* L).1. a hydroponic screen. *Theor Appl Gen* 95, 132-142.
- Qu, L.J., and Zhu, Y.X. (2006). Transcription factor families in Arabidopsis: major progress and outstanding issues for future research - Commentary. *Curr Opin Plant Biol* 9, 544-549.
- Raghothama, K.G. (1999). Phosphate acquisition. *Annu Rev Plant Physiol* 50, 665-693.
- Raghothama, K.G., and Karthikeyan, A.S. (2005). Phosphate acquisition. *Plant Soil* 274, 37-49.
- Ramirez, L., Zabaleta, E.J., and Lamattina, L. (2010). Nitric oxide and frataxin: two players contributing to maintain cellular iron homeostasis. *Ann Bot* 105, 801-810.
- Rausch, C., and Bucher, M. (2002). Molecular mechanisms of phosphate transport in plants. *Planta* 216, 23-37.
- Ravet, K., Touraine, B., Boucherez, J., Briat, J.F., Gaymard, F., and Cellier, F. (2009). Ferritins control interaction between iron homeostasis and oxidative stress in Arabidopsis. *Plant J* 57, 400-412.

- Remans, T., Nacry, P., Pervent, M., Girin, T., Tillard, P., Lepetit, M., and Gojon, A. (2006a). A central role for the nitrate transporter NRT2.1 in the integrated morphological and physiological responses of the root system to nitrogen limitation in *Arabidopsis*. *Plant Physiol* 140, 909-921.
- Remans, T., Nacry, P., Pervent, M., Filleur, S., Diatloff, E., Mounier, E., Tillard, P., Forde, B.G., and Gojon, A. (2006b). The *Arabidopsis* NRT1.1 transporter participates in the signaling pathway triggering root colonization of nitrate-rich patches. *Proc Natl Acad Sci USA* 103, 19206-19211.
- Reyes, J.C., Muro-Pastor, M.I., and Florencio, F.J. (2004). The GATA family of transcription factors in *Arabidopsis* and rice. *Plant Physiol* 134, 1718-1732.
- Reymond, M., Svistoonoff, S., Loudet, O., Nussaume, L., and Desnos, T. (2006). Identification of QTL controlling root growth response to phosphate starvation in *Arabidopsis thaliana*. *Plant Cell Environ* 29, 115-125.
- Riechmann, J.L., and Ratcliffe, O.J. (2000). A genomic perspective on plant transcription factors. *Curr Opin Plant Biol* 3, 423-434.
- Riechmann, J.L., Heard, J., Martin, G., Reuber, L., Jiang, C.Z., Keddie, J., Adam, L., Pineda, O., Ratcliffe, O.J., Samaha, R.R., Creelman, R., Pilgrim, M., Broun, P., Zhang, J.Z., Ghandehari, D., Sherman, B.K., and Yu, C.L. (2000). *Arabidopsis* transcription factors: Genome-wide comparative analysis among eukaryotes. *Science* 290, 2105-2110.
- Rogers, E.E., and Guerinot, M.L. (2002). FRD3, a member of the multidrug and toxin efflux family, controls iron deficiency responses in *Arabidopsis*. *Plant Cell* 14, 1787-1799.
- Romera, F.J., Alcantara, E., and De la Guardia, M.D. (1999). Ethylene production by Fe-deficient roots and its involvement in the regulation of Fe-deficiency stress responses by strategy I plants. *Ann Bot* 83, 51-55.
- Römheld, V., and Marschner, H. (1981). Effect of Fe stress on utilization of Fe chelates by efficient and inefficient plant species. *J Plant Nutr* 3, 551-560.
- Rouached, H., Arpat, A.B., and Poirier, Y. (2010). Regulation of phosphate starvation responses in plants: signaling players and cross-talks. *Mol Plant* 3, 288-299.
- Rubio, V., Linhares, F., Solano, R., Martin, A.C., Iglesias, J., Leyva, A., and Paz-Ares, J. (2001). A conserved MYB transcription factor involved in phosphate starvation signaling both in vascular plants and in unicellular algae. *Gene Dev* 15, 2122-2133.
- Rus, A., Baxter, I., Muthukumar, B., Gustin, J., Lahner, B., Yakubova, E., and Salt, D.E. (2006). Natural variants of AtHKT1 enhance Na<sup>+</sup> accumulation in two wild Populations of *Arabidopsis*. *Plos Genet* 2, 1964-1973.
- Rushton, P.J., Somssich, I.E., Ringler, P., and Shen, Q.J. (2010). WRKY transcription factors. *Trends Plant Sci* 15, 247-258.
- Russo, M., Sgherri, C., Izzo, R., and Navari-Izzo, F. (2008). *Brassica napus* subjected to copper excess: Phospholipases C and D and glutathione system in signalling. *Environ Exp Bot* 62, 238-246.



- Rutherford, J.C., Ojeda, L., Balk, J., Muhlenhoff, U., Lill, R., and Winge, D.R. (2005). Activation of the iron regulon by the yeast Aft1/Aft2 transcription factors depends on mitochondrial but not cytosolic iron-sulfur protein biogenesis. *J Biol Chem* 280, 10135-10140.
- Sabatini, S., Heidstra, R., Wildwater, M., and Scheres, B. (2003). SCARECROW is involved in positioning the stem cell niche in the Arabidopsis root meristem. *Gene Dev* 17, 354-358.
- Salahudeen, A.A., Thompson, J.W., Ruiz, J.C., Ma, H.W., Kinch, L.N., Li, Q.M., Grishin, N.V., and Bruick, R.K. (2009). An E3 Ligase possessing an iron-responsive hemerythrin domain is a regulator of iron homeostasis. *Science* 326, 722-726.
- Sanchez-Calderon, L., Lopez-Bucio, J., Chacon-Lopez, A., Gutierrez-Ortega, A., Hernandez-Abreu, E., and Herrera-Estrella, L. (2006). Characterization of low phosphorus insensitive mutants reveals a crosstalk between low phosphorus-induced determinate root development and the activation of genes involved in the adaptation of Arabidopsis to phosphorus deficiency. *Plant Physiol* 140, 879-889.
- Sanchez-Calderon, L., Lopez-Bucio, J., Chacon-Lopez, A., Cruz-Ramirez, A., Nieto-Jacobo, F., Dubrovsky, J.G., and Herrera-Estrella, L. (2005). Phosphate starvation induces a determinate developmental program in the roots of *Arabidopsis thaliana*. *Plant Cell Physiol* 46, 174-184.
- Schachtman, D.P., and Shin, R. (2007). Nutrient sensing and signaling: NPKS. *Annu Rev Plant Biol* 58, 47-69.
- Scheres, B., Benfey, P., and Dolan, L. (2002). Root development. In *The Arabidopsis Book*, C.R. Somerville and E.M. Meyerowitz, eds (Rockville: America Society of Plant Biologists).
- Scheres, B., Dilaurenzio, L., Willemsen, V., Hauser, M.T., Janmaat, K., Weisbeek, P., and Benfey, P.N. (1995). Mutations affecting the radial organization of the Arabidopsis root display specific defects throughout the embryonic axis. *Development* 121, 53-62.
- Schikora, A., and Schmidt, W. (2001). Iron stress-induced changes in root epidermal cell fate are regulated independently from physiological responses to low iron availability. *Plant Physiol* 125, 1679-1687.
- Schmidt, W., and Schikora, A. (2001). Different pathways are involved in phosphate and iron stress-induced alterations of root epidermal cell development. *Plant Physiol* 125, 2078-2084.
- Schmidt, W., Tittel, J., and Schikora, A. (2000). Role of hormones in the induction of iron deficiency responses in Arabidopsis roots. *Plant Physiol* 122, 1109-1118.
- Schrettl, M., Kim, H.S., Eisendle, M., Kragl, C., Nierman, W.C., Heinekamp, T., Werner, E.R., Jacobsen, I., Illmer, P., Yi, H., Brakhage, A.A., and Haas, H. (2008). SreA-mediated iron regulation in *Aspergillus fumigatus*. *Mol Microbiol* 70, 27-43.
- Séguéla, M., Briat, J.F., Vert, G., and Curie, C. (2008). Cytokinins negatively regulate the root iron uptake machinery in Arabidopsis through a growth-dependent pathway. *Plant J* 55, 289-300.

- Shikata, M., Matsuda, Y., Ando, K., Nishii, A., Takemura, M., Yokota, A., and Kohchi, T. (2004). Characterization of Arabidopsis ZIM, a member of a novel plant-specific GATA factor gene family. *J Exp Bot* 55, 631-639.
- Shin, H., Shin, H.S., Dewbre, G.R., and Harrison, M.J. (2004). Phosphate transport in Arabidopsis: Pht1;1 and Pht1;4 play a major role in phosphate acquisition from both low- and high-phosphate environments. *Plant J* 39, 629-642.
- Shin, H., Shin, H.S., Chen, R., and Harrison, M.J. (2006). Loss of *At4* function impacts phosphate distribution between the roots and the shoots during phosphate starvation. *Plant J* 45, 712-726.
- Shkolnik-Inbar, D., and Bar-Zvi, D. (2010). ABI4 mediates abscisic acid and cytokinin inhibition of lateral root formation by reducing polar auxin transport in Arabidopsis. *Plant Cell* 22, 3560-3573.
- Signora, L., De Smet, I., Foyer, C.H., and Zhang, H. (2001). ABA plays a central role in mediating the regulatory effects of nitrate on root branching in Arabidopsis. *Plant J* 28, 655-662.
- Sozzani, R., Cui, H., Moreno-Risueno, M.A., Busch, W., Van Norman, J.M., Vernoux, T., Brady, S.M., Dewitte, W., Murray, J.A., and Benfey, P.N. (2010). Spatiotemporal regulation of cell-cycle genes by SHORTROOT links patterning and growth. *Nature* 466, 128-132.
- Stacey, M.G., Patel, A., McClain, W.E., Mathieu, M., Remley, M., Rogers, E.E., Gassmann, W., Blevins, D.G., and Stacey, G. (2008). The Arabidopsis AtOPT3 protein functions in metal homeostasis and movement of iron to developing seeds. *Plant Physiol* 146, 589-601.
- Stahl, Y., Wink, R.H., Ingram, G.C., and Simon, R. (2009). A signaling module controlling the stem cell niche in Arabidopsis root meristems. *Curr Biol* 19, 909-914.
- Stitt, M. (1999). Nitrate regulation of metabolism and growth. *Curr Opin Plant Biol* 2, 178-186.
- Svistoonoff, S., Creff, A., Reymond, M., Sigoillot-Claude, C., Ricaud, L., Blanchet, A., Nussaume, L., and Desnos, T. (2007). Root tip contact with low-phosphate media reprograms plant root architecture. *Nat Genet* 39, 792-796.
- Swaminathan, K., Peterson, K., and Jack, T. (2008). The plant B3 superfamily. *Trends Plant Sci* 13, 647-655.
- Swarup, K., Benkova, E., Swarup, R., Casimiro, I., Peret, B., Yang, Y., Parry, G., Nielsen, E., De Smet, I., Vanneste, S., Levesque, M.P., Carrier, D., James, N., Calvo, V., Ljung, K., Kramer, E., Roberts, R., Graham, N., Marillonnet, S., Patel, K., Jones, J.D., Taylor, C.G., Schachtman, D.P., May, S., Sandberg, G., Benfey, P., Friml, J., Kerr, I., Beeckman, T., Laplace, L., and Bennett, M.J. (2008). The auxin influx carrier LAX3 promotes lateral root emergence. *Nat Cell Biol* 10, 946-954.
- Swarup, R., Friml, J., Marchant, A., Ljung, K., Sandberg, G., Palme, K., and Bennett, M. (2001). Localization of the auxin permease AUX1 suggests two functionally distinct hormone transport pathways operate in the Arabidopsis root apex. *Gene Dev* 15, 2648-2653.

- Swarup, R., Kramer, E.M., Perry, P., Knox, K., Leyser, H.M., Haseloff, J., Beemster, G.T., Bhalerao, R., and Bennett, M.J. (2005). Root gravitropism requires lateral root cap and epidermal cells for transport and response to a mobile auxin signal. *Nat Cell Biol* 7, 1057-1065.
- Swarup, R., Kargul, J., Marchant, A., Zadik, D., Rahman, A., Mills, R., Yemm, A., May, S., Williams, L., Millner, P., Tsurumi, S., Moore, I., Napier, R., Kerr, I.D., and Bennett, M.J. (2004). Structure-function analysis of the presumptive *Arabidopsis* auxin permease AUX1. *Plant Cell* 16, 3069-3083.
- Takano, J., Wada, M., Ludewig, U., Schaaf, G., von Wirén, N., and Fujiwara, T. (2006). The *Arabidopsis* major intrinsic protein NIP5;1 is essential for efficient boron uptake and plant development under boron limitation. *Plant Cell* 18, 1498-1509.
- Teakle, G.R., and Kay, S.A. (1995). The GATA-binding protein CGF-1 is closely related to GT-1. *Plant Mol Biol* 29, 1253-1266.
- Teakle, G.R., Manfield, I.W., Graham, J.F., and Gilmartin, P.M. (2002). *Arabidopsis thaliana* GATA factors: organisation, expression and DNA-binding characteristics. *Plant Mol Biol* 50, 43-57.
- Thibaud, M.C., Arrighi, J.F., Bayle, V., Chiarenza, S., Creff, A., Bustos, R., Paz-Ares, J., Poirier, Y., and Nussaume, L. (2010). Dissection of local and systemic transcriptional responses to phosphate starvation in *Arabidopsis*. *Plant J* 64, 775-789.
- Tian, Q.Y., Sun, P., and Zhang, W.H. (2009). Ethylene is involved in nitrate-dependent root growth and branching in *Arabidopsis thaliana*. *New Phytol* 184, 918-931.
- Ticconi, C.A., and Abel, S. (2004). Short on phosphate: plant surveillance and countermeasures. *Trends Plant Sci* 9, 548-555.
- Ticconi, C.A., Delatorre, C.A., and Abel, S. (2001). Attenuation of phosphate starvation responses by phosphite in *Arabidopsis*. *Plant Physiol* 127, 963-972.
- Ticconi, C.A., Delatorre, C.A., Lahner, B., Salt, D.E., and Abel, S. (2004). *Arabidopsis pdr2* reveals a phosphate-sensitive checkpoint in root development. *Plant J* 37, 801-814.
- Ticconi, C.A., Lucero, R.D., Sakhonwasee, S., Adamson, A.W., Creff, A., Nussaume, L., Desnos, T., and Abel, S. (2009). ER-resident proteins PDR2 and LPR1 mediate the developmental response of root meristems to phosphate availability. *Proc Natl Acad Sci USA* 106, 14174-14179.
- Tran, H.T., Hurley, B.A., and Plaxton, W.C. (2010a). Feeding hungry plants: The role of purple acid phosphatases in phosphate nutrition. *Plant Sci* 179, 14-27.
- Tran, H.T., Qian, W.Q., Hurley, B.A., She, Y.M., Wang, D.W., and Plaxton, W.C. (2010b). Biochemical and molecular characterization of AtPAP12 and AtPAP26: the predominant purple acid phosphatase isozymes secreted by phosphate-starved *Arabidopsis thaliana*. *Plant Cell Environ* 33, 1789-1803.
- Trull, M.C., and Deikman, D. (1998). An *Arabidopsis* mutant missing one acid phosphatase isoform. *Planta* 206, 544-550.

- Ulmasov, T., Murfett, J., Hagen, G., and Guilfoyle, T.J. (1997). Aux/IAA proteins repress expression of reporter genes containing natural and highly active synthetic auxin response elements. *Plant Cell* 9, 1963-1971.
- van den Berg, C., Willemsen, V., Hendriks, G., Weisbeek, P., and Scheres, B. (1997). Short-range control of cell differentiation in the *Arabidopsis* root meristem. *Nature* 390, 287-289.
- Vanneste, S., De Rybel, B., Beemster, G.T., Ljung, K., De Smet, I., Van Isterdael, G., Naudts, M., Iida, R., Gruissem, W., Tasaka, M., Inze, D., Fukaki, H., and Beeckman, T. (2005). Cell cycle progression in the pericycle is not sufficient for SOLITARY ROOT/IAA14-mediated lateral root initiation in *Arabidopsis thaliana*. *Plant Cell* 17, 3035-3050.
- Varotto, C., Maiwald, D., Pesaresi, P., Jahns, P., Salamini, F., and Leister, D. (2002). The metal ion transporter IRT1 is necessary for iron homeostasis and efficient photosynthesis in *Arabidopsis thaliana*. *Plant J* 31, 589-599.
- Vashisht, A.A., Zumbrennen, K.B., Huang, X.H., Powers, D.N., Durazo, A., Sun, D.H., Bhaskaran, N., Persson, A., Uhlen, M., Sangfelt, O., Spruck, C., Leibold, E.A., and Wohlschlegel, J.A. (2009). Control of iron homeostasis by an iron-regulated ubiquitin ligase. *Science* 326, 718-721.
- Vert, G., Grotz, N., Dedaldechamp, F., Gaymard, F., Guerinot, M.L., Briat, J.F., and Curie, C. (2002). IRT1, an *Arabidopsis* transporter essential for iron uptake from the soil and for plant growth. *Plant Cell* 14, 1223-1233.
- Vert, G.A., Briat, J.F., and Curie, C. (2003). Dual regulation of the *Arabidopsis* high-affinity root iron uptake system by local and long-distance signals. *Plant Physiol* 132, 796-804.
- von Wirén, N., Klair, S., Bansal, S., Briat, J.F., Khodr, H., Shioiri, T., Leigh, R.A., and Hider, R.C. (1999). Nicotianamine chelates both Fe-III and Fe-II. Implications for metal transport in plants. *Plant Physiol* 119, 1107-1114.
- Vreugdenhil, D., Aarts, M.G.M., Koornneef, M., Nelissen, H., and Ernst, W.H.O. (2004). Natural variation and QTL analysis for cationic mineral content in seeds of *Arabidopsis thaliana*. *Plant Cell Environ* 27, 828-839.
- Walch-Liu, P., and Forde, B.G. (2008). Nitrate signalling mediated by the NRT1.1 nitrate transporter antagonises L-glutamate-induced changes in root architecture. *Plant J* 54, 820-828.
- Walch-Liu, P., Liu, L.H., Remans, T., Tester, M., and Forde, B.G. (2006). Evidence that L-glutamate can act as an exogenous signal to modulate root growth and branching in *Arabidopsis thaliana*. *Plant Cell Physiol* 47, 1045-1057.
- Wang, H.Y., Klatte, M., Jakoby, M., Baumlein, H., Weisshaar, B., and Bauer, P. (2007). Iron deficiency-mediated stress regulation of four subgroup Ib BHLH genes in *Arabidopsis thaliana*. *Planta* 226, 897-908.
- Wang, R.C., Xing, X.J., Wang, Y., Tran, A., and Crawford, N.M. (2009). A genetic screen for nitrate regulatory mutants captures the nitrate transporter gene NRT1.1. *Plant Physiol* 151, 472-478.

- Wang, Y., Duan, L., Lu, M., Li, Z., Wang, M., and Zhai, Z. (2006). Expression of NAC1 up-stream regulatory region and its relationship to the lateral root initiation induced by gibberellins and auxins. *Sci China C Life Sci* 49, 429-435.
- Wang, Y.H., Garvin, D.F., and Kochian, L.V. (2002). Rapid induction of regulatory and transporter genes in response to phosphorus, potassium, and iron deficiencies in tomato roots. Evidence for cross talk and root/rhizosphere-mediated signals. *Plant Physiol* 130, 1361-1370.
- Ward, J.T., Lahner, B., Yakubova, E., Salt, D.E., and Raghothama, K.G. (2008). The effect of iron on the primary root elongation of *Arabidopsis* during phosphate deficiency. *Plant Physiol* 147, 1181-1191.
- Watanabe, T., Broadley, M.R., Jansen, S., White, P.J., Takada, J., Satake, K., Takamatsu, T., Tuah, S.J., and Osaki, M. (2007). Evolutionary control of leaf element composition in plants. *New Phytol* 174, 516-523.
- Waters, B.M., Chu, H.H., DiDonato, R.J., Roberts, L.A., Easley, R.B., Lahner, B., Salt, D.E., and Walker, E.L. (2006). Mutations in *Arabidopsis* Yellow Stripe-Like1 and Yellow Stripe-Like3 reveal their roles in metal ion homeostasis and loading of metal ions in seeds. *Plant Physiol* 141, 1446-1458.
- Werner, T., Nehnevajova, E., Kollmer, I., Novak, O., Strnad, M., Kramer, U., and Schmulling, T. (2010). Root-specific reduction of cytokinin causes enhanced root growth, drought tolerance, and leaf mineral enrichment in *Arabidopsis* and tobacco. *Plant Cell* 22, 3905-3920.
- Wilkinson, J.Q., and Crawford, N.M. (1993). Identification and characterization of a chlorate-resistant mutant of *Arabidopsis thaliana* with mutations in both nitrate reductase structural genes *Nia1* and *Nia2*. *Mol Gen Genet* 239, 289-297.
- Williamson, L.C., Ribrioux, S.P.C.P., Fitter, A.H., and Leyser, H.M.O. (2001). Phosphate availability regulates root system architecture in *Arabidopsis*. *Plant Physiol* 126, 875-882.
- Wilmoth, J.C., Wang, S., Tiwari, S.B., Joshi, A.D., Hagen, G., Guilfoyle, T.J., Alonso, J.M., Ecker, J.R., and Reed, J.W. (2005). NPH4/ARF7 and ARF19 promote leaf expansion and auxin-induced lateral root formation. *Plant J* 43, 118-130.
- Wu, G., Lewis, D.R., and Spalding, E.P. (2007). Mutations in *Arabidopsis* multidrug resistance-like ABC transporters separate the roles of acropetal and basipetal auxin transport in lateral root development. *Plant Cell* 19, 1826-1837.
- Wu, J.J., Wang, C.A., Zheng, L.Q., Wang, L., Chen, Y.L., Whelan, J., and Shou, H.X. (2011). Ethylene is involved in the regulation of iron homeostasis by regulating the expression of iron-acquisition-related genes in *Oryza sativa*. *J Exp Bot* 62, 667-674.
- Wu, P., Ma, L.G., Hou, X.L., Wang, M.Y., Wu, Y.R., Liu, F.Y., and Deng, X.W. (2003). Phosphate starvation triggers distinct alterations of genome expression in *Arabidopsis* roots and leaves. *Plant Physiol* 132, 1260-1271.
- Xie, Q., Frugis, G., Colgan, D., and Chua, N.H. (2000). *Arabidopsis* NAC1 transduces auxin signal downstream of TIR1 to promote lateral root development. *Genes Dev* 14, 3024-3036.

- Yamasaki, H., Abdel-Ghany, S.E., Cohu, C.M., Kobayashi, Y., Shikanai, T., and Pilon, M. (2007). Regulation of copper homeostasis by micro-RNA in *Arabidopsis*. *J Biol Chem* 282, 16369-16378.
- Yang, T.J.W., Lin, W.D., and Schmidt, W. (2010). Transcriptional profiling of the *Arabidopsis* iron deficiency response reveals conserved transition metal homeostasis networks. *Plant Physiol* 152, 2130-2141.
- Yang, T.J.W., Perry, P.J., Ciani, S., Pandian, S., and Schmidt, W. (2008). Manganese deficiency alters the patterning and development of root hairs in *Arabidopsis*. *J Exp Bot* 59, 3453-3464.
- Yang, X.J., and Finnegan, P.M. (2010). Regulation of phosphate starvation responses in higher plants. *Ann Bot* 105, 513-526.
- Yeh, C.M., Chien, P.S., and Huang, H.J. (2007). Distinct signalling pathways for induction of MAP kinase activities by cadmium and copper in rice roots. *J Exp Bot* 58, 659-671.
- Yi, Y., and Guerinot, M.L. (1996). Genetic evidence that induction of root Fe(III) chelate reductase activity is necessary for iron uptake under iron deficiency. *Plant J* 10, 835-844.
- Yuan, H., and Liu, D. (2008). Signaling components involved in plant responses to phosphate starvation. *J Integr Plant Biol* 50, 849-859.
- Yuan, Y.X., Zhang, J., Wang, D.W., and Ling, H.Q. (2005). AtbHLH29 of *Arabidopsis thaliana* is a functional ortholog of tomato FER involved in controlling iron acquisition in strategy I plants. *Cell Res* 15, 613-621.
- Yuan, Y.X., Wu, H.L., Wang, N., Li, J., Zhao, W.N., Du, J., Wang, D.W., and Ling, H.Q. (2008). FIT interacts with AtbHLH38 and AtbHLH39 in regulating iron uptake gene expression for iron homeostasis in *Arabidopsis*. *Cell Res* 18, 385-397.
- Zakhleniuk, O.V., Raines, C.A., and Lloyd, J.C. (2001). *pho3*: a phosphorus-deficient mutant of *Arabidopsis thaliana* (L.) Heynh. *Planta* 212, 529-534.
- Zhang, H., and Forde, B.G. (2000). Regulation of *Arabidopsis* root development by nitrate availability. *J Exp Bot* 51, 51-59.
- Zhang, H., Jennings, A., Barlow, P.W., and Forde, B.G. (1999a). Dual pathways for regulation of root branching by nitrate. *Proc Natl Acad Sci U S A* 96, 6529-6534.
- Zhang, H.M., and Forde, B.G. (1998). An *Arabidopsis* MADS box gene that controls nutrient-induced changes in root architecture. *Science* 279, 407-409.
- Zhao, Y.X., Medrano, L., Ohashi, K., Fletcher, J.C., Yu, H., Sakai, H., and Meyerowitz, E.M. (2004). HANABA TARANU is a GATA transcription factor that regulates shoot apical meristem and flower development in *Arabidopsis*. *Plant Cell* 16, 2586-2600.
- Zheng, L.Q., Huang, F.L., Narsai, R., Wu, J.J., Giraud, E., He, F., Cheng, L.J., Wang, F., Wu, P., Whelan, J., and Shou, H.X. (2009). Physiological and transcriptome analysis of iron and phosphorus interaction in rice seedlings. *Plant Physiol* 151, 262-274.

Zhou, L.W., and Marzluf, G.A. (1999). Functional analysis of the two zinc fingers of SRE, a GATA-type factor that negatively regulates siderophore synthesis in *Neurospora crassa*. *Biochemistry-Us* 38, 4335-4341.

Zhou, L.W., Haas, H., and Marzluf, G.A. (1998). Isolation and characterization of a new gene, sre, which encodes a GATA-type regulatory protein that controls iron transport in *Neurospora crassa*. *Mol General Gen* 259, 532-540.

## 8 Acknowledgements

I would like to thank Prof. Dr. Nicolaus von Wirén for giving me the opportunity of working in his lab under his supervision. I greatly acknowledge your trust and advices. Thank you for always sharing your enthusiasm for science and for being always ready to help me in all critical times.

I am very thankful to Joni Lima for our fruitful cooperation in the lab and for nice sessions of discussion. I also thank his friendship inside and outside the lab and for great sessions of Brazilian food tasting. I really enjoyed the time we spent in Hohenheim and hope we can maintain our cooperation in the future. Valeu Joni!

I wish to thank Prof. Dr. Gerd Weber (University of Hohenheim) for reviewing the present PhD thesis and for his constructive criticism and discussions. I would also like to thank Prof. Dr. Klaus Harter (University of Tübingen) for participating in the oral examination. I am also thankful to the Vice-Dean Prof. Dr. Andreas Fangmeier for taking part during the thesis defence.

Many thanks to the members of the “Fe group” (Ben, Nicole, Seckin, Fanghua, Rongli and Nunun) for the good interaction and for the fruitful discussion sessions.

I thank Anne Kriegel, Alberto and Uli for their help in the lab and for “allowing” me to supervise them. Your contribution to my work and to my academic formation was undoubtedly very important.

I also thank the other members from the former “S1-group” (currently known as “MPE group”): Anne Bohner, Alberto, Uli, Claudia, Bernhard, Dmitriy, Sebastian, Fengying, Julia, Stefan, Baris *et al.* Thank you also Dr. Mohammad-Reza (Mo), Young-Min, and Mohammad Reza. I specially thank Dmitriy for endless discussion sessions about various (usually unrelated) topics.

I also want to thank the former members of the lab, Lixing, Olga *et al.* and specially the Brazilian team Anderson, Lilia, Joni and Fabiano for their friendship, for helping me to get established in the lab, for sharing their experiences and for being such good friends.



I thank all technicians of the MPE group, especially Susanne and Lisa for their support in many experiments. A special thanks to Heike Nierig and Melanie Ruff for the help with cloning and plant transformation. I am also grateful to the members of the AG Plant Structural Biology (Dr. Melzer, Dr. Twan Rutten, Dr. Diaa Daghma and Mrs. Wiesner) for their outstanding support with the microscope analyses.

I am grateful to Mrs. Schöllhammer and Mrs. Berghammer (Uni Hohenheim) for their unconditional help during our stay in Stuttgart. I also thank Mrs. Leps and Mrs. Fischer (IPK) for supporting our establishment in Gatersleben.

Thanks all members of the Institute for Plant Nutrition (Uni Hohenheim), specially Prof. Dr. Torsten Müller, Prof. Dr. Volker Römheld and Dr. Günter Neumann for the excellent discussions during the progress seminars. Special thanks also to Mrs. Dachtler and Mrs. Ruckwied for technical assistance and nutrient analyses.

I also wish to thank Prof. Dr. Fritz Bangerth for sharing with me his enthusiasm for science and for the helpful discussions about plant hormones.

I also thank the members of the Landesanstalt für Landwirtschaftliche Chemie (Uni Hohenheim) for their help with the elemental analyses.

I am grateful to CAPES (Ministry of Education, Brazil) for the scholarship and for the overall support throughout the whole Ph.D. I would also like to thank the Deutscher Akademischer Austausch Dienst (DAAD, Germany) for the financial support during the four months of intensive German lessons in Marburg, Germany.

I would like to express my gratitude to my family. I thank my parents Armando and Iris for their constant support and for their example of dedication and honesty. I also thank my brother Eduardo for his support and for sharing with me his interest on biology, music and guitars. Muito obrigado a vocês!

Finally, I want to thank my lovely wife Ana Cristina. Thank you for your love, support and help. Many thanks for always being with me whenever I needed and for sharing with me the whole experience of living abroad. You are my constant source of inspiration. Te amo demais!

## 9 Curriculum vitae

### Ricardo Fabiano Hettwer Giehl

Date of birth: May 21st, 1982

Place of birth: Boa Vista do Buricá, RS, Brazil

Address: Leibniz Institute of Plant Genetics and Crop Plant Research (IPK),  
Corrensstraße 3, D-06466 Gatersleben, Germany

Telephone: +49 (0)39482 58798

Email: hetgiehl@yahoo.com.br

### Education

April 2007 – current: **PhD in Agricultural Sciences** – Molecular Plant Nutrition, Institute of Plant Nutrition, University of Hohenheim, Germany. PhD Thesis: “Identification of regulatory factors determining nutrient acquisition in Arabidopsis”. Supervisor: Prof. Dr. Nicolaus von Wirén. Scholarship: CAPES, Ministry of Education, Brazil.

March 2005 – September 2006: **Msc. in Agronomy**, Department of Crop Sciences, Federal University of Santa Maria, RS, Brazil. Master thesis: “Control of mealiness, in ‘Chiripá’ peaches, using controlled atmosphere and ethylene”. Supervisor: Prof. Dr. Auri Brackmann. Scholarship: CNPq, Brazil.

March 2000 – December 2005: **Graduation in Agronomy**, Federal University of Santa Maria, RS, Brazil.

### List of articles published during the PhD study

**Giehl, R.F.H.**, Lima, J.E., von Wirén, N (2012). Regulatory components involved in altering lateral root development in response to localized Fe: evidence for natural genetic variation. **Plant Signaling and Behavior**. *Accepted*.

**Giehl, R.F.H.**, Lima, J.E., von Wirén, N. (2012) Localized iron supply triggers lateral root elongation in Arabidopsis by altering the AUX1-mediated auxin distribution. **Plant Cell** 24, 33-49.

**Giehl, R.F.H.**, Meda, A.R., and von Wirén, N. (2009). Moving up, down, and everywhere: signaling of micronutrients in plants. **Current Opinion in Plant Biology** 12, 320-327.

## **Participation in scientific conferences during the PhD study**

**Giehl, R.F.H.**, Takahashi, H., von Wirén, N. Nutriomics-based identification of transcription factors involved in nutrient accumulation and efficiency in *Arabidopsis thaliana*. In: Genetics of Plant Nutrition, 2010, Hannover, Germany (**poster presentation**).

**Giehl, R.F.H.**, Lima, J.E., von Wirén, N. Local supply of iron distinctly defines lateral root number and elongation in *Arabidopsis thaliana*. In: XVII Congress of the Federation of European Societies of Plant Biology, 2010, Valencia, Spain (**poster presentation**).

**Giehl, R.F.H.**, Takahashi, H., von Wirén, N. Nutriomics-based identification of transcription factors involved in nutrient accumulation and efficiency in *Arabidopsis thaliana*. In: 9th International Plant Molecular Biology Congress, 2009, St. Louis, USA (**poster presentation**).

## **Supervision and teaching activities**

Supervision of master's thesis (*Diplomarbeit*) of Ulrich Lutz: "The role of the transcription factor ANAC020 in iron nutrition and flowering time regulation in *Arabidopsis thaliana*". Advisor: Prof. Dr. Nicolaus von Wirén (June 2010 to March 2011).

Supervision of master's thesis (*Diplomarbeit*) of Anne Kriegel: "Identification of transcription factors involved in Fe-deficiency responses in *Arabidopsis thaliana*". Advisor: Prof. Dr. Nicolaus von Wirén (October 2009 to March 2010).

Supervision of master's thesis (*Diplomarbeit*) of Alberto M. Laginha: "Physiological characterization of the ammonium transporter AMT2;1 in *Arabidopsis thaliana*". Advisor: Prof. Dr. Nicolaus von Wirén (October 2009 to May 2010).

Supervision of the practical course "Fe-acquisition mechanisms in plants" for undergraduate students in the frame of the course "Mineral Plant Nutrition", at the Institute of Plant Nutrition, University of Hohenheim, (March 2008 and March 2009).

Supervision of one undergraduate student (Ines Ullmann) for research on molecular plant nutrition, in the frame of the course "Agricultural Biotechnology", University of Hohenheim (April to June 2008).